

**For Reference**

---

**NOT TO BE TAKEN FROM THIS ROOM**

# For Reference

---

NOT TO BE TAKEN FROM THIS ROOM

Ex LIBRIS  
UNIVERSITATIS  
ALBERTAENSIS



## Regulations Regarding Theses and Dissertations

[illegible]









THE UNIVERSITY OF ALBERTA

MEASUREMENTS OF THE BED-LOAD DISCHARGE  
OF THE ELBOW RIVER

by

Albert Bill Hollingshead



A THESIS  
SUBMITTED TO THE FACULTY OF GRADUATE STUDIES  
IN PARTIAL FULFILMENT OF THE REQUIREMENTS FOR THE DEGREE OF  
MASTER OF SCIENCE

DEPARTMENT OF CIVIL ENGINEERING

EDMONTON, ALBERTA

FEBRUARY, 1968



## UNIVERSITY OF ALBERTA

## FACULTY OF GRADUATE STUDIES

The undersigned certify that they have read, and recommend to the Faculty of Graduate Studies for acceptance, a thesis entitled

## MEASUREMENTS OF THE BED-LOAD DISCHARGE

## OF THE ELBOW RIVER

submitted by Albert Bill Hollingshead in partial fulfilment of the requirements for the degree of Master of Science.



## ABSTRACT

Estimates of the bed-load discharge of a gravel bed river were made by the following four methods:

1. direct measurements using two types of portable bed-load samplers;
2. the injection of tracer bed material and the sampling of tracer concentrations within the bed-load;
3. direct measurements of the refilling rate of a large pit excavated in the river bed;
4. the application of several bed-load discharge formulae, using measured hydraulic parameters.

Field observations were carried out during the summer of 1967 on a short reach of the Elbow River near Bragg Creek, Alberta. Surveys of the channel geometry and longitudinal bed and water surface profiles were carried out. The bed material was sampled using various methods. The velocity distribution was measured at three cross sections at several stages of flow, and hydrophone observations were used to determine the start of bed movement. A number of bed-load discharge samples were obtained and a short period of tracer injection was accomplished.

The basket and VUV type samplers gave reasonable estimates of the bed-load discharge; however, a larger number of samples, requiring





improved handling equipment would be advantageous. The use of tracers gave the highest estimates of bed-load discharge however the period of injection was insufficient to satisfy the assumptions on which the method was based. Estimates based on the pit excavation and refilling rate are limited because of the unfortunate timing of the field work. This pit was partially excavated prior to a large flood which occurred on May 30, 1967. The application of the sediment transport formulae gave a wide range of estimates of bed-load discharge for all stages of flow. The applicability of each formula to the range of hydraulic and sediment parameters is discussed. An assessment of hydraulic conditions corresponding to the first displacement of bed material from field observations is most useful for checking and altering the formulae used.

A continuation of the bed-load discharge sampling program is recommended with the use of a more efficient winch system. A study of the total sediment transport and channel processes along the Elbow River, including sediment accumulation in the Glenmore Reservoir, is suggested.



## ACKNOWLEDGEMENTS

This study was a joint project with the following agencies participating: Water Resources Division, Alberta Department of Agriculture; Highways Division, Research Council of Alberta; Department of Civil Engineering, University of Alberta; and Water Survey of Canada, Department of Energy, Mines and Resources.

Acknowledgements are expressed to Dr. T. Blench, thesis supervisor; and to Dr. L. Rakoczi, Research Institute for Water Resources Development, Budapest, Hungary; for their advice and assistance.

Mr. C. R. Neill, Research Council of Alberta, gave many helpful suggestions. Mr. E. Yaremko, Provincial Water Resources Division, cooperated in supplying the survey crews and much of the equipment. All of the staff in the Calgary Office of Water Survey of Canada were most cooperative in supplying equipment and technical assistance. Water Survey of Canada supplied the Canadian pattern bed-load samplers used throughout the study.



## TABLE OF CONTENTS

	Page
Title Page .....	i
Abstract .....	iii
Acknowledgements .....	v
Table of Contents .....	vi
List of Tables .....	x
List of Figures .....	xi
List of Photographs .....	xiii
CHAPTER I. INTRODUCTION .....	1
1.1. Reasons for the Study .....	1
1.2. Objects of the Study .....	2
1.3. Methods .....	2
1.4. Definitions .....	2
1.5. Symbols .....	4
1.6. Abbreviations .....	7
CHAPTER II. THEORY .....	9
2.1. Direct Bed-load Sampling .....	9
2.2. Bed-load Discharge by Tracers .....	11
2.3. The Determination of Bed-load Discharge by Formulae .....	12





CHAPTER III. FIELD EQUIPMENT AND METHODS .....	16
3.1. Introduction .....	16
3.2. Basket Samplers .....	16
3.3. VUV Samplers .....	17
3.4. Bed-load Discharge Sampling .....	18
3.5. Equipment Used in the Tracer Study .....	20
3.6. Tracer Material and Preparation .....	20
3.7. Tracer Injection .....	22
3.8. Sampling of Tracer Material .....	23
3.9. Hydrophone .....	23
3.10. Hydrophone Use .....	24
3.11. Method of Pit Excavation .....	25
3.12. Recording Fathometer .....	26
3.13. Velocity Measurements and Equipment .....	26
3.14. Bed Material Sampling .....	27
CHAPTER IV. FIELD OBSERVATIONS .....	30
4.1. The Study Reach .....	30
4.2. Hydrologic Data .....	30
4.3. Channel Geometry .....	32
4.4. Slope Observations .....	37
4.5. Velocity Observations .....	39
4.6. Analysis of Bed Material .....	40



	Page
4.6.1. Bed Material Samples .....	40
4.6.2. Recovery of Tracer Material .....	43
4.6.3. Shape Analysis of Bed Material .....	45
4.6.4. Specific Gravity of Bed Material .....	46
4.7. Bed-load Discharge Sampling .....	47
4.8. Tracer Study Observations .....	49
4.9. Hydrophone Observations .....	51
4.10. Pit Excavation Observations .....	54
4.11. Other Observations .....	55
4.11.1. Leopold Chains .....	55
4.11.2. Bank Erosion and Channel Shift .....	57
CHAPTER V. ANALYSIS OF DATA .....	59
5.1. Bed-load Discharge Calculations from Direct Sampling ....	59
5.2. Bed-load Discharge Calculations from Tracer Concentrations .....	61
5.3. Bed-load Discharge Calculations from the Volumetric Pit .....	63
5.4. Calculations of Bed-load Discharge Using Formulae .....	64
5.4.1. Calculations Based on the Regime Slope Equations of Blench .....	64
5.4.2. Calculations Based on the Formula of Meyer-Peter, Müller .....	67
5.4.3. Calculations of Bed-load Discharge by the Methods of Einstein .....	68



	Page
5.4.4. Calculations of Bed-load Discharge by the Modified Einstein Method of Colby and Hubbell .....	71
5.5. Comparison of Results and Calculation of Annual Bed-load Discharge .....	74
5.5.1. Comparison of Results .....	74
5.5.2. Estimates of Annual Bed-load Discharge .....	76
5.6. Analysis of Channel Roughness .....	77
5.7. Analysis of Unit Bed-load Discharge Measurements .....	78
5.8. Discussion of Competent Conditions and Calculations of the Average Bed Shear Stress .....	80
CHAPTER VI. CONCLUSIONS AND RECOMMENDATIONS .....	84
6.1. Conclusions .....	84
6.2. Recommendations .....	88
LIST OF REFERENCES .....	92
APPENDIX A. Calculations of Bed-load Discharge by the Methods of Einstein.	
APPENDIX B. Figures.	
APPENDIX C. Photographs.	



## LIST OF TABLES

CHAPTER IV		Page
IV-1	Discharge Measurements, Elbow River at Bragg Creek 1967 (5BJ <sub>4</sub> ) .....	33
IV-2	Channel Geometry .....	36
IV-3	Velocity Fluctuations at Station 60, 12+18 D/S .....	39
IV-4	Bed Material Sampling .....	41
IV-5	Bed-load Sampling .....	48
IV-6	Hydrophone Observations .....	52
CHAPTER V		
V-1	Bed-load Discharge Results from Direct Sampling Calculations .....	60
V-2	Bed-load Discharge Calculated from Tracer Concentration .....	62
V-3	Bed-load Discharge Calculated from the Regime Slope Equation .....	66
V-4	Bed-load Discharge Calculations from Meyer-Peter and Müller Formula .....	69
V-5	Bed-load Discharge by Einstein Method .....	70
V-6	Bed-load Discharge Calculations by Modified Einstein Procedure .....	72
V-7	Sample Calculation Using Modified Einstein Procedure .....	73
V-8	Calculated Values of Shields' Parameter $\frac{\tau_o}{\gamma_s D}$ .....	82
APPENDIX A		
A-1	Calculations by Einstein Method .....	A4
A-2	Calculations by Einstein Method .....	A6





## LIST OF FIGURES

## CHAPTER III

## Appendix B

- 3-1 Assembly Drawing of 24-10-30 Basket Sampler.
- 3-2 Assembly Drawing of Half Size VUV Sampler.

## CHAPTER IV

- 4-1 Topographic Map of Elbow River Basin.
- 4-2 Frequency Curve, Elbow River at Bragg Creek.
- 4-3 Hydrographs, Elbow River at Bragg Creek, 1951, 1953.
- 4-4 Hydrographs, Elbow River at Bragg Creek, 1961, 1964.
- 4-5 Hydrograph, Elbow River at Bragg Creek, 1967.
- 4-6 Flow Duration Curve, Elbow River at Bragg Creek.
- 4-7 Stage Discharge Curves, Elbow River at Bragg Creek.
- 4-8 River Trace from Air Photographs of May 26, 1967.
- 4-9 River Trace from Air Photographs of June 22, 1967.
- 4-10 Cross Sections from 1+24 U/S to 22+03 U/S.
- 4-11 Cross Sections from 0+18 D/S to 12+18 D/S.
- 4-12 Curves of Area vs. Discharge.
- 4-13 Curves of Surface Breadth vs. Discharge.
- 4-14 Curves of  $A/b_w$  vs. Discharge.
- 4-15 Curves of Mean Velocity vs. Discharge.
- 4-16 Water Surface and Bed Longitudinal Profiles.
- 4-17 Velocity Distribution at Various Stages of Flow at Cross Section 22+03 U/S.
- 4-18 Velocity Distribution at Various Stages of Flow at Cross Section 0+18 D/S.



## LIST OF FIGURES

## CHAPTER IV - (Cont'd.)

## Appendix B

- 4-19 Velocity Distribution at Various Stages of Flow at Cross Section 12+18 D/S.
- 4-20 Particle Size Distribution Curves for the Totals of Each Sample Type.
- 4-21 Particle Size Distribution Curves Tape Samples No. 12 to No. 16.
- 4-22 Particle Size Distribution Curves of Bed-load Samples.
- 4-23 Particle Size Distribution Curves of Pit Samples Nos. 1, 2, 4, and 5.
- 4-24 Particle Size Distribution Curve of Pit Sample No. 8 and Tape Sample No. 15.
- 4-25 Particle Size Distribution Curves of Recovered Tracer Material.
- 4-26 Shape Ratios of Tape Sample No. 36 and Excavation Sample No. 58.
- 4-27 Shape Ratios of Bed-load Material.
- 4-28 Cross Sections 12+58 D/S to 13+18 D/S Across Pit Excavation.

## CHAPTER V

- 5-1 Bed-load Discharge Versus Fluid Discharge.
- 5-2 Bed-load Discharge Versus Fluid Discharge.
- 5-3 Distribution of Bed-load Discharge at Cross Section 12+18 D/S.
- 5-4 Velocity Distribution Normal to Bed at Cross Section 12+18 D/S



## LIST OF PHOTOGRAPHS

## CHAPTER III

## Appendix C

- 3-1 Front View of Large Basket Sampler (24-10-30) With 1/4 Inch Mesh Basket.
- 3-2 Side View of Large Basket Sampler (24-10-30) With 1/4 Inch Mesh Basket.
- 3-3 Side View of Small Basket Sampler (12-6-15) With 1/4 Inch Mesh Basket.
- 3-4 Top-front View of Small Basket Sampler (12-6-15) With 1/4 Inch Mesh Basket.
- 3-5 Full Size VUV Sampler, Showing Mouth Opening.
- 3-6 Full Size VUV Sampler, Showing Rear Gate Open.
- 3-7 Half Size, VUV Sampler, Side View.
- 3-8 Half Size VUV Sampler, Top-front View.
- 3-9 Lowering Large Basket Sampler at Station 110 Feet, 12+18 D/S.
- 3-10 Recovering Sampler to Left Bank.
- 3-11 Hydrophone Assembly.
- 3-12 Bottom View of Hydrophone Showing Position of Enclosed Microphone.
- 3-13 Drag Line Equipment.

## CHAPTER IV

- 4-1 Mosaic of Study Reach from Air Photographs of May 26, 1967.
- 4-2 Mosaic of Study Reach from Air Photographs of June 22, 1967.
- 4-3 Upstream Stage Recorder from Right Bank at 23+35 U/S.
- 4-4 Surface Wave, from Stage Recorder at 23+35 U/S on Left Bank.





## LIST OF PHOTOGRAPHS

## CHAPTER IV - (Cont'd.)

## Appendix C

- 4-5      Photographic Grid Sample at Pit Sample No. 1.
- 4-6      Photographic Grid Sample at Pit Sample No. 2.
- 4-7      Photographic Grid Sample at Pit Sample No. 4.
- 4-8      Photographic Grid Sample at Pit Sample No. 5.
- 4-9      Location of Tape Sample No. 15.
- 4-10     Photographic Grid Sample at Pit Sample No. 8.
- 4-11     Location of Bed Excavation, from Left Bank at  
12+38 D/S. Q = 7,000 c.f.s., May 31, 1967.
- 4-12     View from Right Bank at 12+00 D/S. Flow Over  
Bed Rock in Foreground. Q = 7,000 c.f.s., May  
31, 1967.
- 4-13     Bedrock on Right Bank at 12+18 D/S.
- 4-14     Bank Material Eroded at High Stage.



## CHAPTER I

### INTRODUCTION

#### 1.1. Reasons for the Study

Many hydraulic engineering works have been built on sediment-bearing streams. Some of these works have experienced operating and economical difficulties because of an inadequate consideration for the amount of sediment that can be transported. A study of sediment transport may give insight into problems of bank erosion, bed scour, and bed aggradation that may cause structural failure and flooding.

One of the major studies in sediment transport is the determination of the total sediment discharge of a given stream or river. In some rivers the majority of this sediment travels as bed-load, that is by sliding, rolling or saltating along the bed. The determination of bed-load discharge has been attempted in many ways. These all fall into three main categories. First is the direct measurement by some type of apparatus; this includes means of subtracting suspended load discharges from the total sediment discharge. Second are the empirical relations defined by a set of physical observations of a river reach. The third includes all methods based on observations of the results of sedimentation processes.



Unfortunately there are no means, empirical or by direct measurement, which have proven completely adequate over a wide range of sediment and hydraulic conditions in actual rivers.

### 1.2. Objects of the Study

The object of this study was to compare four methods of estimating the bed-load discharge in a gravel bed river. The comparison, to be of maximum use, must concern the ease of operation, the economics of each method, the need for special equipment and trained personnel, and the reliability of the results.

Other objectives of the study were to collect hydrologic data on the river and determine hydraulic conditions for first displacement or incipient motion of the various sizes of material present.

### 1.3. Methods

One method used was direct sampling using several types of portable bed-load samplers. The second method was by tracer injection and bed-load sampling for tracer concentrations. The third was by measuring the rate of refilling of a volumetric pit excavated in the stream bed. The results of these methods are compared with estimates of bed-load discharge calculated by empirical formulae and measured hydraulic parameters.

### 1.4. Definitions

The following definitions have been adopted and used throughout:

BED-LOAD	Bed material that moves by saltating, rolling or sliding along the stream bed.
----------	--





BED-LOAD CHARGE	Bed-load discharge expressed as a ratio to the fluid discharge by weight.
BED-LOAD DISCHARGE	The quantity of bed-load by dry weight passing a given cross section per unit of time.
BED MATERIAL	The alluvial material that makes up the stream bed.
BED MATERIAL DISCHARGE	The quantity of bed material passing a given cross section per unit of time, and composed of bed-load plus bed material transported as suspended load.
COMPETENT CONDITIONS	Hydraulic conditions corresponding to the first displacement of bed material.
GRAVEL	Sediment particles larger than 2 mm. in size.
HYDRAULIC EFFICIENCY	Used with the bed-load samplers and defined as the ratio of the fluid discharge passing through the sampler to the discharge that would have passed through the sampler mouth area without the sampler present.
LEOPOLD CHAIN	An open link chain driven vertically into the stream bed or a bar and used to indicate the maximum depth to which the bed moves thereafter.
SALTATION	Movement of particles that are not in contact with the bed at all times, and which may go into suspension for short periods of time.





SAMPLING EFFICIENCY	Used with bed-load samplers and defined as the ratio of weight of bed-load collected during a given sampling time to the weight of bed-load that would have passed through the sampler mouth area if the sampler was not present.
SAND	Sediment particles between 0.062 mm. and 2 mm. in size.
SEDIMENT (FLUVIAL SEDIMENT)	Fragmentary material that originates from the weathering of rocks and is transported by, suspended in, or deposited from, water.
SEDIMENT DISCHARGE (TOTAL LOAD)	The total quantity of sediment that is carried through any cross section of a stream in a unit of time. This quantity is the bed material discharge plus suspended load which is not bed material.
SILT	Sediment particles between sand and clay sizes 0.004 mm. to 0.062 mm.
THALWEG	Longitudinal plan of the locus of greatest depth along the channel.

### 1.5. Symbols

The following symbols have been adopted, with the dimensions given using force, length and time notation.

Symbol	Meaning	Dimensions
A	Cross-sectional area of flow	$L^2$



Symbol	Meaning	Dimensions
a	Length of long axis of particle	L
a	Area beneath concentration curve	L
b	Channel breadth, general	L
b	Length of intermediate axis of particle	L
$b_w$	Water surface breadth	L
$b_s$	Width of bed contributing to bed-load discharge	L
C	Bed-load charge	
c	Length of short axis of particle	L
c	Tracer concentration	
D	Particle diameter or equivalent diameter	L
$D_x$	The specified size at which x percent of the total sample weight is smaller than	L
d	Depth of flow, general	L
$F_b$	Blench's bed factor $V^2/d$	$L/T^2$
$F_{bo}$	Zero bed factor	$L/T^2$
$G_s$	Sediment discharge, dry weight	F/T
$G_s'$	Sediment discharge, submerged weight	F/T
$G_{tr}$	Tracer material discharge, dry weight	F/T
g	Gravitational acceleration	$L/T^2$
$g_s$	Sediment discharge per unit width, dry weight	F/LT
$g_{tr}$	Tracer material discharge per unit width, dry weight	F/LT
$i_b$	Fraction of specified size range of total bed sample by weight	
k	Slope correction coefficient in regime slope equation	
$k_s$	Equivalent sand-grain roughness	L



Symbol	Meaning	Dimensions
$l$	Effective width of bed-load sampler mouth	$L$
$p$	Wetted perimeter of channel cross section	$L$
$Q$	Fluid discharge	$L^3/T$
$q$	Fluid discharge per unit width	$L^2/T$
$q_s$	Sediment discharge per unit width	$L^2/T$
$R$	Hydraulic radius of channel cross section	$L$
$R_b'$	Partial hydraulic radius with respect to grain size roughness	$L$
$R_b''$	Partial hydraulic radius for channel irregularities	$L$
$S$	Slope, general	
$S_e$	Slope of energy gradient	
$S_w$	Slope of water surface	
$s_s$	Density ratio, solids to fluid	
$V$	Velocity, general	$L/T$
$V_m$	Mean velocity	$L/T$
$V_*$	Shear velocity	$L/T$
$y$	Distance from bed	$L$
$\gamma$	Specific weight of fluid	$F/L^3$
$\gamma_s$	Specific weight of solids	$F/L^3$
$\gamma_s'$	Submerged specific weight of solids	$F/L^3$
$\delta$	Boundary layer thickness	$L$
$\Delta$	Apparent roughness diameter	$L$
$\mu$	Dynamic viscosity of fluid	$FT/L^2$
$\nu$	Kinematic viscosity of fluid	$L^2/T$
$\nu_{70}$	Kinematic viscosity of fluid at 70 degrees fahrenheit	$L^2/T$



Symbol	Meaning	Dimensions
$\rho$	Mass density of fluid	$FT^2/L^4$
$\rho_s$	Mass density of solids	$FT^2/L^4$
$\tau_o$	Shear stress at boundary	$F/L^2$
$\tau_c$	Boundary shear stress for beginning of motion	$F/L^2$
$\Phi$	Intensity of transport	
$\Psi$	Intensity of shear on particle	

### 1.6. Abbreviations

The following abbreviations are used throughout:

c.f.s.	cubic feet per second
D/S	downstream of reference point
Fig.	figure
f.p.s.	feet per second
ft.	foot
g.h.	gage height
H.W.	high water
lb.	pound
Lt.	left
min.	minute
mm.	millimeter
log.	logarithm to the base 10
p.s.i.	pounds per square inch
Ref.	reference
Rt.	right
Sec.	second







Sta.	station
U/S	upstream of reference point
vs.	versus
W.L.	water level
%	percent



## CHAPTER II

### THEORY

#### 2.1. Direct Bed-load Sampling

The bed-load discharge of a river varies rapidly and erratically with time and with distance. Therefore a short period of measurement will not provide representative data at a sampling point. Because of these fluctuations, numerous samples over a long sampling period are necessary for reasonable estimates of the bed-load discharge through any cross section at a river stage.

Most bed-load samplers are constructed for a limited range of sediment sizes and hydraulic conditions. To be of maximum use they should be capable of trapping all sizes of material that are moving as bed-load, should be aligned parallel to the flow, should not present an obstruction to the flow pattern, and should not doze the bed or drop any portion of the sample when lifted.

Because no sampler has been successful in meeting all of these requirements, it is necessary to determine efficiency coefficients which can be applied to sampling results. Tests for sampling and hydraulic efficiencies of the many types of samplers have been attempted and reported many times in the past (Hubbell, 1964). Most of these tests have been carried out in laboratory flumes with sampler models. Similitude



of the sediment and hydraulic factors involved is not readily obtainable and efficiencies determined are therefore questionable when applied to field observations.

Basket type samplers usually have a large capacity and are most suitable for the trapping of large sediment sizes.

Pressure difference type samplers have expanded cross sections in the direction of flow. The resulting lower velocities in the downstream portion allow the sediment load to drop out into a sample retaining compartment. Many different samplers of this type have been designed for the trapping of sand sizes; Arnhem, Sphinx, etc. The Hungarian VUV sampler which is an improvement on the original Karolyi sampler is of this type but designed for use with particle sizes up to 100 mm.

Bed-load discharges are calculated from the direct measurements in much the same way water discharges are. From the weight and duration of the sample and the width of bed sampled the unit bed-load discharge intensity is calculated. Using these unit discharges and either a mean section or mid section, the discharges are multiplied by sampling strip widths to arrive at the total bed-load discharge. Efficiencies, if known for different sample sizes, are applied to the individual samples. If only a general efficiency is known, it is applied to the total calculated bed-load discharge.





## 2.2. Bed-load Discharge by Tracers

The use of tracers in the study of sediment transport has become a popular method. Radioactive isotopes, as well as fluorescent and luminescent dyes and paints have been used to trace bed material in a number of studies.

Ramette and Heuzel (1962) used a radioactive tracer to determine first displacement for three different size ranges of gravel in the Rhone River downstream of its confluence with the Saone River. They then used the tractive force for beginning of motion in the well known Meyer-Peter and Muller formula, in order to calculate bed-load discharges. Many of the studies using tracers are for the study of sand and silt movement along coasts, in estuaries and in maritime rivers (Putman and Smith, 1956; Jolliffe, 1960; Reid and Morgan, 1961). Most of this work is qualitative and measures only the distance tracer particles have traveled and in some cases the velocity of their movement. Experiments by Crickmore and Lean (1962) indicated transport rates can be deduced from measurements of the distribution of tracers in flumes. Measurements of bed material discharge both in the field and the laboratory flume have been reported by Hubbell and Sayre (1964). Rakoczi (1966), and Rakoczi and Stelczer (1965) described studies using luminescent tracers in the laboratory and in the Danube River which were mainly qualitative but extend up into the fine gravel range.

The tracer method used in this study is similar to that of estimating the water discharge by chemicals. A small but known amount





of tracer material  $G_{tr}$  is injected continuously into the unknown sediment discharge per unit width  $g_s$ , at a point within the moving bed strip. Successive samples of bed-load are taken across a cross section downstream of the injection point and far enough for complete mixing of tracer and bed-load material. The concentration of tracer material within each sample is the ratio of  $g_{tr}/g_s$  over the sample width. The area under a concentration versus width curve can be measured and an average concentration calculated by dividing this area by the total width of the bed-load strip. In the use of this method, it is assumed that there is no accumulation of tracer material between the injection point and the sampling cross section and that the total bed-load discharge is the same throughout the reach. Therefore the stipulation of complete mixing assumes that tracer material moves at the same average speed as the bed-load and extends to the full width of the moving bed-load strip over the mixing length. If these assumptions are satisfied the total bed-load discharge  $G_s = \frac{G_{tr}}{c_{average}}$ . An average value of the unit bed-load discharge over the width  $b_s$  equals  $G_s/b_s$ .

### 2.3. The Determination of Bed-load Discharge by Formulae

A large number of sediment transport formulae have evolved since the classical Du Boy's equation, proposed in 1879. Leliavsky (1966), Henderson (1966) and Raudkivi (1967) present many of the formulae and discuss some aspects of the popular forms. In many cases, the range of sediment and hydraulic conditions to which these formulae are applicable, is not clear. Some formulae that are generally known as bed-load formulae appear to cover the suspended load as well. The distinction



between the suspended load and bed-load is difficult to differentiate by hydraulic parameters, therefore creating an additional problem. The following paragraphs briefly describe the formulae used in the calculations of CHAPTER V.

One of the most widely used equations is that of Einstein (1950)

where  $\Phi_* = \text{function } (\Psi_*)$

with  $\Psi = \frac{\gamma_s' D_{35}}{\gamma R_b' S}$

and  $\Phi = \frac{g_s}{\gamma_s} \left( \frac{\rho}{\rho_s'} \right)^{1/2} \left( \frac{1}{g D^3} \right)^{1/2}$ .

By the methods of Einstein, the hydraulic parameters  $S$ ,  $A$ ,  $p$ ,  $R$  are calculated for a representative cross section taken for the selected reach of study. The grain size distribution is taken from bed material samples and split into ranges, each with an average size. The apparent roughness is calculated using the  $D_{65}$  of the total sample with corrections for the thickness of the laminar sublayer and transition from smooth to rough boundary conditions. Average flow velocities are determined according to the works of Keulegan. In order to obtain the total hydraulic radius, a component due to the pressure differences over bed forms and bars  $R_b''$  is added to the component with respect to the grain size roughness  $R_b'$ . Corrections are applied to  $\Psi$  in order to calculate  $\Psi_*$ . From Einstein's FIGURES 9 or 10  $\Phi_*$  is obtained from the calculated values of  $\Psi_*$ . The components of bed-load discharge for each size range are obtained by calculating  $i_b g_s = \Phi_* i_b \rho_s g^{3/2} D^{3/2} (s_s - 1)^{1/2}$  where  $i_b$  is the fraction of the total bed material sample of



each size range. By addition of the  $i_b g_s$  values calculated for each size range at different values of  $R_b'$ , the total bed-load discharge  $G_s$  is obtained by multiplying by the wetted perimeter for each stage. Additional steps are required to calculate the amount of bed material that goes into suspension, and a total bed material discharge can be obtained.

The use of a modified Einstein method was described by Colby and Hubbell (1961). Using this method, values of  $\sqrt{(RS)_m}$  are determined from a nomograph for known values of the mean velocity and the mean depth at a cross section. The bed material sample is used in several size ranges and  $\Psi_m$  is calculated using  $\Psi_m = (s_s - 1) D_{35} / (RS)_m$  or  $\Psi_m = (s_s - 1) (0.4) D_m / (RS)_m$  (where  $D_m$  is the geometric mean size of the range) whichever is greater. These values of  $\Psi_m$  are then used as  $\Psi_*$  in the  $\Psi_* - \Phi_*$  function to obtain values of  $\Phi_*$ . The bed-load discharge can then be calculated for each size range using

$$i_b G_s = p \times 43.2 \times 1200 \times D_m^{3/2} \times 1.39 \times \frac{\Phi_*}{2}$$

and added to give a total  $G_s$  for the cross section in lbs/min. dry weight. Additional steps are used to estimate that portion of bed material that goes into suspension as part of the suspended load.

Meyer-Peter and Müller (1948) developed an equation for bed-load discharge which is of the form:

$$0.25 \rho^{1/3} g_s'^{2/3} = \gamma RS \left( \frac{K_b}{K_b'} \right)^{3/2} - 0.047 \gamma_s' D_m$$

for a channel having negligible bank resistance, where  $K_b$  is a measure





of resistance to flow and equals the mean velocity  $V_m$  divided by  $R^{2/3}$   $S^{1/2}$  and  $K_b'$  is a measure of flow resistance due to grain size resistance only and equals  $\frac{26}{D_{90}^{1/6}}$  with  $D_{90}$  expressed in meters. The last term in the equation represents the bed shear force at competent conditions where  $D_m$  is the mean value of the intermediate diameter of each size range weighted for the fraction each size range is of the total.

Blench (1966) calculates the bed-load charge by the use of the regime slope equation in the form:

$$f'''(C) = \frac{S K b^{1/6} Q^{1/12}}{k F_{bo}^{11/12}}$$

$$\text{where } K = \frac{3.63 g}{v^{1/4}},$$

$$f'''(C) = \frac{(1+0.12C)^{11/12}}{1 + C/233} \quad \text{and is given in}$$

FIG. 7.2 (Blench, 1966),

$k$  is the meander correction coefficient and varies from 1.25 to 2.75

$$F_{bo} = 7.3 \frac{m}{w} D_f^{1/4} \left( \frac{v_{70}}{v} \right)^{1/6}, \quad \text{for } \frac{d}{D} > 50$$

$$\text{also } F_{bo} \approx F_b = \frac{V^2}{d} \quad \text{when } C \rightarrow 0$$

In the regime equations  $D$  is used as  $D_{50}$  in feet by weight and  $C$  is the charge in parts per hundred thousand by weight of the fluid discharge.





## CHAPTER III

### FIELD EQUIPMENT AND METHODS

#### 3.1. Introduction

The following paragraphs describe the field equipment used throughout the study and give a brief description of the field methods. The bed-load samplers and sampling methods used were not familiar to those involved in the study although much related information can be found in the literature. Many difficulties were incurred because of this lack of experience. The hydrophone was constructed just prior to the study and had never been used in the field. Many of the procedures used in the tracer portion of the study were also different than those normally used. A sonic fathometer was used in a slightly different way than normal. Methods that are generally well known are not described. It is hoped that the following paragraphs will assist others in the planning and carrying out of a similar study in the future under similar conditions.

#### 3.2. Basket Samplers

A basket sampler consists of a large rectangular frame and tail section into which fits a basket with one open end. The two sizes used were; large, 30 inches long, 24 inches wide, 10 inches deep and; small, 15 inches long, 12 inches wide, 6 inches deep. The weights of these samplers are 240 lbs. and 80 lbs. respectively. An assembly drawing of



the large sampler is shown in FIG. 3-1 and different views are shown in PLATES 3-1 and 3-2. The smaller sampler is constructed of the same materials but on the reduced scale indicated and shown in PLATES 3-3 and 3-4. With each size sampler there are three baskets with different size meshes. The mesh sizes are as follows:

	Large <u>3/4"</u>	Medium <u>1/2"</u>	Small <u>1/4"</u>
Top	1 inch	3/4 inch	1/2 inch
Sides and back	3/4 inch	1/2 inch	1/4 inch
Bottom	1/2 inch	1/4 inch	3/16 inch

The design and use of basket type samplers were reported by Hubbell (1964) who describes the Muhlhofer, Ehrenberger, Nesper, and the Swiss Federal Authority samplers. The average efficiency of basket type samplers is reported at about 45 percent. Einstein measured efficiencies with the Nesper sampler from about 90 to 20 percent, depending on the particle size and discharge of the bed-load (Hubbell, 1964). Studies are presently under way at the University of Alberta to estimate hydraulic efficiencies of the small basket sampler under different flow conditions and different sample sizes.

### 3.3. VUV Samplers

The second type of bed-load sampler used was the VUV Hungarian sampler with modifications. An assembly drawing of the half size sampler is shown in FIG. 3-2. The large sampler has a mouth width of 18 inches and height of 5 inches (inside measurements) with total length including tail section of 94 inches. The weight of this sampler is



about two hundred lbs. Views of this sampler can be seen in PLATES 3-5 and 3-6. The half size VUV sampler has a mouth width of 8-1/2 inches and height of 4-1/4 inches (inside measurements) with a total length of 41 inches. The photographs of PLATES 3-7 and 3-8 show the small sampler. The total weight is 95 lbs.

This type of sampler is called a pressure-difference type sampler and is recommended for particles from one to one hundred mm. in diameter. Descriptions of the field use and laboratory calibration of this type of sampler are contained in (Hubbell, 1964). Novak (1957) recommends an over-all field sampling efficiency of 70 percent, with a hydraulic efficiency of 101 percent.

The difference between the large and small VUV samplers, other than the dimensions, is that the small sampler has been recently modified with a spring loaded catch that will keep the rear door open during lowering into the water. The rear door of the large sampler is closed when there is pull on the lifting slings.

#### 3.4. Bed-load Discharge Sampling

All bed-load sampling was carried out at the downstream end of the study reach using the cableway at 12+18 D/S. Truck winches were used in conjunction with a pulley system and traveller in order to position the sampler and raise and lower it. Samples were taken at 10 ft. stations across the width using the left bank tower as station zero. At each sampling location the following data were collected:

Date  
Time  
Sampler Type





Sampler Size  
Mesh Size  
Sample Time  
Total Weight of Sample  
Mean Velocity in Vertical  
Depth  
Weight of Tracer Material  
Size of Largest Particle  
Size of Tracer Material

In some cases the sample was saved for grain size analysis and specific weight tests. The sampling procedure is shown in the photographs of PLATES 3-9 and 3-10. The sampling procedure used was very time-consuming because of the slow line speed of the truck winches, and the difficulties in locking the traveller in a fixed position as well as the hooking up and unhooking of the samplers to the cable traveller. The small basket and the small VUV samplers could only be used at the lower stages because of their limited weight and tendency to drift downstream before coming into contact with the bed. It is more difficult to select sampling times with the smaller samplers, because of the small capacity and the large fluctuation of bed-load discharge.

Some difficulty was also experienced in the handling of the large VUV sampler at higher flows. Because the gate must remain closed on lowering, there was a large amount of drag and the sampler would move downstream. Once on the bed, it required no anchor to hold it in position because of the lower velocities and the gate being open. In order not to doze the material off the bed it was necessary to lift the nose of the sampler with a small winch and separate cable, before lifting the sampler with the power winch and lifting slings. For these reasons the majority of the bed-load discharge sampling was carried out with the large basket sampler. It was assumed that the basket mesh size





would have a small effect on the hydraulic efficiency, with the smaller meshes causing a very slight increase in obstruction. The smallest mesh baskets were used most of the time because of the increased sample efficiency as a result of a smaller loss of fine material.

### 3.5. Equipment Used in the Tracer Study

The following paragraphs describe equipment and methods used in conjunction with the tracer study. In order to use this method one must have a tracer material which is suitably marked, a means of injecting this material into the existing bed-load at a known rate, a means of sampling the bed-load at some point downstream and a means of determining the width of the moving strip of bed-load.

### 3.6. Tracer Material and Preparation

A large quantity of bed material was required for the tracer part of the study. Since material that moves at all stages of flow was desired, it was decided to use the natural bed material excavated from the river bed across the entire width of the river. For this reason the material from the excavation of the volumetric pit below the downstream cableway was used. The cleaner material was transported to the painting site for washing, drying and painting.

The washing of this material was carried out with a small pump and spray nozzle. Material smaller than 1/4 inch sieve size was not used. The material was then laid out on large polythene sheets for drying. After drying, painting consisted of dipping the material, contained in a piece of window screening, into a ten gallon pail, half filled with the paint mixture. Three different paint types were used.



The first was a mixture used by Van Der Giessen (1966):

1/3 gal. Day Glo Paint 202 line

1/3 gal. Methyl-ethyl Ketone (M.E.K.) with 10 per-  
cent by weight Bakelite Vinyl Resin (V.M.C.H.)

5/8 gal. Toluene.

This mixture was used in three different colours: red, yellow and green, all of which were fluorescent Day Glo paints. The most difficult part of the mixing is dissolving the V.M.C.H. into the M.E.K. It must be added very slowly with a great deal of agitation or else it will coagulate. Since this resin solution is the binding agent for the paint it is very important that the full amount of V.M.C.H. is dissolved. This mixture proved satisfactory, with the red and yellow colours best seen under water. After 3,400 ft. of bed movement the tracer material coated with this mixture was easily detected with the paint worn off exposed surfaces but remaining on rough surfaces and in grooves. The application of this mixture proved best if it was allowed to dry in the direct sunlight at temperatures not less than 70°F.

The second mixture was of the type used in line painting on highways. It is thinned with a special thinner and was reduced by about 30 percent. This paint is not fluorescent but is waterproof and abrasion resistant. It was much easier to use this mixture as no special mixing was required, it dried faster and did not require sunlight or a high temperature. The material painted with this mixture was as easy to detect as the fluorescent material and was equal in abrasion resistant qualities. The yellow paint was the only available suitable color.





The third type of paint mixture used was a poly-epoxilene coating. Only the red colour was tried. This type gave the most resistant coating to abrasion and was therefore easy to detect in a sample or lying under water. This mixture was again simpler in that the paint is mixed with equal parts of reactor and the solution may be thinned by up to 20 percent. The only disadvantage noted is the fact that once a mixture is made, it must be used or refrigerated to store.

It was found that washing, drying, and painting the tracer material required the majority of the time and labour available for the study. About one gallon of mixture was required to coat 400 lbs. of bed material for all mixtures. The total amount of tracer material prepared was about seven tons. The approximate cost of paint mixtures was 2.9 cents per lb. of tracer using fluorescent paint, 3.0 cents per lb. of tracer using the poly-epoxilene paint and 0.6 cents per lb. of tracer using the highway paint.

### 3.7. Tracer Injection

The painted bed material was injected into the moving bed-load material at the upstream cableway, 22+03 U/S, in order to determine the bed-load discharge within the study reach. This injection was carried out from the rear of an 11 ft. boat which was held captive to the overhead cable. Half filled sample bags with 70 lbs. of tracer material were lowered to the river bed and dumped by lifting up on tag lines attached to the lower end of the bags.





### 3.8. Sampling of Tracer Material

For the tracer study, concentrations from the bed-load discharge sampling were used. With this method the actual amount caught is not important since the calculations are based on concentration only. Other tracer material was recovered from the bed by personnel wading in the upstream direction at low flows, and picking up and noting the location of each observed tracer particle.

### 3.9. Hydrophone

In order to detect bed movement by acoustic means a model DEA-7 directional crystal transducer was used as a hydrophone. The transducer unit is a lead zirconate crystal motor encapsulated in polyurethane and enclosed in a machined brass housing. This housing was fitted into a cast iron, fish-shaped weight which was cast from the mould of a US-D49 suspended sediment sampler. The casting, hydrophone and hanger weighed approximately 83 lbs. The hydrophone was equipped with 40 feet of waterproof coaxial cable which leads from the top of the casting. The model DEA-7 has a resonant frequency in the region of 30 to 35 kc. Its working pressure is 1,500 p.s.i. and it has a nominal electrical capacity of 0.0065 microfarad.

The coaxial cable leads to a small operational amplifier powered by 9 volt batteries, and fitted with a gain control. The operator can wear the amplifier around his waist and use headphones to listen to the bed movement sounds. The complete hydrophone setup is shown in PLATES 3-11 and 3-12.



In this study the hydrophone was suspended from a B-3 reel and an A frame from the bridge, and a cable car bracket and B-3 reel at the cableways. The total cost of the hydrophone equipment was \$270.00.

### 3.10. Hydrophone Use

The hydrophone observations were carried out at the three cross sections where overhead structures existed. At each point of observation; the station, total depth, depth of hydrophone during listening, and sounds heard, were noted. From these sounds the observer would conclude if there was bed movement or not. These observations were carried out to determine the width of the moving strip of bed-load in conjunction with the tracer study. The observations were also useful in determining the locations for tracer injection, and gave good indications of the stage of flow coinciding with competent conditions at the various cross sections.

No attempt was made at relating the level of sound to a quantitative measure of the bed-load discharge. This has been attempted using a similar type of equipment and was reported by Hubbell (1964).

The very heavy weight of this equipment, which was necessary at high stage, makes handling difficult. This particular equipment created turbulence which resulted in sounds very similar to those resulting from bed particle movement. Because of these unwanted sounds a practiced operator is required to make the observations. After the hydrophone has been in use for a long period of time, the operator will find it difficult to distinguish the sounds of particle movement from other



sounds, and it was found that injecting a few particles of small gravel into the river immediately upstream of the hydrophone was useful in regaining this ability.

### 3.11. Method of Pit Excavation

In order to estimate the bed-load discharge by another means, it was decided to dig a large pit in the river bed at low stage and measure the rate at which this pit filled during stages of active bed movement. The site selected for this pit was immediately downstream of the cableway, from 12+28 D/S to 13+08 D/S. The size planned was 100 feet in width, 90 feet long and about 3 feet deep, giving a volume of 1,000 cubic yards. The site was selected in order to use the cableway and fathometer equipment for periodic sounding of cross sections across the pit, in order to calculate the rate of refilling at different stages of flow.

Excavation was carried out using a 5/8 cubic yard drag bucket working from the center of the river. PLATE 3-13 shows a photograph of this equipment. The majority of the material excavated was cast to the left bank, with the remainder being hauled away by truck. About 20 cubic yards of this material was hauled to the tracer injection site for washing and painting.

The results of bed surveys before and after excavation along with the other pit observations are presented in section 4.10.





### 3.12. Recording Fathometer

Some cross sections on the study reach were obtained using a Ratheon Model DE-119D portable recording fathometer. Where no cableway or bridge exists and it is not possible to wade, this method gives useful survey information. On this study reach a boat could not be used effectively and the fathometer was operated from one bank with the transducer, float mounted, and suspended from a portable overhead cable.

This equipment is a complete echo depth sounder designed to provide detailed records of under water topography in water depths up to 240 feet. The fathometer includes a recorder chassis and a transducer connected by coaxial cable.

With this equipment cross sections were obtained at high flows where normal survey methods were not possible. Up to 250 feet of coaxial cable was used between the transducer and recorder units when working downstream of an overhead structure. At high stages the small transducer floats were not stable resulting in a variable depth reading at a fixed location. This was mainly due to the large surface waves that tipped the float through some angle. For this reason the minimum depth readings were used at each point. Generally, results were reliable and of sufficient accuracy for this type of study.

### 3.13. Velocity Measurements and Equipment

Velocity measurements were required for discharge calculations and were also taken in conjunction with bed-load sampling and competent condition observations. All velocities were obtained with the use of





Gurley current meters, pattern 622. All measurements were taken at the three cross sections where overhead structures existed. From the cableways the equipment was suspended by using a B-3 reel and cable car bracket. From the bridge, a standard bridge frame was used.

It was found necessary to use a minimum of a 30 lb. sounding weight, except for very low flows. With the standard hanger locations for the meter, this limits readings to a distance greater than 0.7 feet from the bed. In order to get readings down to 0.5 feet of the bed and maintain the 30 lb. weight, one meter was specifically rated for this position.

Attempts were made, using a Pigmy Gurley meter, to get measurements within 0.5 feet of the bed. These proved unsuccessful because of the difficulty in wading at high flows and extended wading rods could not be used successfully from the cable cars.

The results of velocity observations are given in section 4.5.

#### 3.14. Bed Material Sampling

Bed material samples were obtained by three methods. In order to assess the bed surface roughness a series of tape and toe samples were taken. These sampling methods are discussed by Wolman (1954). For the tape sample, a 100 foot survey tape is stretched out over the area to be sampled. The stone under each foot mark is picked up. This method is simple on bars and banks but if bed samples are desired in deeper water, toe samples are used. For this method, the observer picks up each particle that lies at the toe of his right foot or some other



suitable but consistent place. In this study several tape and toe samples were taken at each cross section. Since the sieves used were only 3 inches and smaller, sizes reported over 3 inches are intermediate axis. For all material not passing a 3 inch sieve the long axis, the intermediate axis and the short axis were measured. The intermediate axis is very close to the sieve size; the more spherical the stone the closer the agreement. The results of the tape and toe samples along with several photographs are presented in section 4.6.

In order to assess the grain size distribution of the bed material that is available for transport a number of pit samples were taken. For these samples an area is marked out and all the material within this area, to the depth of the largest particle, is excavated as part of the sample. These samples were also taken on bars and on the stream bed at low flows. The pit cannot be excavated under water without the loss of fines, if they are present. These samples were analysed by weight, with sizes over 3 inches reported by intermediate diameter. Grain size distribution curves and photographs of the sampling method are given in section 4.6.

The third type of sample taken is called a photographic grid sample. A grid system with 3 inch squares and over-all size of 24 inches square, is placed over the bed and a vertical photograph is taken. Most of these samples were taken near a pit sample in order that the surface material can be visually compared to the grain size distribution curve obtained from the pit samples. In addition to this regular bed material sampling, several large samples of the material



taken from the excavation at 12+18 D/S were analysed. Also, many of the bed-load samples taken with VUV and Basket samplers were analysed.

Qureshi (1962) and Kellerhals (1963) discuss several of the common sampling methods and point out some of the problems involved in analysing the size distribution of natural bed material.

The locations of all samples are shown in FIG. 4-8. TABLE IV-4 contains all of the sampling results which are discussed in section 4.6.







## CHAPTER IV

### FIELD OBSERVATIONS

#### 4.1. The Study Reach

The reach selected for this study was on the Elbow River at Bragg Creek about thirty miles southwest of Calgary. The reach from 22+00 feet upstream of the Bragg Creek bridge to 12+00 feet downstream was studied in detail. This reach was selected mainly because of the known bed-load movement at relatively low stages. This was reported by Van Der Giessen (1966) from his study of several gravel rivers in Southern Alberta. The study reach was readily accessible and was crossed by a bridge. A cableway already existed at the upstream end of the reach and a second cableway was constructed at the downstream end. These overhead structures were most important in order to use the bed-load discharge samplers, the hydrophone, and the velocity measurement equipment, since a boat could not be used effectively and at most stages it was impossible to wade. FIG. 4-8 shows the reach studied with the locations of the bridge and cableways.

#### 4.2. Hydrologic Data

Above the study reach the Elbow River basin has an area of about 306 square miles. The basin area is outlined in FIG. 4-1 which was taken from a 1:250,000 topographic map. This figure shows that the basin is composed of foothills and mountains with more than half of this area above the 5,000 foot elevation contour.



Water Survey of Canada have a water stage recorder (station 5BJ<sub>4</sub>) within the study reach, located about 4,000 feet below the mouth of Bragg Creek and about 100 feet downstream of the existing bridge. For this station there are fairly reliable discharge records for a period of 30 years. This station has had a self recording gage in operation since 1949 and operates from March to October each year. The long-term mean daily discharge for this period, using 13 years record, is approximately 390 c.f.s. The two year maximum mean daily flow is about 1,850 c.f.s. From the flood frequency curve of FIG. 4-2 the 10 year and 100 year return periods give maximum mean daily flows of 4,300 c.f.s. and 8,500 c.f.s. respectively. Thirty two years of record were used in the construction of FIG. 4-2, and therefore the 100 year flood is only a rough estimate.

The hydrographs of mean daily discharge are plotted in FIGS. 4-3 and 4-4 for several years. The incomplete hydrograph of 1967 is FIG. 4-5. The flow duration curve of FIG. 4-6 is plotted using mean daily discharges vs. the number of days per year at which a flow was equalled or exceeded. This curve was obtained from all of the mean daily discharges reported from May 1945 to October 1964. This period covers about 245 days each year between March 1949 and October 1965 and only 1 May to 30 July from 1945 to 1948. Only the last sixteen years were used for the over 500 c.f.s. to 1,000 c.f.s. bracket. Also plotted is a curve for 1967 which is taken from the incomplete hydrograph FIG. 4-5. The average flow duration curve is used in section 5.5.2 to estimate the annual bed-load discharge of the Elbow River at Bragg Creek.



The rating curve for station 5BJ<sub>4</sub> is not stable and the curves used since March 1965 are shown in FIG. 4-7. Curve number nine was used in this study prior to the flood of 30 May 1967. A new curve was constructed from discharge measurements taken after the 30 May flood. These discharge measurements are given in TABLE IV-1. The large change in the rating curve is the result of the shift of a bar which was located upstream of the bridge at 1+00 U/S to 0+50 D/S prior to the flood and was replaced by a bar from 0+50 U/S to 2+75 D/S during the June flood recession. The shift in position of this bar is observed in the mosaics of the study reach, PLATES 4-1 and 4-2, which are taken from air photographs taken on 26 May 1967 and 22 June 1967 respectively.

#### 4.3. Channel Geometry

The river trace of FIG. 4-8 shows the location of the nineteen cross sections that were surveyed in order to define the channel geometry. The cross sections are designated by the distance from the upstream side of the bridge. Chainages are given in feet and taken along the right bank. The cross sections from 22+03 U/S to 1+24 U/S are shown in FIG. 4-10 and those from 0+18 D/S to 12+18 D/S are shown in FIG. 4-11. These cross sections show the bed and bank profile from surveys carried out during the period 25 May to 15 June 1967. In most cases the cross sections were resurveyed on the 10th and 11th of August, and the new bed profiles are shown. Water surface elevations from longitudinal surveyed profiles are also shown for the high water line of 30 May and a selected reference low stage of 410 c.f.s. on 10 August. A discharge of 15,000 c.f.s. has been selected as a conservative estimate of the flow at high water, which peaked at about 11:00 p.m. on 30 May.





TABLE IV-1

DISCHARGE MEASUREMENTS - ELBOW RIVER - 1967,  
STATION 5BJ4

	Day	Time	Mean Gage at Bridge ft.	Discharge in c.f.s.	Location
1	31 May	1145	6.65	8006	Bridge
2	1 June	1300	5.68	3928	Bridge
3	2 June	0930	5.30	2993	Bridge
4	2 June	1030	5.34	3008	Bridge
5	5 June	1200	4.87	1635	U/S Cable
6	6 June	0830	4.82	1596	U/S Cable
7	6 June	1030	4.82	1660	Bridge
8	7 June	1200	4.80	1629	U/S Cable
9	8 June	1200	4.79	1665	D/S Cable
10	14 June	1300	4.52	1150	U/S Cable
11	17 June	2000	4.84	1751	D/S Cable
12	19 June	1300	4.88	1733	U/S Cable
13	20 June	1500	4.78	1557	U/S Cable
14	22 June	1000	4.69	1431	D/S Cable
15	26 June	1000	4.43	1076	U/S Cable
16	27 June	1100	4.50	1297	D/S Cable
17	30 June	1200	4.29	992	Bridge
18	4 July	1200	4.23	883	U/S Cable
19	7 July	1400	4.05	715	U/S Cable
20	11 July	1400	3.91	562	U/S Cable
21	10 Aug.	1100	3.67	410	D/S Cable





Several methods were used in an attempt to extend the new rating curve of FIG. 4-7. The maximum discharge measured was 8,006 c.f.s. at a mean gage height of 6.65 ft. The gage height at high water was 8.0 ft. after the effect of surging in the recorder well was taken into account. A method based on the Chezy formula, in which the square root of the slope times the roughness coefficient is assumed constant, gives a maximum discharge of 12,500 c.f.s. from values of A and R taken for the cross section as surveyed at a flow of 8,006 c.f.s. with a gage height of 8.0 ft. The slope area method uses the Manning equation and gives a slightly higher estimate of 13,000 c.f.s. since R in this formula is to the  $2/3$  power, whereas it is to the  $1/2$  power in the Chezy formula.

The slope of the total energy line at high water was not significantly different than at measured discharges and is discussed in section 4.4. Therefore, the assumption of constant slope seems reasonable. The assumption of a constant Manning's n or Chezy's C value does not fit the observed data and is not reasonable for a mobile bed river with an irregular channel. For this reason, the estimates by these methods are probably low.

Another common method of extending rating curves, assumes that the curve is parabolic with an equation in the form  $Q = k(g.h.-a)^b$ . The term  $(g.h.-a)$  reduces actual gage heights to a gage height above that corresponding to zero flow. Different values of "a" can be selected and the values of Q versus  $(g.h.-a)$  plotted on log paper. The "a" value giving the best fit straight line is then used to extend the curve. It was found that values of "a" equal to 1 or 2, gives the best fit lines.



Previous rating curves at this cross section indicate that the value should be about 2. A value of  $a = 1$  gives  $Q_{\max} = 19,500$  c.f.s. and  $a = 2$  gives 17,500 c.f.s. From the above discussion an arbitrary value of maximum instantaneous discharge of 15,000 c.f.s. is assumed to correspond to high water conditions.

Values of  $Q$ ,  $A$ ,  $V_m$ ,  $b_w$  and  $A/b_w$  are tabulated in TABLE IV-2 for each cross section at high water stage, surveyed stages, and low water reference stage. Included in this table are the results of the discharge measurements at 22+03 U/S, 0+18 D/S and 12+18 D/S.

All elevations refer to an assumed datum of 100.00 feet at BM No. 1 which is located on the right bank, 36 feet upstream of the stage recorder shelter, below the bridge.

FIG. 4-12 shows curves of  $A$  versus  $Q$  for the three cross sections where discharge measurements were taken. The average curve is taken from the average values of all nineteen cross sections. Similarly, FIGS. 4-13, 4-14 and 4-15 show curves of surface breadth versus discharge,  $A/b_w$  versus discharge and mean velocity versus discharge for the same three cross sections and the average curves of all cross sections. It must be pointed out that these average curves include cross sections 19+00 U/S to 9+00 U/S where the flow is in two separate channels at high stages.

All of the cross sections have been marked with semi-permanent reference points and have been tied into a base line for future surveys. A set of photographs, one from each bank, has been taken to enable the cross sections to be located with reasonable accuracy.





TABLE IV-2  
CHANNEL GEOMETRY

Number	Cross Section	Date	Water Elevation Above Datum ft.	Discharge Q c.f.s.	Area A ft. <sup>2</sup>	Mean Velocity V <sub>m</sub> f.p.s.	Water Surface Width b <sub>w</sub> ft.	Depth A/b <sub>w</sub> ft.	Remarks
1	22+03 U/S	23 May		1,080	196	5.51	104	1.88	Discharge Measurement
		29 May	110.23 RB*	950	243	3.91	109	2.23	Survey
		30 May	114.4 RB	15,000	808	18.55	163	4.95	High Water
		5 June		1,635	286	5.72	105	2.72	Discharge Measurement
		6 June		1,600	276	5.79	100	2.76	" "
		14 June		1,150	244	4.70	105	2.32	" "
		19 June		1,730	288	6.01	100	2.88	" "
		20 June		1,557	268	5.81	106	2.52	" "
		22 June		1,430	269	5.32	106	2.54	" "
		26 June		1,076	239	4.50	104	2.30	" "
		4 July		883	201	4.40	104	1.93	" "
		7 July		715	184	3.87	102	1.80	" "
		11 July		562	157	3.58	99	1.59	" "
		10 Aug.	108.91 RB	410	140	2.93	76	1.84	Survey
2	21+00 U/S	29 May	109.99 RB	950	236	4.02	166	1.42	Survey
		30 May	114.1 RB	15,000	1,053	14.22	292	3.61	High Water
		10 Aug.	108.38 RB	410	126	3.26	72	1.75	Survey
3	19+00 U/S	30 May	113.0 RB	15,000	1,489	10.00	340	4.38	High Water
		14 June	108.44 RB	1,200	256	4.69	134	1.91	Survey
		10 Aug.	107.52 RB	410	139	2.95	84	1.56	"
4	17+00 U/S	30 May	111.9 RB	15,000	1,243	12.07	380	3.28	High Water
		14 June	107.59 RB	1,200	217	5.53	125	1.74	Survey
		10 Aug.	106.11 RB	410	103	3.98	76	1.40	"
5	14+75 U/S	30 May	110.6 RB	15,000	1,344	11.15	320	4.20	High Water
		14 June	104.45 RB	1,200	267	4.50	120	2.22	Survey
		10 Aug.	103.26 RB	410	110	3.73	59	1.87	"
6	12+35 U/S	30 May	106.8 RB	15,000	1,085	13.80	296	3.66	High Water
		14 June	103.33 RB	1,200	251	4.78	127	1.98	Survey
		10 Aug.	102.00 RB	410	121	3.39	84	1.44	"
7	11+07 U/S	30 May	106.0 RB	15,000	920	16.30	212	4.34	High Water
		14 June	102.23 RB	1,200	234	5.13	136	1.72	Survey
		10 Aug.	101.30 RB	410	97	4.22	103	.92	"
8	9+00 U/S	30 May	104.6 RB	15,000	909	6.51	236	3.85	High Water
		15 June	101.38 RB	1,300	227	5.72	148	1.53	Survey
		10 Aug.	100.00 RB	410	101	4.06	80	1.26	"
9	3+00 U/S	25 May	94.90 RB	900	215	4.18	130	1.65	Survey
		30 May	99.0 RB	15,000	832	18.00	154	5.40	High Water
		10 Aug.	93.06 RB	410	172	2.38	93	1.85	Survey
10	1+24 U/S	30 May	98.2 RB	15,000	1,183	12.68	182	6.50	High Water
		7 June	93.14 RB	1,650	232	7.11	153	1.51	Survey
		10 Aug.	92.18 RB	410	146	2.81	133	1.10	"
11	0+18 O/S	30 May	97.6 RB	15,000	1,010	14.83	175	5.77	High Water
		31 May		8,006	706	10.68	144	4.90	Discharge Measurement
		1 June		3,928	455	8.65	120	3.79	" "
		2 June		3,010	354	8.50	118	3.00	" "
		6 June	92.58 RB	1,660	265	6.26	135	1.96	Survey
		30 June		992	222	4.46	116	1.91	Discharge Measurement
		10 Aug.	91.78 RB	410	179	2.29	103	1.74	Survey
12	1+00 O/S	4 May	91.2 RB	109	77	1.40	62	1.24	Discharge Measurement
		30 May	96.2 RB	15,000	834	18.00	171	4.87	High Water
		7 June	92.93 RB	1,650	319	5.18	148	2.16	Survey
		10 Aug.	92.10 RB	410	193	2.12	127	1.52	"
13	3+00 O/S	25 May	90.75 LB	900	217	4.15	156	1.39	Survey
		30 May	95.3 LB	15,000	881	17.00	180	4.90	High Water
		10 Aug.	89.00 LB	410	105	3.90	91	1.15	Survey
14	3+13 O/S	30 May	95.2 LB	15,000	875	17.15	165	5.30	High Water
		9 June	90.80 LB	1,600	246	6.50	157	1.57	Survey
		10 Aug.	90.20 LB	410	129	3.18	82	1.57	"
15	5+00 O/S	30 May	94.0 LB	15,000	938	16.00	190	4.95	High Water
		9 June	89.40 LB	1,600	267	6.00	160	1.67	Survey
		10 Aug.	87.34 LB	410	94	4.36	91	1.03	"
16	7+00 O/S	30 May	92.1 LB	15,000	798	18.75	188	4.25	High Water
		9 June	86.45 LB	1,600	236	6.78	99	2.62	Survey
		10 Aug.	85.85 LB	410	113	3.63	59	1.91	"
17	8+85 O/S	30 May	90.8 LB	15,000	894	16.78	203	4.40	High Water
		9 June	86.50 LB	1,600	242	6.61	113	2.14	Survey
		10 Aug.	85.11 LB	410	121	3.39	87	1.39	"
18	11+08 O/S	30 May	89.6 LB	15,000	1,070	14.00	248	4.32	High Water
		9 June	85.30 LB	1,600	276	5.80	137	2.01	Survey
		10 Aug.	83.90 LB	410	156	2.62	116	1.34	"
19	12+18 O/S	26 May	83.98 LB	800	204	3.90	96	2.14	Survey
		30 May	89.1 LB	15,000	1,150	13.00	174	6.60	High Water
		7 June		1,630	296	5.52	104	2.85	Discharge Measurement
		8 June		1,665	304	5.48	104	2.92	" "
		9 June	86.03 LB	1,670	320	5.21	127	2.52	Survey
		17 June		1,751	302	5.81	104	2.90	Discharge Measurement
		22 June		1,496	246	6.07	102	2.41	" "
		27 June		1,297	234	5.55	103	2.28	" "
		10 Aug.	83.22 LB	410	83	4.95	89	.93	Survey

\* RB - Right Bank  
LB - Left Bank.





#### 4.4. Slope Observations

One of the major difficulties in a study of this type is the choice of slope to be used in the empirical relations. Most of the relations given in section 2.3 contain slope and are reasonably sensitive to the value used. Slope measurements in the field vary greatly and are dependent on the length of the reach observed, the steadiness and uniformity of the flow, as well as the method of observation. In order to have a continuous record of slope between two stations a water stage recorder was installed just above the upstream cableway at 23+35 U/S. These records give fairly reliable water surface slopes over a length of 2,425 feet. The effect of surging in the recorder wells at high discharges is due to surface waves and contributes to the observation difficulties. PLATES 4-3 and 4-4 show the location of the gage and water surfaces at a flow of about 7,000 c.f.s. For this length, the slopes calculated vary from a maximum of  $7.50 \times 10^{-3}$  on a rising stage to a minimum value of  $7.26 \times 10^{-3}$ , on a falling stage. An average value of  $7.35 \times 10^{-3}$  is the result of the slopes taken at noon on each day during May, June and July.

Longitudinal profiles of the water surface were surveyed at several stages of flow. In some cases the elevation of the water was taken at both the left and right banks at one hundred foot stations. At low flows a bed shot was also attempted at the thalweg. In order to obtain slopes over a short time interval, for unsteady flow conditions, some profiles were taken along one bank only, working from upstream to downstream. FIG. 4-16 shows a few of the water surface profiles at



various stages of flow. This figure also shows the lowest observed bed elevations from longitudinal surveys and the cross section surveys of June. Bed elevations can vary by 2 ft. within a very short length along the thalweg, because of the large bed material that is present and the difficulty in knowing where to place the rod. It was found that the water was super-elevated by large amounts at high flows. At some sections water levels varied by 3 ft. from one bank to the other. The large differences in levels is not all due to the curvature of flow but partly due to the transverse flow across large submerged bars. It was also observed that at certain cross sections, at high flood stages, the elevation of the water surface at the thalweg could be 18 inches higher than either bank. This effect is thought due to a sudden expansion in the flow section.

Slopes from the total drop between 22+03 U/S to 12+18 D/S from FIG. 4-16 are  $7.40 \times 10^{-3}$  at H.W.,  $7.65 \times 10^{-3}$  at 11,000 c.f.s.,  $7.45 \times 10^{-3}$  at 1,470 c.f.s.,  $7.48 \times 10^{-3}$  at 410 c.f.s. and  $8.25 \times 10^{-3}$  for the bed profile. If best fit straight lines are drawn by eye, the resulting slopes range from 7.50 to 8.50 ft. per thousand. For a discharge of 15,000 c.f.s. the velocity head varies from 1.5 ft. to 5.5 ft. without a correction factor applied. At low reference stage the range of  $V_m^2/2g$  is from 0.07 ft. to 0.38 ft. The variability of the velocity head caused by a series of constrictions and expansions, only makes the choice of a slope more difficult. A slope of  $7.45 \times 10^{-3}$  seems to be a good estimate for the entire reach. Van Der Giessen (1966) used  $S = 7.05 \times 10^{-3}$  in the reach about 1 mile upstream of the present study.





#### 4.5. Velocity Observations

The velocity distribution with respect to depth and distance across a section are represented in FIGS. 4-17, 4-18 and 4-19 for the three cross sections where routine observations were carried out. The distribution is shown at a few stages at each section. The arrows indicate actual observations within the vertical. The closest bed observations were at 6 inches from the bed. The observed values in FIGS. 4-17 and 4-18 are mainly from routine discharge measurements while those of FIG. 4-19 correspond to times at which bed-load discharge samples were taken.

In a gravel river of this type, with a  $d/D$  ratio generally less than 50, fluctuations of velocities near the bed are very obvious. A typical set of readings at the same depth and location are given in TABLE IV-3.

TABLE IV-3  
VELOCITY FLUCTUATIONS

June 1, 1967 - Cross Section 12+18 D/S - Station 60 ft.					
Depth (ft.)	Depth of Observation (ft.)	Revolutions	Time (sec.)	Velocity at Point (f.p.s.)	Average Velocity at Point
2.8	1.6	500	141.3	7.94	7.94
	1.6	200	56.1	8.00	8.25
	1.6	200	54.1	8.30	
	1.6	200	54.9	8.19	
	1.6	200	50.8	8.84	
	1.6	20	4.8	9.33	
	1.6	20	5.2	8.64	8.66
	1.6	20	5.6	8.02	
	1.6	20	5.4	8.32	
	1.6	20	5.0	8.98	





TABLE IV-3 indicates a maximum range of 1.31 f.p.s. for velocities determined from short counts and a range of 0.90 f.p.s. from the long counts. These time fluctuations were largest at points near the bed, while surface velocities at 0.2 d remained relatively constant. For this reason, long counts were used throughout the study hoping to average out some of these time fluctuations. Most of the velocities used in the construction of FIGS. 4-17 to 4-19 were average figures based on two long counts at each depth.

#### 4.6. Analysis of Bed Material

##### 4.6.1. Bed Material Samples

The types of bed material samples taken are discussed in section 3.14. The results of the size analysis of all samples taken are given in TABLE IV-4 as percent by weight or number greater than selected sizes. The sizes from 1/4 to 3 inches are actual sieve sizes, while those over 3 inches were measured by the intermediate axis of the particle. The table gives the approximate location of each sample as a chainage from the bridge while FIG. 4-8 shows the detailed location.

The size distribution curves for the total of each sample type are shown in FIG. 4-20. Tape and toe samples are plotted by number with the others plotted by weight. The points plotted can be fitted with straight lines indicating logarithmic normal probability distribution. FIG. 4-21 shows several of the tape samples that were analysed by both weight and number. If curve one on FIG. 4-20 was plotted by weight it would fall slightly above curve number four on FIG. 4-20. Curve number



TABLE IV-4  
8EO MATERIAL SAMPLING

Sample Number	Type of Sample	Sample Location	Analysis	Percent Retained By										
				8	6	5	4	3	2	1-1/2	1	3/4	7/16	1/4
				Size in Inches										
1	Pit	21+00 U/S	Weight					11.6	22.7	40.4	59.0	67.3	82.5	89.9
2	Pit	12+35 U/S	Weight		5.3	11.9	20.9	26.8	47.8	56.5	63.8	67.7	74.2	79.2
3	Pit	8+15 U/S	Weight		11.5	39.6	57.0	67.4	72.5	75.5	79.6	81.1	84.6	85.5
4	Pit	0+35 U/S	Weight					2.9	18.9	30.3	50.8	64.7	82.4	90.1
5	Pit	1+45 O/S	Weight						1.7	7.9	29.5	43.0	69.4	79.4
6	Pit	3+13 O/S	Weight						5.8	13.0	32.4	46.7	71.9	82.6
7	Pit	7+00 O/S	Weight					3.0	13.5	28.4	49.5	62.8	82.1	89.5
8	Pit	8+85 O/S	Weight					5.4	7.0	19.5	43.8	57.9	84.5	91.4
9	Pit	11+00 O/S	Weight					3.3	20.1	35.6	60.0	74.7	92.7	95.6
10	Pit	5+00 O/S	Weight					16.4	40.7	57.1	74.3	84.1	96.8	99.2
11	Pit	11+75 O/S	Weight					2.8	11.0	19.9	41.1	55.2	78.1	86.9
12	Tape	20+00 to 21+00 U/S	Weight				33.6	59.6	70.0	82.7	94.5	95.5	100.0	
13	Tape	20+00 to 21+00 U/S	Weight			43.3	62.3	71.2	89.0	95.4	98.8	99.4	99.9	100.0
			Number			3.0	7.0	11.0	28.0	44.0	60.0	75.0	93.0	100.0
14	Tape	10+50 to 11+50 O/S	Weight			13.5	40.1	40.1	71.2	87.4	98.5	99.5	99.9	100.0
			Number			1.0	3.0	3.0	19.0	37.0	77.0	88.0	99.0	100.0
15	Tape	8+50 to 9+50 O/S	Weight				16.4	49.8	77.4	92.0	97.6	99.6	99.9	100.0
			Number				2.0	10.0	27.0	51.0	75.0	91.0	98.0	100.0
16	Tape	6+50 to 7+50 O/S	Weight					11.0	48.5	70.3	96.6	98.9	99.8	100.0
			Number					1.0	11.0	26.0	70.0	81.0	93.0	100.0
17	Tape	10+50 to 11+50 O/S	Number					3.0	21.0	35.0	67.0	78.0	98.0	100.0
18	Tape	10+50 to 11+50 O/S	Number					5.0	21.0	31.0	59.0	77.0	100.0	
19	Tape	5+00 to 6+00 O/S	Number					5.1	21.4	42.8	71.5	87.8	100.0	
20	Tape	5+00 to 6+00 O/S	Number					1.0	10.0	28.0	69.0	86.0	97.0	100.0
21	Toe	21+00 to 22+00 U/S	Number					9.0	27.0	53.0	82.0	88.0	99.0	100.0
22	Toe	21+00 to 22+00 U/S	Number					17.0	44.0	61.0	82.0	89.0	98.0	100.0
23	Toe	19+50 to 20+50 U/S	Number	1.0	4.0	10.0	25.0	32.0	69.0	80.0	91.0	94.0	97.0	100.0
24	Tape	20+00 to 21+00 U/S	Number	9.0	15.0	20.0	28.0	34.0	59.0	69.0	87.0	93.0	100.0	
25	Tape	20+00 to 21+00 U/S	Number	9.0	34.0	42.0	54.0	59.0	82.0	91.0	96.0	99.0	100.0	
26	Tape	19+00 to 20+00 U/S	Number	4.0	17.0	25.0	31.0	35.0	52.0	66.0	76.0	93.0	100.0	
27	Toe	16+97 to 17+03 U/S	Number					6.0	28.0	44.0	83.0	98.0	100.0	
28	Tape	16+50 to 17+50 U/S	Number					1.0	8.0	28.0	72.0	92.0	100.0	
29	Toe	14+72 to 14+75 U/S	Number						4.0	9.0	49.0	75.0	100.0	
30	Tape	14+55 to 15+55 U/S	Number	1.0	14.0	15.0	20.0	24.0	39.0	47.0	76.0	90.0	100.0	
31	Tape	12+60 to 13+60 U/S	Number	1.0	11.0	24.0	42.0	53.0	66.0	74.0	89.0	100.0		
32	Tape	10+58 to 11+58 U/S	Number	2.0	2.0	4.0	9.0	13.0	41.0	61.0	82.0	98.0	100.0	
33	Toe	11+07 U/S	Number	4.0	12.0	28.0	42.0	68.0	82.0	92.0	98.0	100.0		
34	Tape	8+66 to 9+66 U/S	Number	5.0	12.0	19.0	27.0	33.0	52.0	74.0	90.0	100.0		
35	Toe	9+00 U/S	Number	4.0	12.0	16.0	25.0	34.0	53.0	74.0	90.0	100.0		
36	Toe	16+50 to 17+50 U/S	Number	2.0	10.0	30.0	45.0	66.0	87.0	96.0	100.0			
37	Tape	14+25 to 15+25 U/S	Number	4.0	12.0	19.0	34.0	53.0	81.0	94.0	100.0			
38	Tape	14+25 to 15+25 U/S	Number	3.0	9.0	13.0	20.0	27.0	51.0	70.0	92.0	100.0		
39	Tape	11+85 to 12+85 U/S	Number	3.0	7.0	11.0	21.0	28.0	55.0	75.0	90.0	97.0	100.0	
40	Toe	11+85 to 12+85 U/S	Number	3.2	10.9	19.5	32.6	39.1	67.4	80.4	93.5	96.7	100.0	
41	Tape	10+57 to 11+57 U/S	Number		1.0	4.0	11.0	21.0	52.0	72.0	95.0	100.0		
42	Toe	10+57 to 11+57 U/S	Number	1.0	9.0	19.0	29.0	46.0	80.0	93.0	97.0	100.0		
43	Tape	8+50 to 9+50 U/S	Number		5.0	7.0	22.0	35.0	69.0	86.0	100.0			
44	Toe	8+50 to 9+50 U/S	Number	2.0	14.0	19.0	37.0	54.0	79.0	92.0	100.0			
45	Tape	11+85 to 12+85 U/S	Number	3.0	5.0	9.0	15.0	24.0	62.0	84.0	100.0			
46	Tape	8+50 to 9+50 U/S	Number	5.0	17.0	23.0	32.0	45.0	68.0	83.0	99.0	100.0		
47	Tape	2+75 to 3+75 U/S	Number	2.0	6.0	8.0	11.0	16.0	33.0	60.0	95.0	100.0		
48	Tape	1+00 to 1+50 U/S	Number	1.0	3.0	9.0	20.0	30.0	60.0	85.0	98.0	100.0		
49	Tape	0+50 U/S to 0+50 O/S	Number					2.0	3.9	11.8	60.8	82.4	100.0	
50	Tape	1+05 to 2+05 O/S	Number						4.0	8.0	43.0	77.0	99.0	100.0
51	Toe	3+13 to 3+16 O/S	Number					3.0	31.0	48.0	79.0	94.0	100.0	
52	Toe	5+00 to 5+03 O/S	Number					3.0	29.0	61.0	87.0	97.0	100.0	
53	Toe	7+00 to 7+03 O/S	Number						14.6	47.9	90.6	96.9	100.0	
54	Toe	8+82 to 8+91 O/S	Number			1.0	5.0	16.0	45.4	66.6	79.7	86.8	100.0	
55	Toe	11+00 to 11+03 O/S	Number		1.0	2.0	10.1	17.3	36.7	58.1	86.7	94.9	100.0	
56	Toe	12+15 to 12+21 O/S	Number		2.0	5.0	11.6	16.5	49.5	70.9	91.3	99.0	100.0	
57	Excavation	12+18 O/S	Weight			11.3	16.2	45.0	74.4	87.9	97.2	99.1	99.9	100.0
			Number			0.6	1.1	5.4	17.0	29.4	54.0	67.2	85.6	100.0
58	Excavation	12+18 O/S	Weight	8.9	21.0	33.4	46.1	56.9	75.4	84.8	94.4	97.2	99.5	100.0
59	Excavation	12+18 O/S	Weight		19.3	24.3	30.5	38.7	53.2	67.5	86.0	93.0	98.8	100.0
60	Excavation	12+18 O/S	Weight						20.3	45.8	74.6	85.5	96.8	100.0
61	Excavation	12+18 O/S	Weight		14.7	39.7	58.8	66.7	74.2	82.3	93.4	96.7	100.0	
62	Bed-load	22+03 U/S	Weight						2.6	14.0	46.5	63.9	88.8	98.0
			Number						0.04	0.4	3.7	8.4	28.7	68.2
63	Bed-load	12+18 O/S	Weight						22.4	32.2	43.5	54.4	73.5	84.5
64	Bed-load	12+18 O/S	Weight					3.8	14.5	27.2	66.5	78.5	95.5	100.0
65	Bed-load	12+18 O/S	Weight					5.0	20.0	34.1	63.0	79.8	98.6	100.0
66	Bed-load	12+18 O/S	Weight					10.9	28.8	43.4	72.3	86.0	98.1	100.0
67	Bed-load	12+18 O/S	Weight					6.6	26.2	41.5	65.5	76.8	92.5	100.0
68	Bed-load	12+18 O/S	Weight						1.9	4.9	15.0	28.2	63.5	87.5

\* Basket size.

\*\* Basket mesh size in inches.





one of FIG. 4-20 is an analysis of surface material only, and therefore should be an indicator of grain size roughness of the bed at flows below competent conditions. If curve number one by weight is compared with curve three, it is obvious that the bed surface is paved with a portion of the larger material at the sampled stage.

The material used for the tracer injection (curve number four) is generally larger than the material sampled as bed-load or that taken from the pit samples. The reasons for this are; that most of the fines were washed out of the excavated material during dragging, much of this material was taken from the bed beneath the thalweg, a greater portion of large material was taken from the stock piles for painting, and additional fines were lost during the washing before painting.

FIG. 4-20 shows a close agreement of curves two and three. This is a result of the pit samples being obtained at a low stage with most of this material being deposited during and subsequent to the stage at which the bed-load samples were taken. The difference in distribution is a result of fines passing through the bed-load samplers and the limited size that they are capable of trapping. This affect is represented in FIG. 4-22 which shows curve three of FIG. 4-20 and curve number two as separate plots for the basket and VUV bed-load samples. When the bed-load discharge is calculated, the loss of fines through the basket sampler is taken into account by assuming that the loss is included in the over-all reported sampler efficiency. The samples indicate that the 1/4 inch basket mesh passes about 13% of the sample weight, at the stage at which the sampling was carried out.





Several photographic grid samples were taken along the study reach. The size of the grid is two feet square with a smaller grid system of 3 inches square. These photographs were taken on June 29 with the survey stake indicating the D/S direction. PLATE 4-5 is a photograph taken at the location of pit sample number 1. The photograph of PLATE 4-6 is at the location of sample number 2, PLATE 4-7 at the location of sample number 4, and PLATE 4-8 at the location of sample number 5. FIG. 4-23 gives the grain size distribution curves of these pit samples, for comparison with the photographs. The photographs give a good indication of the size range of the surface material of the bed and bars with the sieve curves from the pit samples giving the distribution of the material to some depth.

PLATE 4-9 shows tape sample number 15 being collected, along a line on top of the bar between 8+50 D/S and 9+50 D/S. PLATE 4-10 is a photograph of the grid at a position just left of this line at 9+00 D/S. Pit sample number 8 was taken just right of this line about 15 feet U/S of the grid photograph. FIG. 4-24 gives the grain size distribution of pit sample number 8 and tape sample number 15 for comparison with the photograph of PLATE 4-10.

#### 4.6.2. Recovery of Tracer Material

Tracer material was recovered from bars and the stream bed D/S of the injection point on September 20 and 21. All particles visible to the observers between 20+00 U/S and 20+00 D/S were picked up. From the hydrograph of FIG. 4-5 it is observed that from the time of



injection, the discharge decreased to about 900 c.f.s. within a twelve day period. From section 4.7 and 4.9 it is concluded that very little movement occurs below this discharge. During July, August, and September the hydrograph continued to drop and therefore the locations of the recovered particles are probably those which they attained sometime during this twelve day period immediately after injection. The flow on September 20 was estimated at 250 c.f.s. from the gage height of 3.40 feet. The locations of large concentrations of tracer material were noted, and the material was analysed by grouping it into three lengths in order to assess the dependence of the distance travelled on the size and shape of the material. FIG. 4-25 gives the grain size distribution curves based on these three groups 20+00 U/S to 2+00 U/S, 2+00 U/S to 12+18 D/S, and 12+18 D/S to 20+00 D/S. A large amount of tracer material was present on the bed between the injection point and 20+00 U/S, but was not recovered.

From FIG. 4-25 a few general observations can be made. The majority of the injected material smaller than  $D_{50}$  by weight (3" from FIG. 4-20, curve 4), passed through the study reach during a relatively short period after injection. Very little of the material larger than this size travelled further than 3,400 feet and most of the material in the three to five inch intermediate diameter range travelled an average distance of about 2,000 feet. The small material recovered within the 3,400 feet downstream of the injection point was probably stopped by the sheltering effect of larger material.





#### 4.6.3. Shape Analysis of Bed Material

In order to assess the effect of material shape on bed-load movement, the three axes of particles in several samples were measured. The shape ratios of the material larger than three inch intermediate axis for two bed material samples, are plotted in FIG. 4-26, in the form of a Zingg's classification chart. One group of points is from a tape sample, and therefore includes only surface material, while the second group is from the excavation at 12+18 D/S, includes the material at depth, and was the material used for tracer injection.

An immediate observation from this figure is that more than 90 percent of the material has  $b/a + c/b$  greater than one. The most obvious difference in the two samples is the smaller percentage of particles within the spheroids category for the tape sample. This indicates that the more spherical particles for a given intermediate axis are less stable on the bed.

For a further analysis of the effect of shape, the size of particles of several bed-load samples were measured. In order to acquire a reasonable number of particles for analysis it was necessary to include some material less than three inch but greater than two inch intermediate axis. The ratios of the axis lengths of this material are plotted in FIG. 4-27. This material is grouped for plotting into tracer and non-tracer bed-load material, the difference being that an approximate rate of travel is known for the tracer portion. This figure compared to FIG. 4-26 indicates a much higher percentage of spheroids





and very few particles within the blades category. While the tracer material that was injected indicated 24 percent of the particles within the spheroid category, that which was sampled as bed-load indicates nearly 60 percent. This material is known to have travelled the 3,400 feet from the injection point within a four day period and is discussed in section 4.8. Nearly 50 percent of the non-tracer material also falls within the spheroid class. These observations indicate that the more spherical portion of the bed material made up most of the bed-load at the sampled stages which were from 1,250 to 3,850 c.f.s. This would indicate that the bed-load movement is primarily by rolling, as opposed to sliding. A detailed analysis of each tracer particle and its travel time indicates that the more spherical particles have higher average velocities over the 3,400 feet for a given intermediate size.

#### 4.6.4. Specific Gravity of Bed Material

Specific gravity tests were run on four large samples of bed material that were sampled as bed-load. The samples were taken from a common pile of material that was obtained throughout the sampling period, and represent material that moved at all sampled stages. Tests were conducted in accordance with American Standards A 37.5 - 1964 for bulk specific gravities at both oven dry and saturated surface dry conditions. The average values of the bulk specific gravity at these conditions were 2.63 and 2.64 respectively. In the calculations of CHAPTER V a value of  $s_s = 2.64$  is used in all cases.



#### 4.7. Bed-load Discharge Sampling

TABLE IV-5 gives the observations of all bed-load measurements obtained by the direct sampling apparatus. Only measurements that are considered reliable are tabulated while those in which technical difficulties were involved or are known to be unreliable are neglected. The missing data include cases where the sampler turned oblique to the flow, material was dozed off the bed, the sampler rested on a large boulder above the bed, part of the sample was lost during recovery, the sampler was full when recovered or the sampler was obstructed by debris floating under the surface. Obviously, some of these factors could also be present within the existing data but were not observed.

Column 4 indicates the distances from the left bank tower at which the samples were taken. The corresponding water edges at cross section 12+18 D/S are about 35 ft. and 135 ft. for the main channel during the sampling period. Column 7 gives the time from when the basket sampler touched the bed to the time it was lifted from the bed. For the large VUV sampler it is from the time the rear gate opened to the time it was closed by lifting, and for the small VUV sampler it is from the time it contacts the bed to the time at which the gate is closed by lifting. Column 8 gives the actual weight of the material taken from the bed-load sampler. This material often included a large amount of debris, such as small water saturated wood chips and roots. Although the volume of this material was usually significant, the total weight is effected very little if it is disregarded. In the case of the VUV sampler, it is necessary to pour water into the sampler mouth with





TABLE IV-5  
8EO-LOAD SAMPLING

(1) Sample Number	(2) Date  1967	(3) Time	(4) Station  ft.	(5) Sampler Type	(6) Basket Mesh  ins.	(7) Sample Time  min.	(8) Sample Weight  lbs.	(9) Unit Bed-load Discharge  lb/ft.min.	(10) Depth  ft.	(11) Mean Velocity in Vertical f.p.s.	(12) Unit Discharge  c.f.s/ft.	(13) Bridge Gage  ft.	(14) Mean Gage  ft.	(15) Mean Discharge  c.f.s.	(16) Colored Rock Concen- tration x 10 <sup>3</sup>	(17) b Axis of Largest Particle  ins.
1	1 June	1500	60	Large Basket	3/4	10	330	16.5	2.6	8.01	20.8	5.65	5.65	3,850		7.3
2	2 June	1030	40	" "	"	5			1.9	4.59	8.7	5.32				
3		1100	50	" "	"	5	43.6	4.40	2.2	6.34	13.9	5.32				2.8
4		1130	60	" "	"	5	296	29.6	1.9	7.60	14.4	5.31				3.0
5		1145	60	" "	"	4	183	22.9	1.9	7.60	14.4	5.31				3.8
6		1200	70	" "	"	3	125	20.8	2.1	7.50	15.8	5.31				3.8
7		1225	80	" "	"	2.5			3.2	7.90	25.3	5.31	5.30	2,900		
8		1235	80	" "	"	3	1.0	0.16	3.2	7.90	25.3	5.31				
9		1245	80	" "	"	2			3.2	7.90	25.3	5.31				
10		1400	80	" "	"	3	3.0	0.50	3.2	7.90	25.3	5.28				2.3
11		1415	90	" "	"	3	1.0	0.16	3.9	7.77	30.3	5.27				1.0
12		1430	90	" "	"	4	3.0	0.38	3.9	7.77	30.3	5.26				2.0
13		1445	90	" "	"	10	0.5	0.02	3.9	7.77	30.3	5.25				1.0
14		1500	100	" "	"	10			5.6	6.94	38.8	5.26				
15	5 June	1030	50	" "	1/4	3			2.2	5.90	13.0	4.90				
16		1100	60	" "	"	5			1.8	7.28	13.1	4.91				
17		1115	70	" "	"	5			2.0	6.12	12.2	4.91				
18		1125	80	" "	"	10	0.5	0.03	2.3	6.73	15.5	4.90	4.89	1,850		1.0
19		1150	90	" "	"	10	0.2	0.01	2.5	7.54	18.8	4.89				1.0
20		1430	100	" "	"	20			2.5	7.01	17.5	4.87				
21		1500	110	" "	"	20			3.8	6.65	25.3	4.86				
22		1530	120	" "	"	20			5.1	5.96	30.5	4.85				
23	7 June	1400	70	VUV Large	---	10			2.2	6.12	13.5	4.80				
24		1430	90	" "	---	10	0.5	0.034	2.2	6.12	13.5	4.79				1.0
25		1500	90	Small Basket	1/4	10	0.1	0.010	2.2	6.12	13.5	4.79	4.79	1,600		1.0
26		1530	90	" "	1/2	20			2.2	6.12	13.5	4.78				
27		1600	90	Large Basket	1/4	20	1.5	0.038	2.2	6.12	13.5	4.78				1.5
28		1630	90	VUV Large	---	20	0.7	0.0236	2.2	6.12	13.5	4.78				0.8
29	16 June	1100	50	Small Basket	1/4	80	2.0	0.025	1.7	5.89	10.0	4.65	4.65	1,350		0.5
30		1130	50	VUV Small	---	20	1.0	0.073	1.7	5.89	10.0	4.65				1.0
31	17 June	1400	50	Large Basket	1/4	10	147	7.40	2.2	5.90	13.0	4.95				2.0
32		1430	40	" "	"	10	1.0	0.05	1.8	3.70	7.3	4.92				0.5
33		1445	60	" "	"	10	1.0	0.05	1.8	7.28	13.1	4.94				0.5
34		1510	70	" "	"	10	107	5.3	2.0	6.12	12.2	4.94	4.91	1,900		3.5
35		1530	80	" "	"	10	324	16.2	2.3	6.73	15.5	4.92				5.0
36		1600	90	" "	"	10	182	9.1	2.5	7.54	18.9	4.90				3.5
37		1620	100	" "	"	10	146	7.3	2.5	7.01	17.5	4.89				3.0
38		1645	110	" "	"	10	3	0.15	3.8	6.65	25.3	4.87				3.0
39		1700	120	" "	"	10			5.1	5.96	30.5	4.86				
40	19 June	0930	50	VUV Large	---	5	87	11.90	2.2	5.90	13.0	4.92				2.0
41		0945	60	" "	---	5	34.9	4.71	1.8	7.28	13.1	4.92				2.5
42		1000	70	" "	---	5	147.5	19.95	2.0	6.12	12.2	4.93				3.5
43		1020	80	" "	---	5	1.0	0.15	2.3	6.73	15.5	4.92				1.0
44		1030	90	" "	---	5	28.8	3.90	2.5	7.54	18.9	4.91	4.91	1,900		1.5
45		1045	100	" "	---	5	1.5	0.20	2.5	7.01	17.5	4.91				2.0
46		1100	110	" "	---	5	0.8	0.11	3.8	6.65	25.3	4.90				0.75
47		1120	120	" "	---	5			5.1	5.96	30.5	4.89				
48		1130	130	" "	---	5			3.9	4.98	14.5	4.88				
49		1400	40	Large Basket	1/4	10			1.8	3.70	7.3	4.86				
50		1415	50	" "	"	10			2.2	5.90	13.0	4.85				
51		1434	60	" "	"	10	19	0.95	1.8	7.28	13.1	4.84				3.0
52		1442	70	" "	"	10	126	6.3	2.0	6.12	12.2	4.84				4.0
53		1513	80	" "	"	10			2.3	6.73	15.5	4.83	4.83	1,650		
54		1535	80	" "	"	10	0.5	0.025	2.3	6.73	15.5	4.83				
55		1551	80	" "	"	10	22.5	1.13	2.3	6.73	15.5	4.82				3.5
56		1610	70	" "	"	10			2.0	6.12	12.2	4.82				
57		1625	60	" "	"	10			1.8	7.28	13.1	4.81				
58		1632	60	" "	"	10	0.5	0.025	1.8	7.28	13.1	4.81				0.5
59	20 June	0930	70	" "	"	10	2.0	0.10	1.8	5.85	10.5	4.87				3.0
60		0950	90	" "	"	30	161.0	2.68	2.3	7.07	16.3	4.86				4.0
61		1035	100	" "	"	30	2.0	0.10	2.6	6.74	17.5	4.85				1.0
62		1115	80	" "	"	30	316.0	5.27	2.0	6.29	12.6	4.84			1.050	6.0
63		1200	70	" "	"	45	259	2.88	1.8	5.85	10.5	4.83			0.051	4.0
64		1335	60	" "	"	30			1.5	5.76	8.65	4.81	4.81	1,630		
65		1410	80	" "	"	10	1.0	0.05	2.0	6.29	12.6	4.80				
66		1430	80	" "	"	30			2.0	6.29	12.6	4.79				
67		1520	90	" "	"	30	5.25	0.088	2.3	7.07	16.3	4.78				2.0
68		1550	50	" "	"	30			1.7	5.89	10.0	4.77				
69		1630	70	" "	"	20	303	7.56	1.8	5.85	10.5	4.76			1.46	3.0
70		1715	70	" "	"	20	206	5.14	1.8	5.85	10.5	4.75			2.41	3.5
71	21 June	0915	50	" "	"	20	0.04	0.001	1.7	5.89	10.0	4.79				
72		0945	60	" "	"	30	109	1.81	1.5	5.76	8.64	4.78			0.143	2.8
73		1030	70	" "	"	20	193	4.83	1.8	5.85	10.5	4.77			0.750	4.3
74		1100	80	" "	"	20	222	5.55	2.0	6.29	12.6	4.77			8.55	3.8
75		1130	90	" "	"	20	328	8.20	2.3	7.07	16.3	4.77			1.63	3.3
76		1230	100	" "	"	82	326	1.99	2.6	6.74	17.5	4.76	4.76	1,560		3.0
77		1405	110	" "	"	20			3.5	7.02	24.6	4.75				
78		1430	120	" "	"	20			4.5	6.35	28.6	4.75				
79		1500	100	" "	"	20	83.5	2.08	2.6	6.74	17.5	4.75				3.7
80		1530	90	" "	"	20	306.0	7.65	2.3	7.07	16.3	4.74			0.109	3.4
81		1600	80	" "	"	15	34.2	1.14	2.0	6.29	12.6	4.73				2.8
82		1630	70	" "	"	10	42.4	2.12	1.8	5.85	10.5	4.72			2.34	2.0
83	22 June	1010	50	VUV Large	---	10	0.5	0.034	1.7	5.89	10.0	4.75				
84		1030	60	" "	---	10	7.03	0.475	1.5	5.76	8.64	4.74				2.5
85		1050	70	" "	---	10	54.5	3.68	1.8	5.85	10.5	4.73				3.0
86		1115	80	" "	---	10	9.0	0.608	2.0	6.29	12.6	4.73			1.70	3.0
87		1140	90	" "	---	10	13.25	0.895	2.3	7.07	16.3	4.72				2.0
88		1210	100	" "	---	92			2.6	6.74	17.5	4.72				
89		1350	110	" "	---	10			3.5	7.02	24.6	4.70	4.70	1,480		
90		1410	100	Large Basket	1/4	20	121	3.04	2.6	6.74	17.5	4.69			0.888	3.0
91		1439	90	" "	"	15	55.9	1.86	2.3	7.07	16.3	4.68				4.0
92		1505	80	" "	"	15	272	9.10	2.0	6.29	12.6	4.68			0.283	5.0
93		1530	70	" "	"	10	79.1	3.96	1.8	5.85	10.5	4.67			1.00	3.0
94		1552	60	" "	"	10			1.5	5.78	8.64	4.66				
95		1610	80	" "	"	10	15.2	0.76	2.0	6.29	12.6	4.65				3.0
96	23 June	0900	60	" "	"	10			1.2	4.65	5.54	4.56				
97		0915	55	" "	"	10			1.2	4.84	5.81	4.56				
98		0930	70	" "	"	10			1.5	5.04	7.58	4.55				
99		0940	70	" "	"	20	0.20	0.005	1.5	5.04	7.58	4.55	4.55	1,250		
100		1005	80	" "	"	30	0.66	0.01	1.5	5.37	8.05					





the rear sample door open in order to collect all of the fines that were part of the sample. Column 9 is calculated from columns 7 and 8 using a sampler width of 2.0 ft., 1.0 ft., 1.48 ft., and 0.69 ft. for the large and small baskets, and the large and small VUV samplers respectively. The depths of column 10 and velocities of column 11 were measured with a Gurley meter and 30 lb. weight and were not all taken at the same time as the bed-load samples. They were measured the same day but may have been taken as much as eight hours apart. The unit discharges of column 12 were calculated using the observations of columns 10 and 11. The gage height of column 13 was taken from the stage recorder located at 0+90 D/S and indicates that stage corresponding to the time in column 3. The mean gage height and mean discharge are therefore taken for sampling periods of about six hrs. in most cases. Tracer concentrations are reported in column 16 for the periods of sampling after tracer injection, and are the weight of tracer material divided by the total sample weight. Column 17 indicates the intermediate axis, measured in inches, of the largest particle in each bed-load sample.

The calculations of total bed-load discharge from these observations are presented in section 5.1.

#### 4.8. Tracer Study Observations

Tracer concentrations in bed-load samples obtained from the direct measuring equipment are referred to in section 4.7 and column 16 of TABLE IV-5. Because of the time required for tracer preparation and the stages of flow during the summer of 1967, only one period of continuous tracer injection was possible. Tracer material was injected



on the rising limb of the hydrograph starting at 9:55 A.M., 19 June. All material was injected into the bed-load at 22+03 U/S. About 3,800 lbs. of material coloured with highway yellow paint was injected at 105 ft. from the tower on the right bank at an average rate of 19.5 lbs/min. The injection of fluorescent green material commenced at 2:30 P.M., 19 June at station 80 ft. at the same rate up to a total of 1,500 lbs. Hydrophone observations indicated the bed was actively moving from 50 to 120 feet, with the most intensive movement between 90 and 110 feet. A few bags of the green material were placed on the bed at 120 ft. to check the limits of the moving strip and see if any portion of this material would be transported down the high water channel between 21+00 U/S and 7+00 U/S.

As can be seen from TABLE IV-5, the first sample that contained tracer material was collected at 11:15 A.M., 20 June 1967. This gives a time from first injection to first sample of 25 hours and 20 minutes. The distance through which this material travelled was from 22+03 U/S to 12+18 D/S or about 3,400 feet since material was injected slightly downstream of the cableway. The average rate of movement was therefore about 134 feet per hour at a mean discharge of 1,750 c.f.s. Of the six yellow tracer particles contained in this sample the largest had an intermediate diameter of 1.4 inches. The first green tracer particle was sampled at 5:15 P.M., 20 June 1967 giving a maximum travel time of 26 hours and 45 minutes over the same distance which corresponds to an average rate of 127 ft/hr. The maximum size particle of green material in this sample was also 1.4 inches intermediate diameter.





The data of TABLE IV-5 indicate the large fluctuations in tracer concentration over a period of relatively constant stage. Part of the reason for this may be due to the falling hydrograph and also the difference in grain sizes between the actual bed-load and the tracer material. The injection period was not sufficiently long.

The calculations of bed-load discharge based on these observations are presented in section 5.2.

#### 4.9. Hydrophone Observations

The use of the hydrophone equipment was discussed in section 3.10. Several routine hydrophone observations were carried out in order to estimate competent conditions and the extent of bed-load movement across the channel. A few of the more useful observations are tabulated in TABLE IV-6. Included in this table is an estimate of the mean discharge during the observation period. The table describes the movement sounds using the following descriptive words and their adopted meaning:

None	- no sounds of bed movement were heard;
Very Intermittent	- the sound of individual particle movement could be heard over a period of time (in the order of one particle movement sound per 20 seconds or longer);
Intermittent	- particle movement sounds were heard every few seconds and could be distinguished as individual particle movement sounds;
Intensive	- the sounds of particle movements were continuous and could not be distinguished as individual particle movement sounds;





TABLE IV-6  
HYDROPHONE OBSERVATIONS

Date	Location ft.	Station ft.	Total Depth ft.	Observation Depth ft.	Mean Discharge c.f.s.	Movement
May 26	22+03 U/S	40 to 130	---	---	800	None
June 1	0+18 D/S	20 to 130	---	---	8000	Intensive
June 7	12+18 D/S	130	3.3	2.3		Very intermittent
		120	5.0	4.0		Intermittent
		110	6.6	5.6		Intermittent
		100	4.6	4.0		Intensive fluctuation
		90	2.7	2.0	1700	Intensive
		80	1.7	1.0		Intensive
		70	1.5	1.0		Intensive
		60	1.5	1.0		Intensive
		50	2.0	1.0		Intensive
		40	2.1	1.0		Intermittent
		30	1.5	1.0		None
June 9	12+18 D/S	130	3.2	2.2		Very intermittent
		120	5.0	4.0		Intermittent
		110	6.5	5.0	1550	Intermittent
		100	3.8	3.8		Intensive
		90	1.9	1.0		Intensive
		80	1.5	1.0		Intensive
		70 to 40				Intermittent
		30	1.5	1.0		None
June 15	12+18 D/S	130	3.3	2.3		Intermittent
		120	4.7	3.7		Intermittent
		110	3.5	2.5	1250	Very intermittent
		100 to 60				None
		50	1.5	1.0		Intermittent
		40	1.7	1.0		None
June 30	22+03 U/S	100	1.8	1.0		None
		90	2.5	1.5		Very intermittent
		80	2.9	1.9	950	Intermittent
		70	2.9	1.9		Intermittent
		60	3.9	2.9		None
		50	2.5	1.5		None



Intensive Fluctuation - the sounds of particle movements were intensive for short periods followed by periods of no movement or intermittent movement.

The hydrophone observations indicate that throughout the study reach, bed movement occurs at a stage corresponding to a discharge of about 800 to 900 c.f.s. Between the start of movement and a stage corresponding to a flow of about 1,300 c.f.s. the movement is intermittent and occurs at isolated locations across the channel width. At all stages above this there seems to be a definite portion of the bed which is moving at all times. The width of this moving strip and its position within the cross section may vary. As the stage increases, this width increases and at flows as high as 8,000 c.f.s., it occupies all but a few feet of the channel near each bank.

Sampling with the bed-load samplers confirmed the stage corresponding to 1,300 c.f.s. as the limit between intermittent and general movement. In order to confirm the stage corresponding to competent conditions a strip of tracer material was placed across the bed at 21+50 U/S on June 29, 1967. At this time the flow was 1,000 c.f.s. This strip of material was a few feet wide, 100 feet long and required 3,000 lbs. of tracer material. The colored strip was visible from the banks as well as the cableway. Although no individual particle movements were observed at that time, by July 6 a portion of the smaller material between 60 and 100 feet had moved up to 50 feet downstream. At this time the flow was 800 c.f.s. The site was next visited on August 10 at which time the flow was 400 c.f.s. There had been a continuous





drop of the hydrograph during this interval. A small amount of additional movement was detected with material located as far as 20+00 U/S. This indicates that movement does occur below 800 c.f.s. but is not detectable over a short period of time, and is probably negligible compared to the bed-load discharge at 1,000 c.f.s. From the amount of movement observed it is likely that only a few particles greater than 1/4 inch sieve size move through a cross section during a day with flows below 800 c.f.s. At this stage most of the material smaller than 1/4 inch is beneath the bed paving so can only move when a larger particle moves.

#### 4.10. Pit Excavation Observations

The excavation site and equipment used are described in section 3.11. Excavation of the pit was started at 7:00 A.M. on May 29. At this time the flow was 900 c.f.s. and hydrophone observations indicated little or no bed movement. During the day of 29 May approximately 210 cubic yards of bed material were removed from the bed. This volume was estimated by the capacity of the excavating and hauling equipment. Most of the 210 cubic yards of material were taken from an area between 12+68 D/S and 13+08 D/S, and within 60 feet of the left bank. The flow was up to 1,000 c.f.s. at 5:30 P.M. when the excavation was discontinued. At this stage there is definite bed movement but it was not considered to be at a high enough rate to affect the volume of the excavation. When excavation resumed at 6:00 A.M. on May 30 the flow was estimated at 1,500 c.f.s. By 9:00 A.M. rough depths taken with the drag bucket indicated that material was depositing within the pit. At 12:00 noon





excavation was discontinued and flow was estimated at 5,500 c.f.s. At this time, material was coming into the pit at a higher rate than it could be removed. During the excavating period of May 30 an additional 50 cubic yards of material was removed. Attempts to resurvey the pit area between noon and 4:00 P.M. proved very difficult. By 4:00 P.M. the entire bed was estimated at a lower level, but from the crude depth measurement taken from a small boat the pit could not be detected. At 4:00 P.M. the flow was estimated at 9,500 c.f.s. Unfortunately, the rating curve shifted during this period and discharges are only rough estimates as no measurements were carried out. FIG. 4-28 shows seven cross sections from 12+58 D/S to 13+18 D/S that were surveyed on May 26. This figure shows the approximate level that excavation reached and was plotted from a few measured depths and an estimated volume of 260 cubic yards. PLATES 4-11 and 4-12 show the site at a flow of about 7,000 c.f.s.

These observations indicate a total of 260 cubic yards of bed material was excavated from a known area between 7:00 A.M. on May 29 and noon on May 30, 1967. The result of this excavation could not be detected at 4:00 P.M. on May 30. Calculations of the bed-load discharge based on certain assumptions are given in section 5.3.

#### 4.11. Other Observations

##### 4.11.1. Leopold Chains

In order to assess the depth to which the bed becomes mobile, at different stages of flow, a number of open link chains were driven into



the bed at several locations. Difficulties were encountered when placing these chains in the bed because of large buried boulders. The chains were placed at the upstream and downstream ends of one gravel bar at 5+00 D/S to 5+80 D/S. The chains were positioned on June 15 and re-surveyed on June 26, 1967. Each survey locates the exact position of the chain, the elevation of the bed at the chain and the elevation of the direction change in the chain if buried. In this way, scour and fill depths are estimated for the period between surveys. Between these successive surveys there was a small peak in the hydrograph with a maximum instantaneous flow of 2,700 c.f.s. at 5:00 A.M. on June 17, 1967. The mean flow for this same day was 2,000 c.f.s. The flows of 15 and 26 June were approximately the same. The flow over this bar was from right to left at about 45 degrees to the downstream direction with a maximum depth of 9 inches over the top of the bar on the 17 June. The Leopold chain observations indicated that scour of the bar occurred during this period but there was little deposition at any of the locations on the falling limb. The following assumed elevations were recorded at the chain locations.

Chain	Bed elevation 15 June	Lowest bed elevation 15 to 26 June	Bed elevation 26 June
1	2.77	2.09	2.09
2	2.77	2.01	2.01
3	2.46	1.92	1.92
4	2.30	2.30	2.33
5	1.81	1.81	1.82
6	1.51	1.26	1.26





In order to get good estimates of scour depths, a large number of chains would be required across the entire cross section at several locations. In order to place and survey these in thalweg locations, a very low stage would be required. Because of this, and the difficulties in driving the chains in large gravel and boulder material, the method was not useful in this study.

#### 4.11.2. Bank Erosion and Channel Shift

Severe bank erosion was observed at isolated locations throughout the study reach as a result of the flood of May 30, 1967. The majority of the length of bank through this reach is composed of alluvial material. The remainder consists of short lengths of exposed sandstone and shale. An example of a bed rock outcrop can be seen in the photograph of PLATE 4-3. PLATE 4-13 shows a bed rock shelf on the right bank at the downstream cable. Most of the alluvial banks have been stabilized by vegetation. PLATE 4-14 shows a portion of a bank that was eroded during the flood. The sites where severe bank erosion was observed had banks opposite them of bed rock. These bed rock outcrops produced severe constrictions on the channel at high flows with resulting higher velocities and bank scour. On the falling limb of the flood hydrograph several of these constrictions were constricted further by the building of gravel bars protruding into the original constriction. This caused increased bank erosion. A good example of bank erosion as a result of this cause is the left bank at the downstream cable. This is clearly indicated in the cross sections at 12+18 D/S in FIG. 4-11.



Between 52+00 and 40+00 U/S the right bank has been protected by rip-rap of about 24 inch intermediate size. The thalweg shifted from the left to right side of the channel during the flood period and can be seen in PLATES 4-1 and 4-2. The flood of May 30, 1967 reached the top of this bank. No loss of rip-rap or bank material was observed. At a site about 65+00 D/S severe erosion of the right bank took place during the May-June flood. This occurred over a length of bank covered by trees and erosion exceeded 50 feet in some places.

The channel shift and changes in major bar locations are indicated by a comparison of FIGS. 4-8 and 4-9. These were taken from the mosaics of May 26 and June 22 at discharges of 800 c.f.s. and 1,500 c.f.s. respectively, with the water surface elevation differing by about five inches in most places.



## CHAPTER V

### ANALYSIS OF DATA

#### 5.1. Bed-load Discharge Calculations from Direct Sampling

From the data of TABLE IV-5 the measured bed-load discharge per foot of width for each sample can be seen in column (9). The large fluctuations in measured bed-load discharge are obvious with respect to time and location. For the same mean velocity, same depth and similar grain sized distribution, rates can vary by 100 times.

If the sample observations are grouped into days containing a sample at several stations across the cross section, these can be used to calculate the total bed-load discharge through that section. The method is similar to the calculation of total fluid discharge by the mid-section method.

The results of these calculations are shown in TABLE V-1. Only those days when a reasonable number of samples were taken are tabulated, with the exception of June 1, which was used because of the high stage. The total width of moving bed strip is taken from the mid points between the last stations at which no sample was obtained to the stations nearest each bank where a sample was obtained. This moving strip was assumed to be continuous over the width in which a sample was obtained every ten feet. The bed-load discharge in lbs/min. is obtained by the





TABLE V-1

## BED-LOAD DISCHARGE RESULTS FROM DIRECT SAMPLING CALCULATIONS

Date 1967	Number of Samples in Calculation	Total Width of Strip ft.	Calculated Bed-load Discharge lbs/min.	Assumed Sampler Efficiency percent	Total Bed-load Discharge lbs/min.	Mean Fluid Discharge c.f.s.
June 1	1	60	990	45	2200	3850
June 12	13	50	522	45	1160	2900
June 17	8	80	456	45	1010	1900
June 19*	7	70	409	70	585	1900
				45	910	
June 20	13	40	72	45	160	1630
June 21	12	50	186	45	413	1560
June 22*	7	50	57	70	82	1550
				45	182	
June 22	7	40	138	45	300	1470
June 23	3	30	0.4	45	0.8	1250

\* VUV Samples.

summation of the unit discharges times the interval width, which in most cases was 10 feet. Assumed general sampler efficiencies are then applied to get the estimated bed-load discharge through the cross section. The efficiencies are presumed to take into account all losses. From the little data available it would appear that the VUV efficiency of 70% is probably high and should be less than that of the baskets. The total bed-load discharge is plotted against fluid discharge in FIGURE 5-1.



This figure shows the VUV sample estimates plotted using an efficiency of 45%. The fluid discharges reported are taken from the mean gage height during the sampling period. The sampled range of discharges from 1,250 c.f.s. to 3,850 c.f.s. indicate bed-load discharges from almost nothing to over one ton per minute.

There are insufficient data to make a comparison of relative efficiencies for the different sampler types, sampler sizes, and basket mesh sizes. Several samples at each location with each type of sampler would be required at each stage of flow to make maximum use of a sampling program. Samples should be taken at shorter intervals across the section. Even with improved equipment many days of flow at these relatively high stages would be required to satisfy this type of sampling program.

#### 5.2. Bed-load Discharge Calculations from Tracer Concentrations

From the bed-load sampling data of TABLE V-5 it is observed that the tracer concentration data of column 16 are very limited. TABLE V-2 gives the results of the calculations based on the method of section 2.2. The data have been grouped into days and calculations of the total bed-load discharge are made for each day. Because insufficient data were available to construct concentration versus distance curves and measure the resulting areas, rough estimates of a mean concentration were calculated. The total bed-load discharge was calculated by dividing an effective tracer injection rate by these mean concentrations. The actual injection rate was 19.5 lbs/min. but if the grain size curves of the injected tracer material and sampled bed-load material are compared





TABLE V-2

## BED-LOAD DISCHARGE CALCULATED FROM TRACER CONCENTRATION

Date 1967	Number of Samples in Calculation	Total Width of Strip ft.	Mean Concentration  $\times 10^3$	Total Bed-load Discharge lbs/min.	Mean Flow Discharge c.f.s.
June 20	4	40	1.22	9,100	1,630
June 21	9	50	1.98	5,100	1,560
June 22	4	40	0.97	10,400	1,480

(FIG. 4-20 curves two and four), it is estimated that only 52 percent of the tracer material, by weight, was of small enough size to move as part of the bed-load. For this reason, an effective tracer injection rate of 10.1 lbs/min. was used in the calculations.

A plot of tracer concentration versus time for some point downstream of the injection point should increase to some steady maximum value if a sufficient injection period is used. In this study the period was insufficient and an equilibrium condition was not reached. The values calculated for June 20 and 22 are on the rising and falling limb of this concentration vs. time curve and are therefore poor estimates of the bed-load discharge. The value calculated for June 21 should be the best estimate but is still high since equilibrium conditions were not reached.

A number of tracer particles were recovered from the bed between



the injection point and the sampling cross section during the visual recovery in September. Some of this material was smaller than 3 inch intermediate diameter indicating an accumulation of tracer material within the study reach. The amount of this material that is buried is not known, but is probably a significant portion of the total material that was injected.

Because of this accumulation of material and the insufficient injection period, observed concentrations are lower than they would have been if the assumptions of the method were satisfied, and the resulting estimate of bed-load discharge of 5,100 lbs/min. is probably high.

### 5.3. Bed-load Discharge Calculations from the Volumetric Pit

From the observations of section 4.10 a crude estimate of the bed-load discharge can be made. The weight of the material deposited in the excavation is estimated at 700,000 lbs. The hydrophone measurements of section 4.9 indicate little movement below 1,000 c.f.s. This is confirmed by the results of the direct bed-load measurements. If the excavation is assumed to have started to fill actively at about 1,300 c.f.s. the total time in which this filling took place is from 5:00 A.M. to 4:00 P.M. on May 30, 1967. Because of the lack of survey information it is not known at what time during this interval the pit was full. Obviously, during the last portion of filling much of the material would not be trapped and would pass through the excavation area. Calculating the bed-load discharge using the total time of 11 hours, gives an estimate of approximately 1,000 lbs/min. Because of the previous discussion this is considered a minimum estimate and the actual bed-load





discharge could be many times this. The mean flow during this same period is 4,500 c.f.s.

#### 5.4. Calculations of Bed-load Discharge Using Formulae

##### 5.4.1. Calculations Based on the Regime Slope Equation of Blench (1966)

The recommended form of the slope equation is:

$$f''' (c) = \frac{S K b^{1/6} Q^{1/12}}{k F_{bo}^{11/12}}$$

with  $K = \frac{3.63 g}{v^{1/4}}$ , and using  $g = 32.2$  ft/sec. and  $v = 1.4 \times 10^{-5}$  at  $52^{\circ}\text{F}$  gives a  $K$  value of 1,910. The regime equations were developed for straight sand bed canals. The meander correction coefficient,  $k$ , is to take into account that portion of the energy slope dissipated through curvature of flow and by irregular section and bed forms. Blench states the range of  $k$  is from 1.25 to 2.75 for natural rivers. Although this study reach does not contain well developed meanders a great deal of transverse flow is generated by the gravel bars. A value of  $k = 2.5$  has been selected as a reasonable estimate of the correction to be applied. A slope of  $7.45 \times 10^{-3}$  is used in these calculations as obtained in section 4.4. In order to assess a value of  $F_{bo}$ , a median grain size by weight of 0.1 ft. was selected from the pit samples of section 4.6, FIG. 4-20. If this is used in the rough formula  $F_{bo} = 7.3 \frac{m_D}{w} f^{1/4} \left( \frac{v_{70}}{v} \right)^{1/6}$  a value of  $F_{bo} = 3.9$  is obtained. Blench warns that the formula should not be trusted in gravel rivers unless  $d/D$  exceeds 50, and further states that the actual value of  $F_{bo}$  may be 3 to 4 times that calculated using the formula if  $d/D$  is less than 50. For this reason it





was decided to obtain an estimate of  $F_{b0}$  from the relation  $F_b = \frac{V_m^2}{d}$  at conditions where the charge was known to be nearly zero. From hydrophone observations, a flow of 1,000 c.f.s. was selected to meet this condition for the study reach in general. From the average curves of channel geometry (FIGS. 4-12 to 4-15), this stage corresponds to a mean velocity of 4.6 f.p.s. and mean depth taken equal to  $A/b_w$  of 1.9 ft. These values give  $F_{b0} \approx F_b = 11.1$  and  $F_{b0}^{11/12} = 9.1$ . If these values are used in the slope equation

$$\begin{aligned} f'''(c) &= \frac{1,910 \times 7.45 \times 10^{-3} b^{1/6} Q^{1/12}}{2.5 \times 9.1} \\ &= 0.63 b^{1/6} Q^{1/12} \end{aligned}$$

The calculation of  $f'''(c)$  is given for several values of  $Q$ , with  $b$  taken as equal to  $b_w$  and read from the average cross section curve of FIG. 4-13. The discharges of TABLE V-1 have been included in TABLE V-3 for comparison. Values of charge were taken from Blench's FIG. 7.2 which plots  $f'''(c)$  vs.  $C$  in parts per hundred thousand from the equation  $f'''(c) = \frac{(1 + 0.12 C)^{11/12}}{1 + C/233}$ . The charge has been converted to the bed-load discharge in lbs. per min. for comparison with the values of TABLE V-1.

It is interesting to note that the charge calculated using the regime slope equation is insensitive to stage and therefore the bed-load discharge is practically proportional to the fluid discharge. Generally this method gives slightly higher results than the direct sampling but it was found that the charges correspond to charges calculated from the sampling. The difference being, that the regime charge is taken for the



TABLE V-3

BED-LOAD DISCHARGE CALCULATED FROM THE REGIME SLOPE EQUATION

Q c.f.s.	$Q^{1/12}$	b ft.	$b^{1/6}$	$f'''$ (c)	$C \times 10^5$	$G_s$ lbs/min.
1,000	1.78	118	2.22	2.48	15	561
1,300	1.82	124	2.24	2.55	16	778
1,470	1.84	128	2.25	2.60	17	935
1,550	1.85	130	2.25	2.61	17	985
1,630	1.86	131	2.25	2.62	17	1,040
1,900	1.88	136	2.27	2.68	18	1,280
2,900	1.94	150	2.31	2.80	20	2,170
3,850	1.99	160	2.33	2.90	21	3,020
5,000	2.03	170	2.36	3.00	22	4,110
7,000	2.09	183	2.38	3.12	24	6,280
10,000	2.16	200	2.42	3.28	26	9,720
15,000	2.23	220	2.46	3.44	28	15,700

entire cross section while the direct sampling results correspond to only a portion of the cross section.

Obviously, one of the major difficulties in the use of this method is the assessment of values for  $F_{b0}$  and  $k$ . Without some idea of competent conditions the assessment would be even more difficult.





#### 5.4.2. Calculations Based on the Formula of Meyer-Peter, Müller (1948)

---

The Meyer-Peter, Müller equation can be written in the form:

$$0.25 \rho^{1/3} g_s'^{2/3} = \gamma R S \left( \frac{K_b}{K_b'} \right)^{3/2} - 0.047 \gamma_s' D_m$$

for a channel having negligible bank resistance. The following parameters remain constant throughout the calculations:

$$\rho = 1.94 \text{ lb. sec.}^2/\text{ft.}^4$$

$$\gamma = 62.4 \text{ lb./ft.}^3$$

$$S = 7.45 \times 10^{-3}$$

$$\gamma_s' = (2.64 - 1) 62.4 = 102 \text{ lbs./ft.}^3$$

$$K_b' = \frac{48}{D_{90}^{1/6}} = 60, \text{ with } D_{90} \text{ in feet}$$

$$D_m = \Sigma i_b D = 0.083 \text{ ft.}$$

The  $K_b$  and  $K_b'$  values in these calculations correspond to the units of feet and seconds and not to the metric system used normally with the Strickler equation,  $V_m = K R^{2/3} S^{1/2}$ .

$$\text{Therefore } K_b' = \frac{48}{D_{90}^{1/6}} = \frac{1.49}{n'}$$

$$\text{with } n' = 0.031 D_{90}^{1/6}$$

$$\text{and } K_b = \frac{1.49}{n} = \frac{V_m}{R^{2/3} S^{1/2}}$$

The values for the calculations of  $D_{90}$  and  $D_m$  are taken from the total of all pit samples with the grain size distribution shown in FIG. 4-20.



With the total resistance to flow  $K_b = \frac{V_m}{R^{2/3} S^{1/2}}$  the equation can be re-written

$$0.312 g_s'^{2/3} = 0.465 R \left( \frac{K_b}{K_{b'}} \right)^{3/2} - 0.398$$

The resulting calculations are given in TABLE V-4. As in TABLE V-3 a range of discharges has been selected to include the stages calculated for in TABLE V-1. Values of  $V_m$  and  $R$  are taken from the average curves of FIGS. 4-14 and 4-15. The hydraulic radius is assumed equal to  $A/b_w$ .

#### 5.4.3. Calculations of Bed-load Discharge by the Methods of Einstein (1950)

---

The results of calculations made by the Einstein method are given in TABLE V-5 for stages corresponding to the range of discharges used in TABLES V-3 and V-4. The detailed calculations and assumptions used are contained in APPENDIX A. The discharges given in TABLE V-5 are calculated from areas corresponding to the total hydraulic radius with respect to the bed and calculated velocities. The mean velocities calculated by this method do not agree with those obtained in FIG. 4-15 for corresponding discharges or values of the hydraulic radii. No adjustment was made since actual velocities and hydraulic radii are used in the method of section 5.4.4. The results given in TABLE V-5 are plotted in FIG. 5-2 for comparison with the results obtained by other methods.

With these calculations of bed-load discharge, it is necessary to realize that many of the figures used are derived from flume



TABLE V-4

BED-LOAD DISCHARGE CALCULATIONS FROM MEYER-PETER, MÜLLER EQUATION

Q c.f.s.	A/b <sub>w</sub> ft.	V <sub>m</sub> f.p.s.	$[A/b_w]^{2/3}$	K <sub>b</sub>	$[\frac{K_b}{K_b'}]^{3/2}$	$0.465 \frac{A}{b_w} [\frac{K_b}{K_b'}]^{3/2}$	$0.312 g_s'^{2/3}$	$g_s'$ lbs/ft.sec.	$g_s$ lb/ft.min.	b <sub>w</sub> ft.	G <sub>s</sub> lbs/min.
1,000	1.87	4.60	1.52	35.0	0.447	0.390	---	---	---	---	---
1,300	2.03	5.20	1.60	37.6	0.498	0.470	0.072	0.110	10.6	124	1,310
1,470	2.12	5.50	1.65	38.6	0.515	0.507	0.109	0.206	19.8	128	2,540
1,550	2.16	5.65	1.67	39.0	0.524	0.526	0.128	0.263	25.4	130	3,300
1,630	2.20	5.80	1.69	39.6	0.536	0.548	0.150	0.333	32.2	131	4,230
1,900	2.30	6.20	1.74	41.2	0.568	0.606	0.208	0.543	52.5	136	7,150
2,900	2.68	7.40	1.93	44.3	0.635	0.791	0.393	1.41	136	150	20,400
3,850	2.94	8.40	2.06	47.1	0.696	0.951	0.553	2.36	228	160	36,500
5,000	3.20	9.40	2.17	50.0	0.761	1.13	0.73	3.58	346	170	59,000
7,000	3.60	10.9	2.35	53.5	0.842	1.41	1.01	5.83	563	183	103,000
10,000	4.00	12.8	2.52	58.8	0.970	1.80	1.40	9.50	916	200	183,000
15,000	4.60	15.1	2.77	63.2	1.0	2.14	1.74	13.2	1,270	220	280,000





TABLE V-5  
BED-LOAD DISCHARGE BY EINSTEIN METHOD

$R_b'$	$R_b$	$Q$	$\Sigma i_b g_s$	$b_w$	$G_s$
ft.	ft.	c.f.s.	lbs/ft.min.	ft.	lbs/min.
0.5	1.85	712		115	
0.8	2.72	2,000	1.31	152	199
1.0	3.22	3,080	7.10	170	1,210
1.2	3.67	4,400	18.5	187	3,460
1.4	4.07	5,840	36.1	200	7,200
1.6	4.54	7,580	63.3	213	13,500
1.8	4.95	9,850	99.5	230	22,900
2.0	5.30	11,700	146	239	34,800
2.5	5.94	17,000	309	260	80,400
3.0	6.68	23,400	521	280	146,000



experiments and may not be directly applicable to the hydraulic and sediment conditions that exist. The use of Einstein's FIG. 5 ( $\Psi$  vs.  $V_m/V_{*'}''$ ) attempts to relate the effect of the irregularities of a natural stream channel to channel roughness. This appraisal is not considered to be accurate when the channel is obstructed by large gravel bars. The curve of the hiding factor  $\xi$  against  $D/X$  given as FIG. 7 in Einstein's work was derived from flume experiments using six mixtures. The values of  $\xi > 1$  used may not be applicable to this study, however the use does not greatly affect the final estimates because of the small contribution to the total weight of bed-load discharge. The curve of  $\Phi_*$  vs.  $\Psi_*$  is theoretical and represents the Einstein bed-load equation. The constants involved were obtained from two series of experiments, one of which used gravel of about 27 mm. average size.

#### 5.4.4. Calculations of Bed-load Discharge by the Modified Einstein Method of Colby and Hubbell (1961)

---

The calculations completed using this method are for the same stages as those in sections 5.4.1 and 5.4.2. Values of  $A/b_w$  and  $V_m$  are taken from the curves for an average cross section in FIGS. 4-14 and 4-15. The first step in computing the bed-load discharge by the modified Einstein procedure is the solution of the equation

$$V_m = 5.75 \sqrt{g(RS)_m} \log_{10} \left( 12.27 \frac{xd}{k_s} \right)$$

for  $\sqrt{(RS)_m}$  using a trial and error solution with the aid of a graph (PLATE 1, Colby and Hubbell, 1961). Using this procedure,  $k_s$  is taken equal to  $D_{65}$  which is 0.125 ft. from the combined pit sample curve of FIG. 4-20. The dimensionless parameter  $x$  is determined from PLATE 1





(Colby and Hubbell, 1961) and is one in all cases. Values of  $xd/k_s$  are given in TABLE V-6. From the values of  $xd/k_s$  and  $V_m$ , values of  $\sqrt{(RS)_m}$  are found from PLATE 1. A value of  $\nu = 1.4 \times 10^{-5}$  corresponding to a water temperature of 52°F. was used to estimate  $x$  values. In these calculations the average water depth  $d$  is taken to equal  $A/b_w$ .

According to the modified relationship the intensity of bed-load transport is  $\phi_*/2$ , if  $\phi_*$  is determined from the relationship between  $\phi_*$  and  $\psi_*$  (Einstein, 1950) by substituting  $\psi_m$  for  $\psi_*$ . TABLE V-7 shows a sample for the remainder of the calculations for one stage. The

TABLE V-6

## BED-LOAD DISCHARGE CALCULATIONS BY MODIFIED EINSTEIN PROCEDURE

Q	A/b <sub>w</sub>	V <sub>m</sub>	$\frac{xd}{k_s}$	$\sqrt{(RS)_m}$	(RS) <sub>m</sub>	$\Sigma i_b \phi_* D^{3/2}$	b <sub>w</sub>	G <sub>S</sub>
c.f.s.	ft.	f.p.s.				x 10 <sup>6</sup>	ft.	lbs/min.
1,000	1.87	4.60	15.0	0.0618	0.00382	3.08	118	13.1
1,300	2.03	5.20	16.2	0.0695	0.00483	38.4	124	171
1,470	2.12	5.50	17.0	0.0728	0.00530	75.3	128	347
1,550	2.16	5.65	17.3	0.0740	0.00548	92.2	130	432
1,630	2.20	5.80	17.6	0.0760	0.00577	134	131	632
1,900	2.30	6.20	18.4	0.0810	0.00656	258	136	1,260
2,900	2.68	7.40	21.4	0.0937	0.00879	965	150	5,200
3,850	2.94	8.40	23.5	0.1040	0.0108	2,240	160	12,900
5,000	3.20	9.40	25.6	0.115	0.0132	4,430	170	27,200
7,000	3.60	10.9	28.8	0.130	0.0169	9,250	183	61,000
10,000	4.00	12.8	32.0	0.151	0.0228	20,690	200	149,000
15,000	4.60	15.1	36.8	0.174	0.0303	38,600	220	306,000



TABLE V-7

## SAMPLE CALCULATION USING MODIFIED EINSTEIN PROCEDURE

Q=1,900 c.f.s.

 $(RS)_m = 0.00656$ 

Size Range ft.	$i_b$ %	D ft.	$D^{3/2}$	$\psi_m$	$\phi_*$	$i_b \phi_* D^{3/2}$ $\times 10^6$
>0.5	1.6					
0.500 to 0.334	6.0	0.409	0.261	40.8		
0.334 to 0.167	17.0	0.236	0.114	23.6	0.00064	12.4
0.167 to 0.0834	27.4	0.118	0.040	15.0	0.016	175
0.0834 to 0.0624	12.0	0.0721	0.019	15.0	0.016	36.5
0.0624 to 0.0364	18.0	0.0477	0.0105	15.0	0.016	30.2
0.0364 to 0.0208	5.0	0.0275	0.0046	15.0	0.016	3.7
< 0.0208	13.0					
$\Sigma i_b \phi_* D^{3/2} = \underline{257.8 \times 10^{-6}}$						

relations  $\psi_m = (s_s - 1) \frac{D_{35}}{(RS)_m}$

or  $\psi_m = 0.4 (s_s - 1) \frac{D}{(RS)_m}$

are used depending on the relation of D to  $D_{35}$  for each size range.

Then the relation  $i_b G_s = i_b b_w D^{3/2} \phi_* \times 36,000$  is calculated to give the bed-load discharge. The size analysis of the material used in these calculations is from the total of all pit samples. The  $D_{35}$  is taken from FIG. 4-20 as 0.06 feet,  $2.5 D_{35}$  equals 0.15 feet and therefore  $\psi_m$  is calculated using the  $D_{35}$  size except for the two largest size ranges.



The totals of the bed-load discharge of each size range are given in the last column of TABLE V-6. These totals would be slightly higher if the total sample were used rather than the size ranges indicated which comprise 85.4% of the sample. The material larger than 0.5 ft. is small by percentage (1.6%) and does not contribute until a flow of 4,000 c.f.s. is attained. The material smaller than 0.0208 feet is 13% of the total sample weight but because of the small particle size, contributes very little to the total weight of bed-load discharge.

It is interesting to note that using this procedure, conditions of zero bed-load discharge coincide to the same stage at which movement begins, as detected by other means. The results of this method are compared to the previous results in section 5.5.

#### 5.5. Comparison of Results and Calculation of Annual Bed-load Discharge

##### 5.5.1. Comparison of Results

The results of the calculations of sections 5.1 to 5.4 are presented as a logarithmic plot of  $G_s$  vs.  $Q$  in FIG. 5-1. The results of the direct measurements come closest to the Modified Einstein curve for discharges of 1,000 to 2,000 c.f.s. There is then an indication that the curve would flatten and follow more closely the curve of Blench. The value plotted from the tracer concentration calculations is expected to be high because of the lack of equilibrium conditions and the accumulation of tracer material within the study reach. The value plotted from the excavation filling rate is expected to be low since the excavation could not be 100 percent efficient and no efficiency was applied to the calculated value.





Below 4,000 c.f.s. the Einstein calculations give the lowest estimates of bed-load discharge. The reason for this is the very large value of  $R_b''$  which are calculated from theoretical shear velocities obtained from FIG. 5 (Einstein, 1950) which may give a poor appraisal of the effect of channel irregularities. The large values of  $R_b''$  cause large values for the total bed hydraulic radii, for relatively small values of the grain size hydraulic radii. The result of this is high values of  $\Psi_*$  and therefore low values for the intensity of transport  $\Phi_*$  for the high stages corresponding to the large values of  $R_b$ .

The modified Einstein method used in section 5.4.4 gives estimates higher than the Einstein method, throughout the range of fluid discharges. Although this method is based on the theory and empirical relation of the original method, it uses actual mean velocities rather than a measured slope in order to obtain values for the shear intensity on a particle. In this study, the result is a smaller correction for roughness due to channel irregularities and therefore higher rates of bed-load discharge for corresponding stages and a given range of particle sizes. It is interesting to note, that using this method, conditions are calculated which correspond to the field observations for the beginning of transport. The Einstein method indicates zero bed-load discharge at this same stage.

Estimates of the bed-load discharge from the regime slope equation indicate that the bed-load discharge increases at a much lower rate with an increase in fluid discharge than indicated by either the



Einstein or modified Einstein procedures. This is a result of the calculated values of charge being insensitive to an increase in stage. It is noted that the value of the zero bed factor is calculated for observed competent conditions and at these conditions a reasonably large estimate of bed-load discharge is obtained. This method would yield estimates closer to the field measurements if the meander correction coefficient was varied inversely with stage. The decreased proportion of energy required to overcome the channel irregularities with increased stage is taken into account by the other methods used. In the Einstein method, ratios of  $R_b'/R_b$  vary from 0.27 to 0.45 with an increase in discharge from 712 to 23,400 c.f.s. In the Meyer-Peter and Müller equation values of  $(K_b/K_b')^{3/2}$  vary from 0.447 to 1.0 with discharges from 1,000 to 15,000 c.f.s., while in the regime slope equation  $1/k$  remains constant at 0.4.

For the range of values given in FIG. 5-1, the Meyer-Peter and Müller equation gives the highest estimates of bed-load discharge. A slightly higher value of the bed shear stress corresponding to the start of bed-load movement, than the  $0.047 \gamma_s' D_m$  used, is indicated in section 5.8 and TABLE V-8.

#### 5.5.2. Estimates of Annual Bed-load Discharge

An estimate of the total quantity of bed-load passing through a given section can be made using a flow duration record and a curve or equation relating bed-load discharge to fluid discharge or stage. This estimate will use the average annual flow duration curve of FIG. 4-6 and an assumed curve of bed-load discharge vs. fluid discharge based on the





field measurements and given as FIG. 5-2. With these two curves the average annual bed-load moved through the study reach is calculated to be about 4,400 tons. This amount is moved during a period of less than 20 days, and is equivalent to approximately two acre ft. of material at 100 lbs/ft.<sup>3</sup>. For the average year 70 percent of this total is contributed by a 5.3 day period of flow between 1,500 and 4,000 c.f.s.

If the same calculation is applied to the 1967 hydrograph with mean daily discharges as shown in FIG. 4-6 the result is 10,600 tons per year considering the period from May 21 to June 30, 1967. With these amounts over a period of 35 years the reduction in capacity of a large reservoir would be insignificant. Preliminary estimates from surveys carried out by Provincial Water Resources Division, indicate a slight reduction in the capacity of the Glenmore Reservoir downstream of the study reach since the construction of the dam in 1933. Much of the material deposited within the reservoir may be transported in suspension and is not included in the previous discussion. Although no suspended sediment samples were obtained at high flows, deposits of sand were observed on the flood plain at locations where flow spilled over the banks, indicating that at high flows sand is transported in suspension. A completed analysis of the reservoir loss and a study of sedimentation processes upstream of the reservoir would be valuable in this connection.

#### 5.6. Analysis of Channel Roughness

The range of values of channel roughness for varying stages of flow are indicated by the column of  $K_b$  values in TABLE V-4 in connection with the Meyer-Peter and Müller calculation. If Manning's  $n$  is



calculated for a reference low water stage of 410 c.f.s., from the average channel geometry, it is 0.050 as compared to a value of 0.024 at the high water stage of 15,000 c.f.s.

If it is accepted that  $\frac{V_m}{V_*} = 5.75 \log_{10} \left( 12.27 \frac{R}{k_s} \right)$  for fully rough flow and this is approximated by  $\frac{V_m}{V_*} = 8.45 \left( \frac{R}{k_s} \right)^{1/6}$  for values of  $7 < \frac{R}{k_s} < 130$  then the grain size roughness is given by a Manning's  $n' = 0.031 k_s^{1/6}$  where  $k_s$  is the equivalent grain size roughness of the bed. In the Meyer-Peter, Müller equation  $k_s$  was taken equal to  $D_{90}$  by weight from the pit samples and corresponds to a  $n' = 0.025$ . In the Einstein calculation  $k_s$  was taken equal to the  $D_{65}$  by weight from the same samples and corresponds to a  $n' = 0.022$ . If the  $D_{50}$  by number of the total of all tape and toe samples is used as an effective grain size roughness, a value of  $n' = 0.023$  is obtained.

These calculations indicate the grain size roughness is not sensitive to the equivalent grain size used and probably remains nearly constant with a change in stage. That portion of the total channel roughness due to channel irregularities and bed shape decreases rapidly with an increasing stage. An energy slope correction of one half at reference low water stage to one at high water seems reasonable when applying the bed-load discharge equations.

### 5.7. Analysis of Unit Bed-load Discharge Measurements

The values tabulated in column 9 of TABLE IV-5 indicate average values of unit bed-load discharge generally higher from 50 to 100 feet than from 100 to 130 feet. The depth readings of column 10 indicate





that these high values correspond to verticals of small depth and the lower unit bed-load discharges are at locations of larger depth. No large differences in the sizes of bed material or bed-load material were found across this section. The mean velocities of each vertical are given in column 11 and do not increase with an increase in the local depth, in most cases. This clearly indicates that the energy slope is not constant at all points across the channel. The vertical velocity distribution as represented in FIG. 4-19, at cross section 12+18 D/S, indicates higher velocities, near the bed at these locations of small relative depth. FIG. 5-3 shows depth, mean velocity, fluid discharge, measured bed-load discharge, and velocities 6 inches above the bed; plotted across cross section 12+18 D/S for 2 June. The distribution of velocity 6 inches above the bed reflects the distribution of bed-load discharge for velocities in excess of about 6 f.p.s. Unfortunately, velocities nearer the bed were not obtained.

These observations contradict the assumption of using an average value of the energy slope for points across a section, on which most bed-load discharge equations are applied. Other observations from both flumes and river models show distinctly that the transport at the points of deepest scour is usually very small and more intense transport occurs at medium depths and on the top of bars. This is explained by the irregular distribution of the energy slope for an irregular channel cross section and indicates the need for measurements of the distribution of shear stress over the entire bed.





### 5.8. Discussion of Competent Conditions and Calculations of the Average Bed Shear Stress

---

The hydrophone observations of section 4.9 and the bed-load sampling data of section 4.7 indicate the substantial range of hydraulic conditions between the first displacement of a bed material particle and the start of general bed-load movement. Individual particle movements were observed at conditions corresponding to a flow of 400 to 800 c.f.s. over the study reach. Between flows of 800 and 1,300 c.f.s. considerable bed particle movement occurred but bed-load charge was not significant. At flows greater than 1,300 c.f.s. bed-load transport increased at a high rate.

The average bed shear stress calculated for the entire section at 12+18 D/S for  $Q = 1,300$  c.f.s. is  $\tau_0 = 1.1$  lbs/ft.<sup>2</sup>, using  $S = 7.45 \times 10^{-3}$  and an average depth of 2.3 ft. The average shear stress calculated from  $\gamma dS$  for the portion of the channel 60 to 110' is  $\tau_0 = 0.93$  lbs/ft.<sup>2</sup>. FIG. 5-4 shows a semi-logarithmic plot of the velocity distribution at cross section 12+18 D/S at a flow of about 1,300 c.f.s. FIG. 5-4 was constructed from the isovels plotted in FIG. 4-19 (June 27) with distances taken normal to the bed. Normals taken within 25 feet of either bank did not plot consistently with the central portion of the channel and are not given in the plot.

The straight line of FIG. 5-4 can be represented by a non-dimensional velocity equation

$$\frac{V}{V_*} = A \log \frac{y}{k_s} + B, \text{ where } V \text{ is the velocity}$$



at a distance  $y$  from the bed,  $k_s$  is Nikuradse's sand grain diameter and A and B are constants. If the value of  $A = 5.75$  is applicable then  $V_*$  can be calculated, without knowing  $k_s$  or B. This value has been used because of the difficulty in assessing  $k_s$  for an alluvial bed of non-uniform size material and the uncertainty of the constant B. Obviously the calculated shear velocity is dependent on the selection of a bed datum. From the slope of the line in FIG. 5-4,  $V_* = 0.85$  ft/sec. giving an average bed shear stress from 60 to 110 ft. of  $\rho V_*^2 = 1.4$  lbs/ft.<sup>2</sup>. If the velocity profiles near each bank are included,  $V_*$  average = 0.6 ft/sec. giving  $\tau_0 = 0.7$  lbs/ft.<sup>2</sup>. Bed shear stresses were determined in the same way for cross section 22+03 U/S at  $Q = 883$  c.f.s. for July 4 (see FIG. 4-17). Over the region 50 to 100 feet,  $V_* = 0.6$  ft/sec. giving  $\tau_0 = 0.7$  lbs/ft.<sup>2</sup> and  $\gamma dS$  using the total average slope gives  $\tau_0 = 1.2$  lbs/ft.<sup>2</sup>. If the values of  $\tau_0$  determined from the velocity profiles are compared to those calculated using  $\gamma dS$  a slope correction of one half seems reasonable when calculating the average bed shear stress for the entire cross section. It also becomes apparent that over a portion of the bed, the actual bed shear stress may be as high or higher than the value calculated using the mean depth and total slope.

TABLE V-8 gives values of the nondimensional Shields' parameter for conditions corresponding to flows of 400, 800, and 1,300 c.f.s. for a few grain sizes. Values of  $\tau_0$  have been calculated using  $R$  equals  $A/b_w$  for the study reach in general and an effective slope of  $\frac{1}{2} \times 7.45 \times 10^{-3}$  consistent with the previous discussion for the average bed shear stress.





TABLE V-8  
SHIELDS' PARAMETER

Q	A/b <sub>w</sub>	$\tau_o$	$\frac{\tau_o}{\gamma_s' D}$		
			D=0.061 ft.*	D=0.083 ft.**	D=0.15 ft.***
c.f.s.	ft.	lbs/ft. <sup>2</sup>			
400	1.4	0.33	0.053	0.039	0.022
800	1.7	0.40	0.064	0.047	0.026
1,300	2.0	0.47	0.076	0.055	0.031

\* D<sub>35</sub> by weight, pit samples.

\*\* D<sub>50</sub> by weight, pit samples.

\*\*\* D<sub>50</sub> by number, tape and toe samples.

The grain size Reynolds' numbers  $\frac{V_* D}{\nu}$  for the conditions of TABLE V-8 are about 2,500 with d/D ratios of about 15 to 25 for D = 0.083 feet. Meyer-Peter and Müller (1948) use a value of  $\frac{\tau_o}{\gamma_s' D_m} = 0.047$  as a start of bed-load movement and 0.03 as a value below which the bed is at complete rest. Other studies have suggested a value of  $\frac{\tau_o}{\gamma_s' D}$  in the range 0.04 to 0.06 for competent conditions in the fully rough phase of flow. Of course one of the greatest problems is the definition of competent conditions and the criterion on which observations are based. From TABLE V-8 using D = 0.083 feet the present study indicates values of 0.039 and 0.055 corresponding to the Meyer-Peter Müller values of 0.03 and 0.047. The effect of bed paving on competent conditions requires further study.



The bed-load sampling observations indicate that the complete range of bed material sizes will move when this upper value corresponding to 1,300 c.f.s. is exceeded. Material of intermediate axis length equal to 5 inches, ( $D_{95}$ , curve 3, FIG. 4-20) was sampled as bed-load at a flow of 1,400 c.f.s. (TABLE IV-5).



## CHAPTER VI

### CONCLUSIONS AND RECOMMENDATIONS

#### 6.1. Conclusions

The observations of section 4.7 and results of section 5.1 lead to the following general conclusions with respect to the measurement of bed-load discharge by direct sampling.

1. Large fluctuations of bed-load discharge with respect to time and location make it necessary to collect a large number of samples for a useful quantitative analysis.
2. Relative efficiencies of the VUV and Basket samplers could be obtained for the various sizes and basket mesh sizes with a good field sampling program. The effect of sample size on sampler efficiency must also be determined.
3. The use of hand winches or truck-mounted power winches with a slow line speed severely limits the number of samples that can be taken during a given period of time.
4. The number of days per year at which the bed-load discharge is high enough to make direct sampling useful may also limit the sampling program.





5. A sample time is simpler to estimate using the larger size of each type sampler, and this reduces the number of samples that must be disregarded because the sampler is full.
6. High stream velocities make the use of the small samplers difficult. The handling of the VUV samplers is more difficult than the basket samplers under all observed conditions. The modification to keep the rear gate of the half size VUV sampler open during lowering is a necessity unless velocities are very low.
7. The VUV sampler has the advantage of trapping a portion of the smaller material that passes through the smallest mesh basket. A decision on which sampler type to use must be based on the grain size distribution of bed material.
8. The use of overhead cableways for direct sampling proved satisfactory for this study and is probably the simplest means on a river of this size with relatively high velocities.

Some general conclusions can be drawn from the observations and results of the tracer method used.

1. A great deal of time and labour is involved in preparing large quantities of tracer material using the hand method described in section 3.6.
2. The use of the fluorescent paint mixture is not considered practical or necessary using this method with large size bed



material. The yellow highway paint proved acceptable in this study and a more abrasive-resistant paint such as the poly-epoxilene coating would be required over longer distances. A separate colour is required for each injection during any one flood season.

3. The rate of injection must be based on an estimate of the bed-load discharge. The rate used in this study was sufficient for the discharge that prevailed.
4. The period of continuous injection used was insufficient and probably should have been several days. For higher stages a shorter period of injection may be used but the rate of injection should then be increased.
5. Since the grain size distribution of the injected tracer material should be similar to that of the bed-load at any one stage, information from bed-load sampling must be available before injection is started. A stage prediction would be most useful in determining the injection rate, the length of period and the grain size distribution required.
6. The results and observations of the method, as used in this study, indicate the difficulty in satisfying the assumptions on which the method is based.

From the limited observations and results given from the bed excavation, the following general conclusions are made.





1. The excavation size is dependent on the amount of expected bed-load movement. Large mechanical methods of excavation and hauling must be used and this becomes expensive.
2. The excavation should be completed at a low stage where there is no bed movement in order that accurate surveys can be made before refilling begins.
3. At high stages, resurveys were not possible by wading. The uses of the fathometer from a boat or with the transducer float mounted and operated from the cableway are not completely satisfactory.
4. The reliability of the method is dependent on the availability of good survey information at several intervals during the refilling. The efficiency of the pit to trap material must be determined or assumed.

Several conclusions can be made with regard to the application of the sediment transport equations of section 5.4.

1. Results can be misleading if only the channel geometry and limited bed material sampling are applied in a rigid manner. For a given set of conditions the equations will yield a wide range of values for the bed-load discharge.
2. There are simple field observations that make the application or adjustment of the formulae reasonable. Measurements of mean



velocities and the velocity distribution prove valuable. An assessment of the hydraulic conditions corresponding to the start of bed movement is useful. The use of suitably marked bed material or an instrument such as the hydrophone make this type of assessment possible. The hydrophone can give valuable information on the extent of bed movement which can be used to supplement the formulae.

3. The pit type bed material sample, analysed on a weight basis, is the most useful when applying these empirical relations. The samples must be large when studying rivers whose beds are composed of large material. The samples must contain the material that moves at all stages of flow and therefore cannot be restricted to small gravel bars. The grain size distribution of actual bed-load samples provides a good check on the results obtained by formulae. Tape or toe samples analysed by number may be sufficient to estimate the grain size roughness of the bed but are not representative of the bed material that is available for transport.

## 6.2. Recommendations

The following recommendations can be made from the conclusions of section 6.1.

1. A continuation of the direct bed-load discharge sampling program will provide useful information as to the quantity of bed-load moving in gravel rivers.



2. A power winch system using portable gasoline engines would make such a program practical. For each sampling site involving an overhead cableway two winches are desirable. These should have a freewheeling clutch and brake system with minimum line speeds of about 200 feet per minute at 500 lbs. pull and 25 feet per minute at 5,000 lbs. pull. With an effective cable traveller this would reduce sampling time to the order of 15 minutes for a 10 minute sample on rivers up to 200 feet in width.
3. The large basket and full size VUV samplers are recommended for use in rivers having sediment and hydraulic conditions comparable to the Elbow River at Bragg Creek as reported. The sample compartment size is small on the VUV sampler which will restrict it to the low rates of movement. When material larger than four inches intermediate diameter moves this sampler becomes unsuitable. A modification to the large VUV sampler similar to the half size sampler in which the gate can be kept open during lowering would make handling less difficult.
4. Consideration should be given to other rivers and locations at which the bed is known to be active for a larger number of days each year.
5. Future studies of this type should include an extensive suspended sediment measurement program in conjunction with the bed-load measurements. This would provide the necessary information to calculate the total sediment discharge and provide a check on





the size of bed material going into suspension as calculated from empirical relations.

6. A larger scale attempt at the use of the tracer injection method would be interesting now that some of the problems have been sorted out. Mechanical methods of sieving, washing and painting the tracer material should be considered because of the large quantity of material that is required. This method is probably best suited to the higher rates of bed-load discharge.
7. The pit excavation method is probably best suited to low rates of bed-load discharge and will include a portion of the suspended sediment in most cases. A suitable and accurate method of resurvey must be found that will yield refilling rates at all stages of flow. As a routine measurement this method is considered impractical.
8. Velocity measurements should be taken in conjunction with direct bed-load measurements and hydrophone observations are considered an important part of this type of study.
9. An improved hydrophone is presently under construction with the hope of reducing the unwanted sounds by streamlining. Laboratory studies are planned to investigate the capabilities of this instrument.
10. A direct method for measuring the distribution of shear stress over a natural gravel bed would provide valuable information on the distribution and amount of bed-load discharge.



11. A study of the over-all sedimentation process along the Elbow River including an analysis of sediment accumulation in the Glenmore Reservoir is proposed for the future.





## LIST OF REFERENCES



## LIST OF REFERENCES

- Blench, T. - "Mobile-Bed Fluviology". T. Blench and Assocs. Ltd., Edmonton, 1966.
- Colby, B.R. - "Fluvial Sediments - a Summary of Source, Transportation, Deposition, and Measurement of Sediment Discharge". Geological Survey Bulletin 1181-A, 1963.
- Colby, B.R. and Hubbell, D.W. - "Simplified Methods, Sediment Discharge, Modified Einstein Procedure". Geological Survey Water-Supply Paper 1593, 1961.
- Crickmore, M.J. and Lean, G.H. - "The Measurement of Sand Transport by Means of Radioactive Tracers". Proceedings of the Royal Society, A, Volume 266, pp. 402-421, 1962.
- Crickmore, M.J. and Lean, G.H. - "The Measurements of Sand Transport by the Time-integration Method with Radioactive Tracers". Proceedings of the Royal Society, A, Volume 270, pp. 27-47, 1962.
- Einstein, H.A. - "The Bed-load Function for Sediment Transportation in Open Channel Flows". Technical Bulletin No. 1026, U.S. Department of Agriculture, Washington, D.C., September, 1950.
- Emmett, W.W. and Leopold, L.L. - "Downstream Pattern of River Bed Scour and Fill". Federal Inter-Agency Sedimentation Conference, Jackson, Mississippi, January 28, 1963.
- Henderson, F.M. - "Open Channel Flow". The Macmillan Company, New York, 1966.
- Hubbell, D.W. - "Apparatus and Techniques for Measuring Bed-load". Geological Survey, Water Supply Paper 1748, U.S. Government Printing Office, 1964.
- Hubbell, D.W. and Sayre, W.W. - "Sand Transport Studies with Radioactive Tracers". Journal of Hydraulics Division, Proceedings of the ASCE, Hy 3, pp. 39-68, May, 1964.
- Jolliffe, I.P. - "The Use of Tracers to Study Beach Movements; and the Measurement of Littoral Drift by a Fluorescent Technique". Revue de Geomorphologie Dynamique, 1960.



- Kellerhals, R. - "Gravel Rivers with Low Sediment Charge". M.Sc. Thesis, Dept. of Civil Engineering, University of Alberta, Edmonton, 1963.
- Keulegan, G.H. - "Laws of Turbulent Flow in Open Channels". National Bureau of Standards Journal of Research, Vol. 21, 1938.
- Leliavsky, S. - "An Introduction to Fluvial Hydraulics". Dover Publications, Inc., New York, 1966.
- Meyer-Peter, E. and Müller, R. - "Formulae for Bed-load Transport". Proc. I.A.H.R., Stockholm, 1948.
- Novak, P. - "Bed-load Meters - Development of a new type and determination of their efficiency with the aid of scale models". Internat. Assoc. Hydraulic Research, Trans. V. 1, pp. A9-1 to A9-11, 7th gen. mtg. Lisbon, 1957.
- Putman, J.L. and Smith, D.B. - "Radioactive Tracer Techniques for Sand and Silt Movements Under Water". International Journal of Applied Radiation and Isotopes, Vol. 1, pp. 24-32, 1956.
- Qureshi, M.A. - "Regime Relations in a Gravel Reach of the Red Deer River". M.Sc. Thesis, Dept. of Civil Engineering, University of Alberta, Edmonton, 1962.
- Rakoczi, L. - "Studies of Sediment Transportation by Luminescent Tracers". Poona Golden Jubilee Symposium, January, 1966.
- Rakoczi, L. and Stelczer, K. - "Sediment Investigations with Tracers on Experimental Areas". Publication No. 66 of the IASH, Symposium of Budapest, pp. 361-371. (1965).
- Ramette and Heuzel. - "A Study of Pebble Movements in the Rhone by Means of Radioactive Tracers". Translation, No. Special A, pp. 389-399, La Houille Blanche, 1962.
- Raudkivi, A.J. - "Loose Boundary Hydraulics". Pergamon Press Ltd., 1967.
- Reid, W.J. and Morgan, H.D. - "The Use of Radioactive and Fluorescent Tracers in England to Measure the Movement of Silt, Sand and Shingle". XXth International Association of Navigation Congress, Baltimore, 1961.
- Shields, A. - "Anwendung der Aehnlichkeitsmechanik und der Turbulenzforschung auf die Geschiebebewegung". (Application of Similarity Principle and Turbulence Research to Bed-load Movement.) Mitteilungen der Preuss Versuchsanst für Wasserbau und Schiffbau, No. 26, 1936.





Subcommittee on Sedimentation - "Determination of Fluvial Sediment Discharge". U.S. Inter-Agency Committee on Water Resources Report No. 14, 1963.

Van Der Giessen, N. - "Report on Observations on Gravel Transport in Four Rivers in Western Alberta". M.Sc. Thesis, University of Alberta, Edmonton, 1966.

Wolman, M.G. - "A Method of Sampling Coarse River Bed Material". Trans. A.G.U., Vol. 35, No. 6, December, 1954.



APPENDIX A

CALCULATIONS OF THE BED-LOAD  
DISCHARGE BY THE METHODS OF EINSTEIN



## APPENDIX A

Calculations of Bed-load Discharge by the Methods of Einstein (1950)

The following calculations follow the step by step procedure of Einstein (1950). Where assumptions or modifications to the procedure are made, they have been noted.

Hydraulic Calculations for Channels in GeneralStep 1 to 4

The effective slope is taken as  $7.45 \cdot 10^{-3}$  from the observations of section 4.4. Average values of the channel geometry for the study reach are plotted in FIGS. 4-12 to 4-15. Although the methods used in determining values of slope and hydraulic geometry are different than those of Einstein, the results are of no appreciable difference.

Step 5 and 6

The grain size composition of the bed is described by bed material samples 1 to 11, TABLE IV-4 and FIG. 4-20. The size which enters the equations of transport is  $D_{35} = 0.06$  feet, and the size characteristic for friction  $D_{65} = 0.125$  feet. The bed material sample is broken into the following size ranges, indicating the percent of the sample within each range and the geometric mean size of each range.

<u>Size Range</u> <u>inches</u>	<u>Percent of</u> <u>Material</u>	<u>D</u> <u>ft.</u>
> 6	1.6	
6 to 4	6.0	0.409
4 to 2	17.0	0.236
2 to 1	27.4	0.118
1 to 3/4	12.0	0.0721
3/4 to 7/16	18.0	0.0477
7/16 to 1/4	5.0	0.0275
< 1/4	13.0	





The bed-load discharge is calculated for grain sizes between 6 in. and 1/4 inch which covers 85.4 percent of the bed material.

### Hydraulic Calculations for Channel Without Bank Friction

#### Step 7

Assumed values of the hydraulic radius with respect to the grain,  $R_b'$ , are given in column (1) of TABLE A-1.

#### Step 8

The friction velocities of column (2) are calculated using  $V_*' = \sqrt{SR_b' g}$  with  $S = 7.45 \times 10^{-3}$  and  $g = 32.2 \text{ ft/sec.}^2$ .

#### Steps 9 to 12

The thickness of the laminar sublayer  $\delta = \frac{11.6 \nu}{V_*'}$  is determined in order to obtain a correction allowing for boundary conditions and thereby calculate the apparent roughness. With  $k_s' = D_{65} = 0.125$  feet, the values of  $k/\delta$  are large and this makes  $x = 1.0$  in all cases. The apparent roughness  $\Delta = k_s/x$  is therefore equal to 0.125 feet in all cases.

#### Step 13

The average flow velocity  $V_m$  is calculated using  $\frac{V_m}{V_*'} = 5.75 \log_{10} \left( 12.27 \frac{R_b' x}{k_s} \right)$  using the values of columns (1) and (2) with the result given in column (3).

#### Step 14

For the determination of the friction contribution of the channel irregularities the parameter  $\Psi'$  is calculated from



TABLE A-1

(1)	(2)	(3)	(4)	(5)	(6)	(7)	(8)	(9)	(10)	(11)
$R_b'$ ft.	$V_*'$ f.p.s.	$V_m$ f.p.s.	$\Psi'$	$V_m/V_*''$	$V_*''$ f.p.s.	$R_b''$ ft.	$R_b$ ft.	$A$ ft. <sup>2</sup>	$b_w$ ft.	$Q$ c.f.s.
0.5	0.346	3.36	26.4	5.9	0.57	1.35	1.85	212	115	712
0.8	0.438	4.78	16.5	7.0	0.68	1.92	2.72	420	152	2,000
1.0	0.490	5.60	13.2	7.7	0.73	2.22	3.22	550	170	3,080
1.2	0.536	6.39	11.0	8.3	0.77	2.47	3.67	690	187	4,400
1.4	0.580	7.12	9.44	8.9	0.80	2.67	4.07	820	200	5,840
1.6	0.620	7.82	8.25	9.3	0.84	2.94	4.54	970	213	7,580
1.8	0.658	8.50	7.32	9.8	0.87	3.15	4.95	1,180	230	9,850
2.0	0.693	9.12	6.60	10.3	0.89	3.30	5.30	1,280	239	11,700
2.5	0.774	10.6	5.28	11.6	0.91	3.44	5.94	1,600	260	17,000
3.0	0.848	12.0	4.40	12.8	0.94	3.68	6.68	1,950	280	23,400
3.5	0.916	13.4	3.77	13.4	1.00	4.16	7.66			

$$\Psi' = (s_s - 1) \frac{D_{35}}{R_b' S} \quad \text{with} \quad D_{35} = 0.06, \quad S = 7.45 \cdot 10^{-3} \quad \text{and} \quad s_s = 2.64.$$

These values are entered in column (4).

#### Step 15

From Einstein's FIG. 5 values  $V_m/V_*''$  are obtained for values of  $\Psi'$  and entered in column (5).

#### Step 16

Values of  $V_*''$  are calculated from columns (3) and (5) and tabulated in column (6).



Step 17

$R_b''$  is calculated from  $R_b'' = \frac{V_*'^2}{S_g}$  with  $S = 7.45 \cdot 10^{-3}$  and  $g = 32.2 \text{ ft/sec.}^2$  and placed in column (7).

Step 18

The two components  $R_b'$  and  $R_b''$  are usually the only components of the hydraulic radius  $R_b$  pertaining to the bed and are added directly and given in column (8).

Step 19

For the values of  $R_b$ , the cross sectional area  $A$  and the channel width  $b_w$  are taken from FIGS. 4-12, 4-13, 4-14 and placed in columns (9) and (10).

Step 20

The fluid discharge is then calculated from  $Q = V_m A$  using the values of columns (3) and (9).

Step 21

An average section rating curve was not constructed.

Steps 18 to 21 (Alternate)

Since the banks consist of similar material to the bed and are not stabilized by vegetation below bank full condition no additional calculations for bank friction are made.

Step 22

Representative grain sizes which are the geometric mean of each size range of step 5 are given in column (1) of TABLE A-2.





TABLE A-2

(1)	(2)	(3)	(4)	(5)	(6)	(7)	(8)	(9)
D ft.	$i_b$ %	$R_b$ ft.	$\Psi$	D/X	$\xi$	$\Psi_*$	$\Phi_*$	$i_b g_s$ lbs/ft.min.
0.409	6.0	0.5	180	4.25	1.0	120	--	--
		0.8	112			80	--	--
		1.0	90			60.1	--	--
		1.2	75			50.0	--	--
		1.4	64.2			42.8	--	--
		1.6	56.2			37.5	--	--
		1.8	50.0			33.4	--	--
		2.0	45.0			30.0	--	--
		2.5	36.0			24.0	0.0005	0.568
		3.0	30.0			20.0	0.0029	3.30
0.236	17.0	0.5	104	2.45	1.0	69.4	--	--
		0.8	65			43.4	--	--
		1.0	52			34.7	--	--
		1.2	43.2			28.8	--	--
		1.4	37.1			24.8	0.00035	0.492
		1.6	32.4			21.6	0.0015	2.11
		1.8	28.8			19.2	0.0040	5.63
		2.0	26.0			17.4	0.0072	10.1
		2.5	20.8			13.9	0.024	33.8
		3.0	17.3			11.6	0.050	70.4
0.118	27.4	0.5	52	1.23	1.03	35.8	--	--
		0.8	32.5			22.4	0.0010	0.796
		1.0	26			17.9	0.0062	4.93
		1.2	21.6			14.9	0.017	13.5
		1.4	18.6			12.8	0.033	26.2
		1.6	16.2			11.1	0.057	45.4
		1.8	14.4			9.87	0.088	70.0
		2.0	13.0			8.92	0.127	101
		2.5	10.4			7.15	0.260	206
		3.0	8.66			5.96	0.42	334
0.0721	12.0	0.5	31.8	0.75	1.50	31.8	--	--
		0.8	19.9			19.9	0.0031	0.513
		1.0	15.9			15.9	0.013	2.15
		1.2	13.2			13.2	0.029	4.80
		1.4	11.3			11.3	0.053	8.77
		1.6	9.93			9.93	0.086	14.2
		1.8	8.84			8.84	0.128	21.2
		2.0	7.95			7.95	0.185	30.6
		2.5	6.36			6.36	0.355	58.8
		3.0	5.30			5.30	0.57	94.3

..... (Cont'd.)



TABLE A-2 (Continued)

(1)	(2)	(3)	(4)	(5)	(6)	(7)	(8)	(9)
D ft.	$i_b$ %	$R_b'$ ft.	$\Psi$	D/X	$\xi$	$\Psi_*$	$\Phi_*$	$i_b g_s$ lbs/ft.min.
0.0477	18.0	0.5	21.0	0.496	3.7	51.9	--	--
		0.8	13.1			32.4	--	--
		1.0	10.5			26.0	0.00017	0.0233
		1.2	8.75			21.6	0.0015	0.206
		1.4	7.50			18.5	0.0050	0.686
		1.6	6.56			16.2	0.0112	1.54
		1.8	5.84			14.4	0.0192	2.63
		2.0	5.25			13.0	0.030	4.12
		2.5	4.20			10.4	0.074	10.2
		3.0	3.50			8.66	0.14	19.2
0.0275	5.0	0.5	12.1	0.286	15.0	121	--	--
		0.8	7.56			75.6	--	--
		1.0	6.05			60.5	--	--
		1.2	5.04			50.4	--	--
		1.4	4.31			43.1	--	--
		1.6	3.78			37.8	--	--
		1.8	3.36			33.6	--	--
		2.0	3.02			30.2	--	--
		2.5	2.42			24.2	0.00044	0.000735
		3.0	2.02			20.2	0.0025	0.00417

Step 23

The fraction by weight for each range of the total of the bed material samples  $i_b$  is given in column (2), expressed as a percent.

Step 24

Values of  $R_b'$  from 0.5 and 3.0 feet corresponding to calculated discharges of 712 to 23,400 c.f.s. are used in column (3).



Step 25

The intensity of shear  $\Psi$  is calculated from  $\Psi = (s_s - 1) D/R_b' S$  with  $s_s = 2.64$ ,  $S = 7.45 \times 10^{-3}$ ,  $D$  and  $R_b'$  from columns (1) and (3).

Step 26

The characteristic distance  $X$  is derived from  $X = 0.77 \Delta$  since in all cases  $\frac{\Delta}{\delta} \gg 1.80$ . Therefore  $X = 0.77 \times 0.125 = 0.0962$ .

Step 27

The ratio of  $D/X$  is placed in column (5) of TABLE A-2 from column (1) with  $X = 0.0962$ .

Step 28

Values of  $\xi$  are taken from Einstein's FIG. 7, from the known value of  $D/X$  in column (5) and placed in column (6).

Step 29

The  $Y$  value is obtained from FIG. 8, for values of  $k_s/\delta$ . Since  $k_s/\delta > 100$  was calculated in steps 9 to 12,  $Y = 0.53$  in all cases.

Step 30

$\beta_x$  is calculated from  $\beta_x = \log_{10} \left( 10.6 \frac{X}{\Delta} \right)$  and equals 0.912 with  $X = 0.0962$ , and  $\Delta = D_{65} = 0.125$  feet.

Step 31

$\beta = \log_{10} (10.6) = 1.025$  is divided by  $\beta_x = 0.912$  and squared to give  $\left( \frac{\beta}{\beta_x} \right)^2 = 1.26$ .





Step 32

The parameter  $\Psi_*$  is calculated from  $\Psi_* = \xi Y \left( \frac{\beta}{\beta_x} \right)^2 \Psi$  and the values are given in column (7). With  $Y = 0.53$  and  $\left( \frac{\beta}{\beta_x} \right)^2 = 1.26$ ,  
 $\Psi_* = 0.668 \xi \Psi$ .

Step 33

Column (8) gives values of  $\Phi_*$  corresponding to the values of  $\Psi_*$  from column (7) using FIG. 10.

Step 34

The bed-load rate  $i_b g_s$  is calculated from  $\Phi_*$  using  $i_b g_s = \Phi_* i_b \rho_s g^{3/2} (s_s - 1)^{1/2} D^{3/2}$  with  $\rho_s = 2.64 \times 1.94 = 5.12$ ,  $g^{3/2} = 185$ , and  $(s_s - 1)^{1/2} = 1.28$  with  $\Phi_*$ ,  $i_b$  and  $D$  from columns (8), (2) and (1) of TABLE A-2. This is given in column (9) of TABLE A-2 in lbs/ft.min. by multiplying by 60 sec/min.

Steps 35 to 42

This part of the calculation involves the determination of the suspended load of particle sizes for which the bed-load function exists. This portion is not considered since results are to be compared with the results of material moving as bed-load only. In all but the smallest size range  $z > 5$  making the expression  $(PI_1 + I_2 + 1)$  approximately 1. The method indicates a good portion of the smallest size range will go into suspension and  $i_T g_T = 1.2 i_b g_s$  but this makes no significant contribution to the total bed material discharge because of the small value of  $i_b g_s$  which results from small material sizes.



Steps 43 and 44

Values of  $i_b g_s$  have been taken from TABLE A-2 and the  $\Sigma i_b g_s$  for each stage given in TABLE V-5. These values have been multiplied by  $b_w$  from TABLE A-1 to give the total bed-load discharge in lbs/min. through the average cross section. These values have been given as  $G_s$  since the 13% of bed material smaller than 1/4 inch is mostly sand and the calculations of steps 35 to 42 indicate a large portion of this material would move in suspension. Any of this material moving as bed-load would not contribute significantly to the total values of  $G_s$  as can be seen from the bottom of TABLE A-2.



## APPENDIX B

### FIGURES





FIG. 3 - I

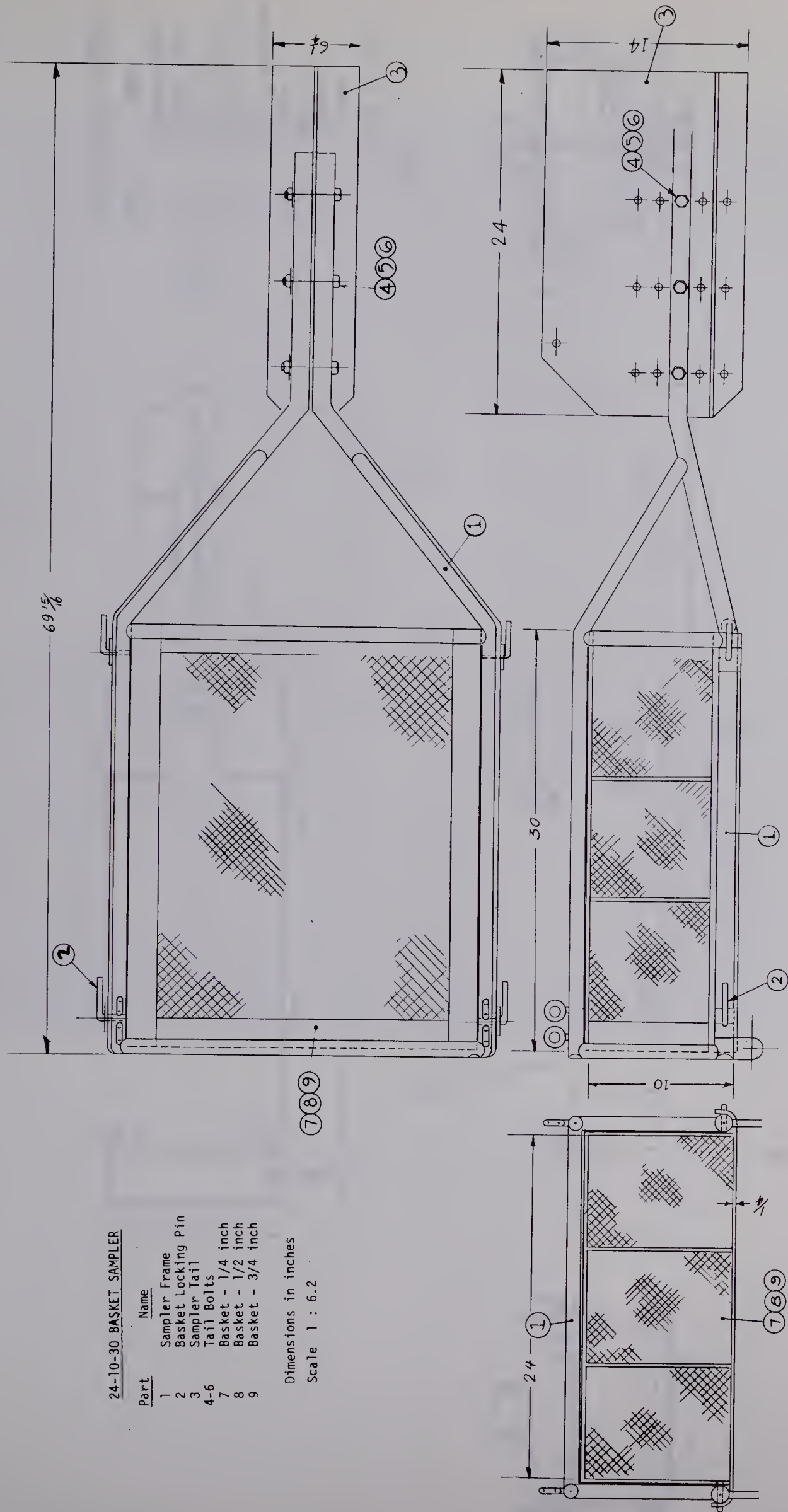




FIG. 3-2

HALF SIZE VUV SAMPLER

Part	Name
1	Sampler Body
2	Washer Lock
3	Tail Fin
4	Tail Frame
5	Tension Spring
6	Bolt
7	Screw Shoulder
8	Screw
9	Nut
10	Washer
11	Hanger

Dimensions in inches  
Scale 1 : 5.6

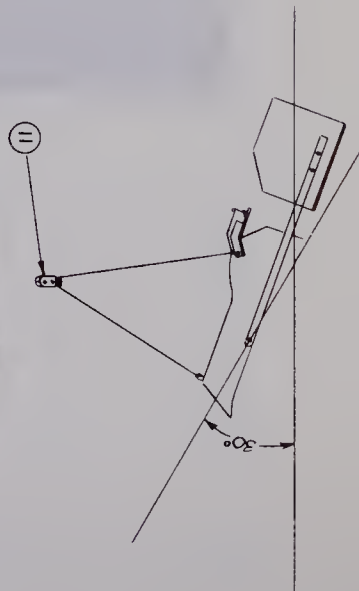
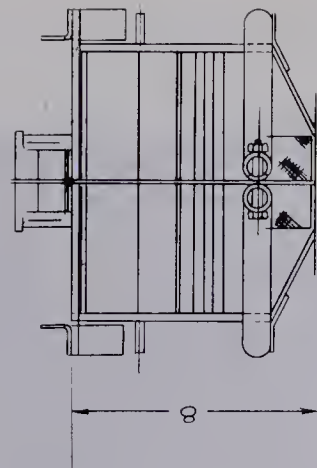
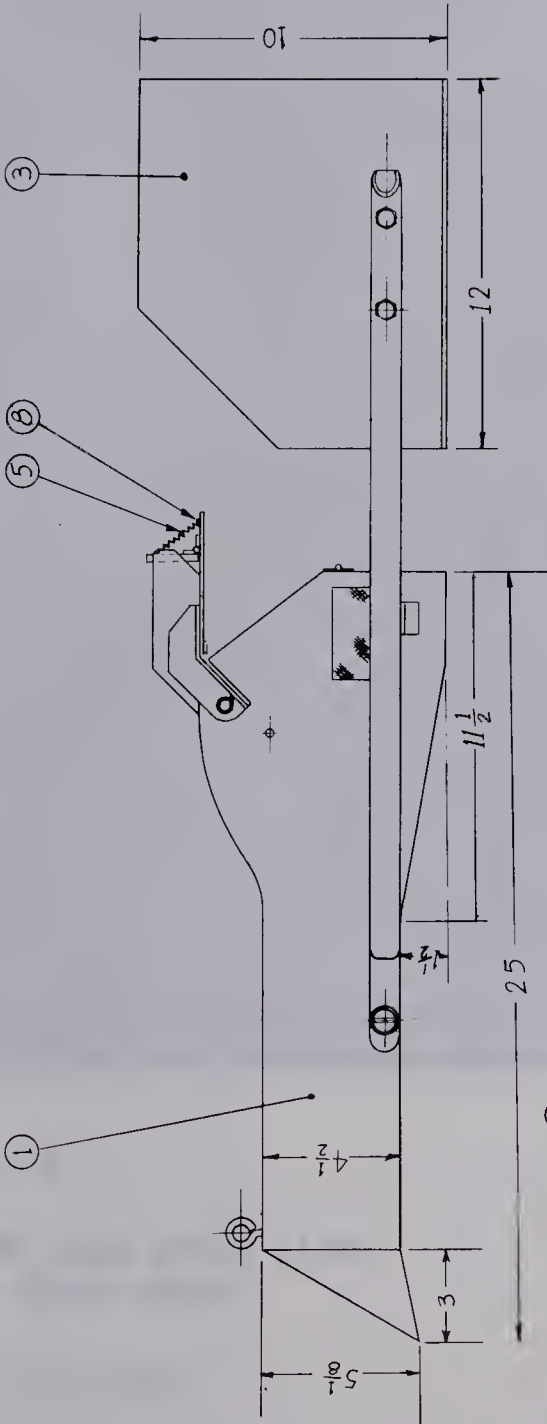
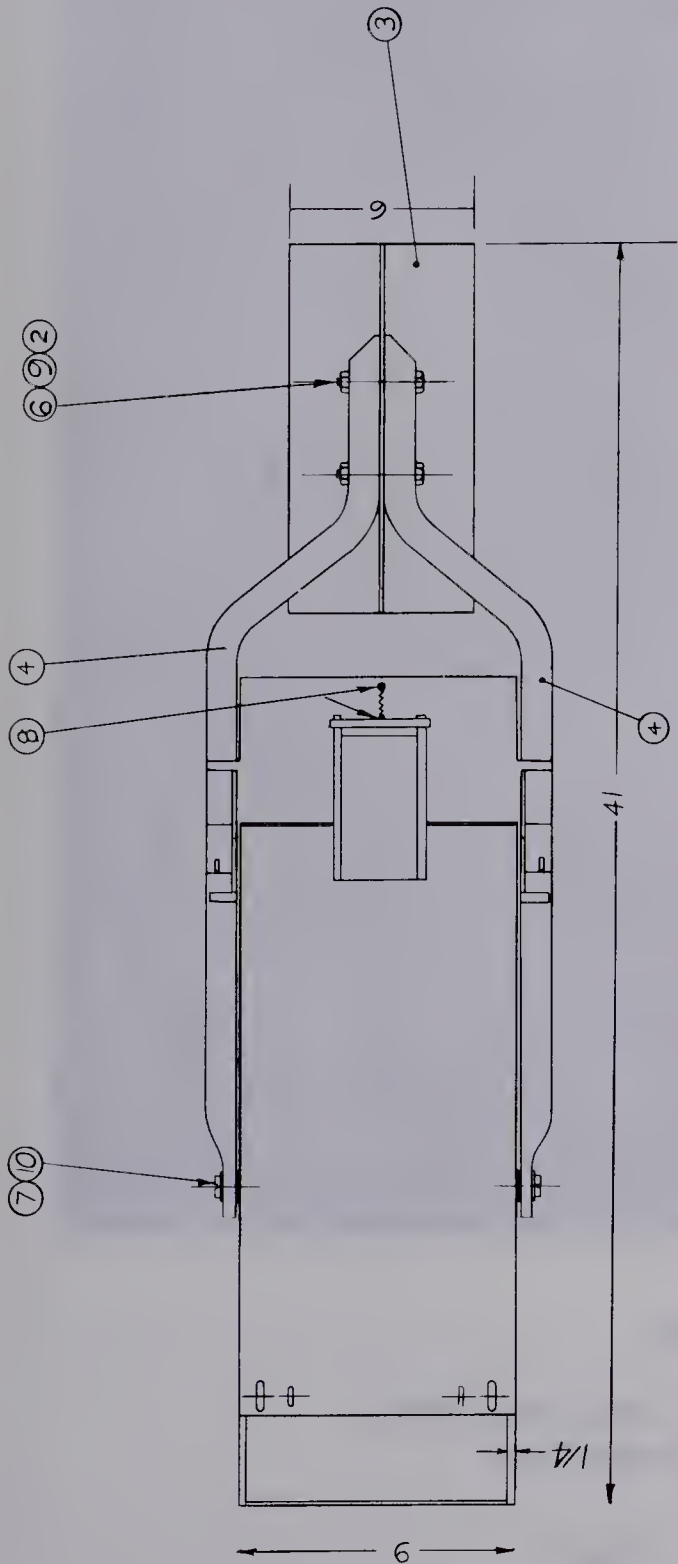








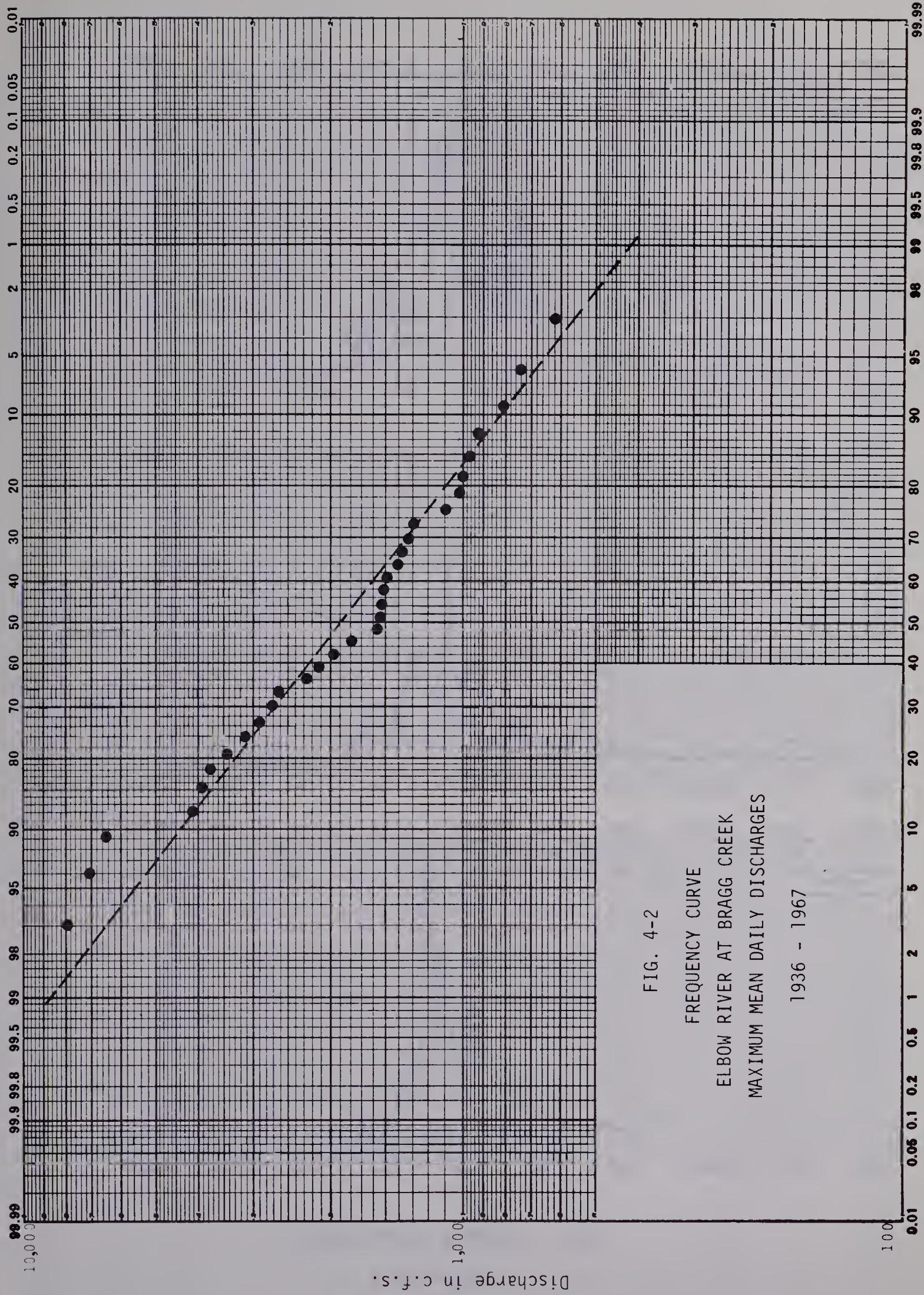
FIG. 4-1

TOPOGRAPHIC MAP OF ELBOW RIVER BASIN  
UPSTREAM OF BRAGG CREEK

Scale: 1:250,000

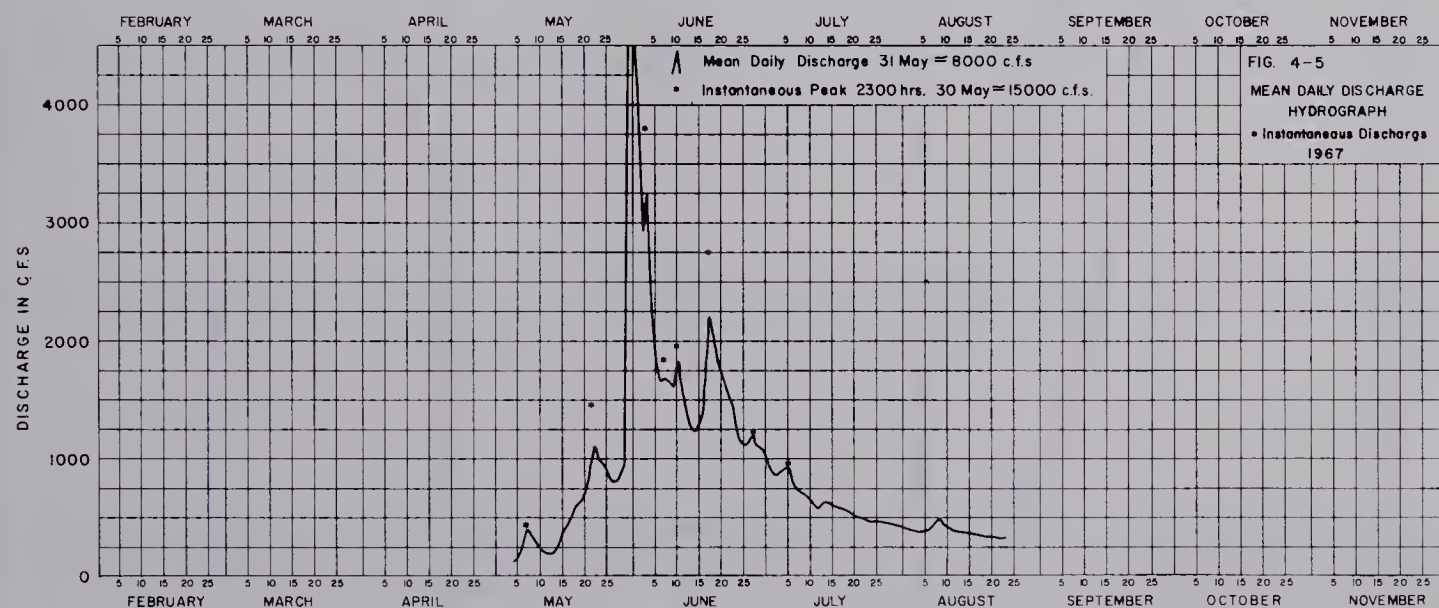
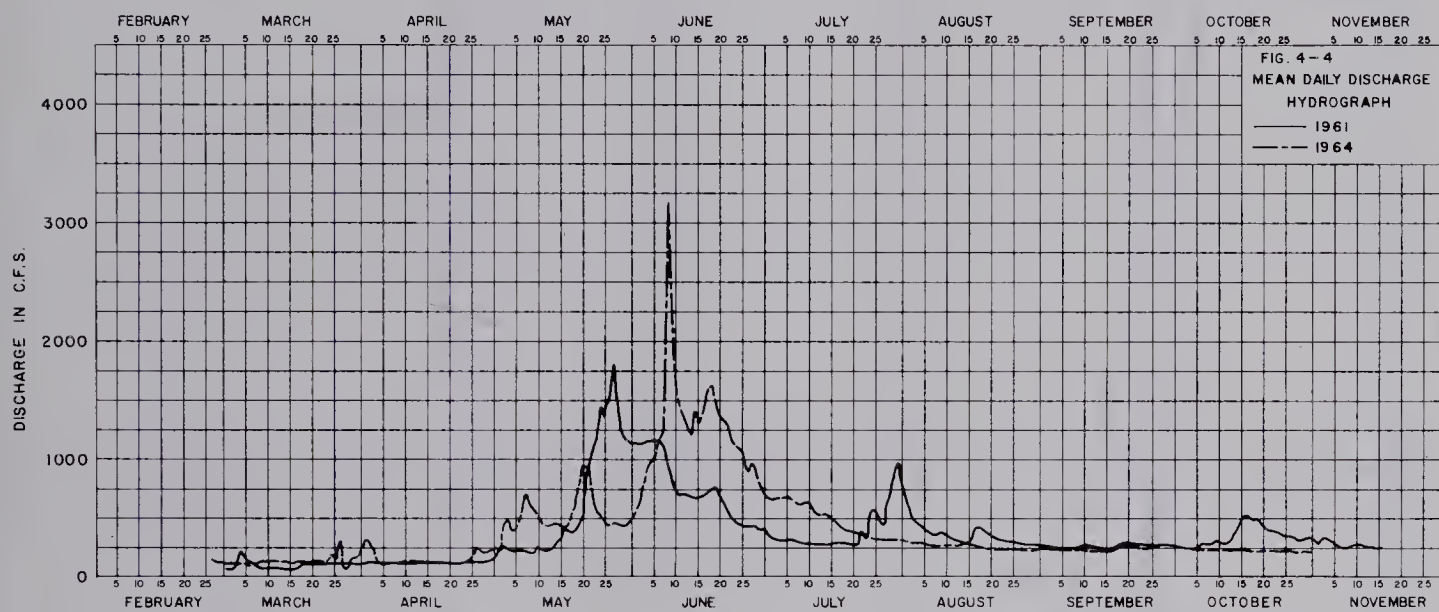
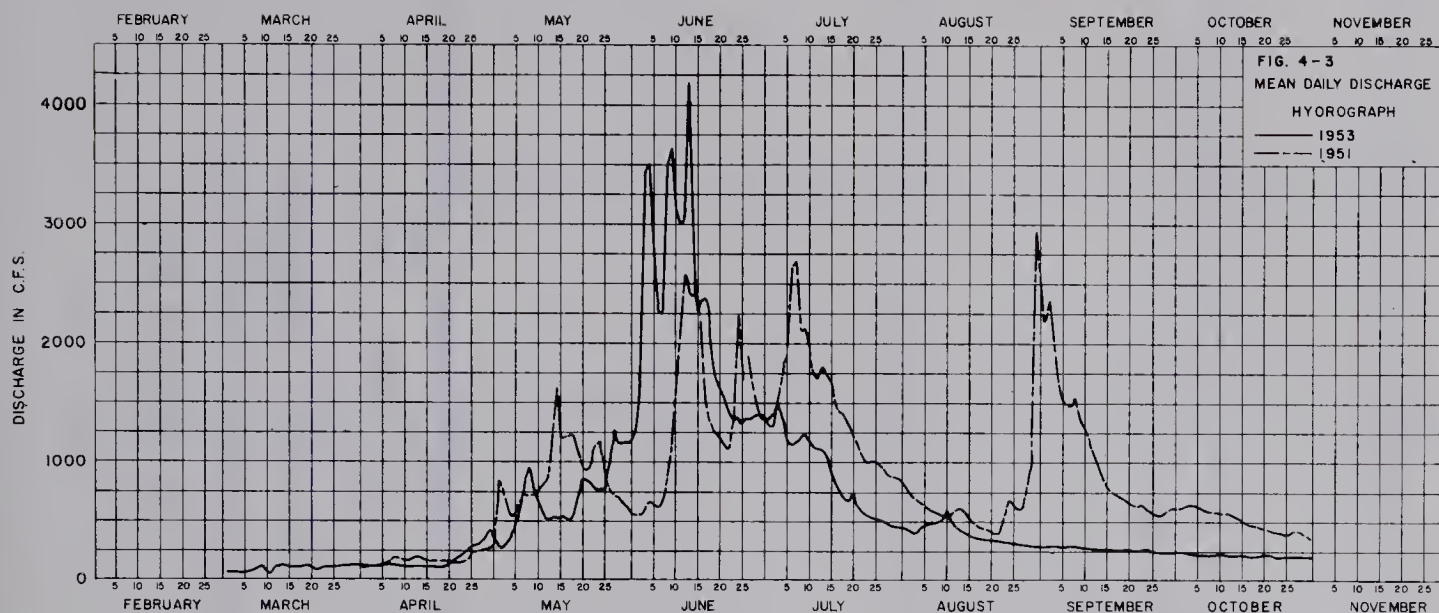












ELBOW RIVER @ BRAGG CREEK

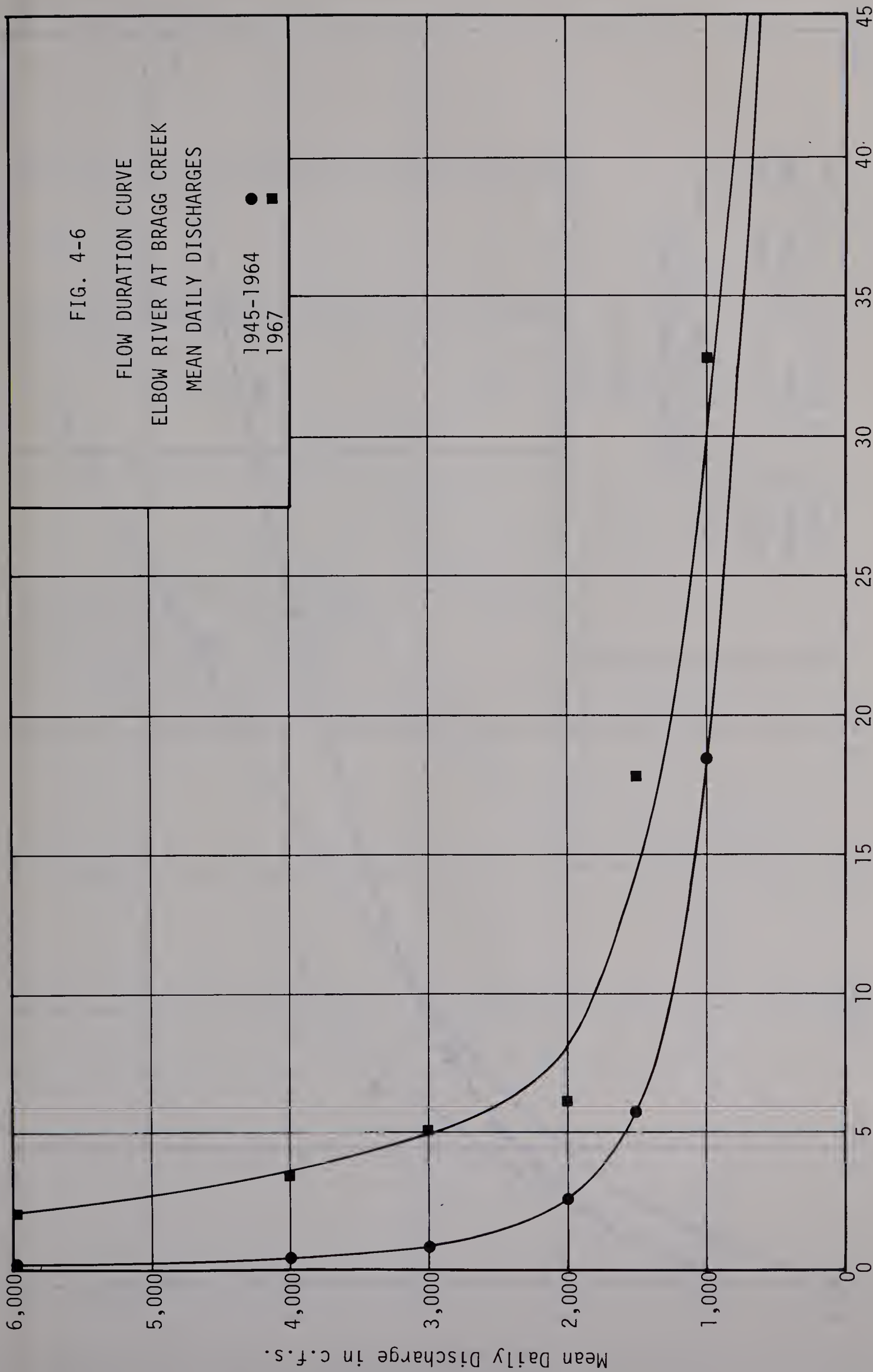
STATION 5BJ4

FIGS.(4-3),(4-4),(4-5)



FIG. 4-6  
 FLOW DURATION CURVE  
 ELBOW RIVER AT BRAGG CREEK  
 MEAN DAILY DISCHARGES

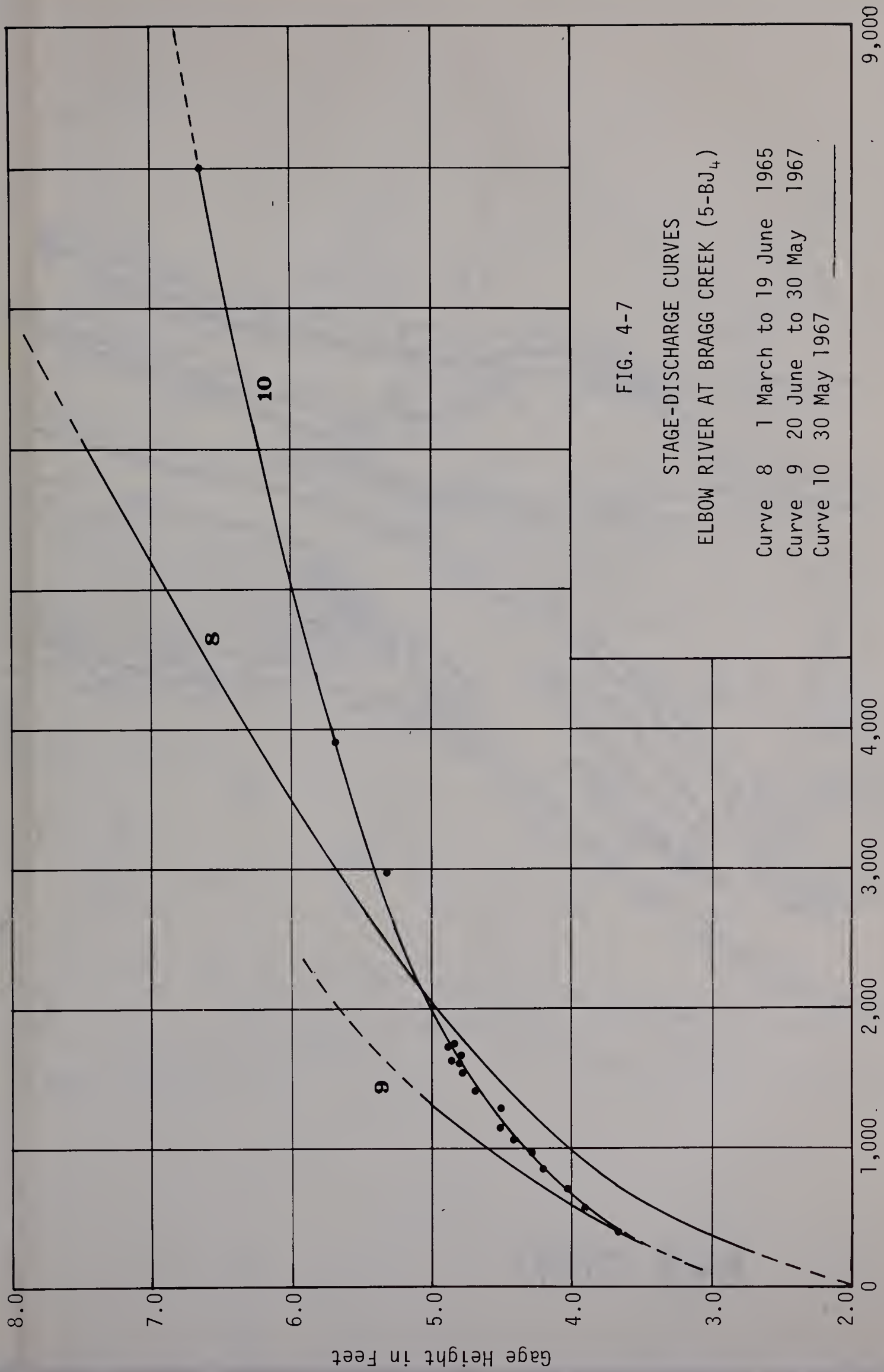
1945-1964 ●  
 1967 ■



Number of Days Per Year, Discharge is Equalled or Exceeded









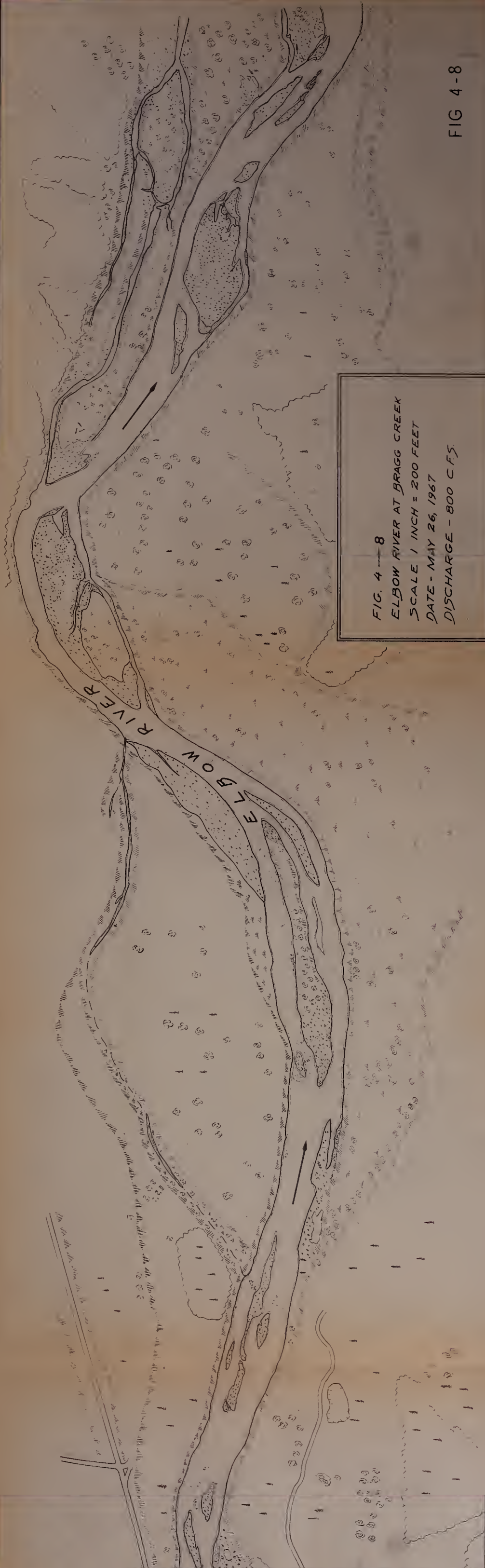


FIG. 4-8

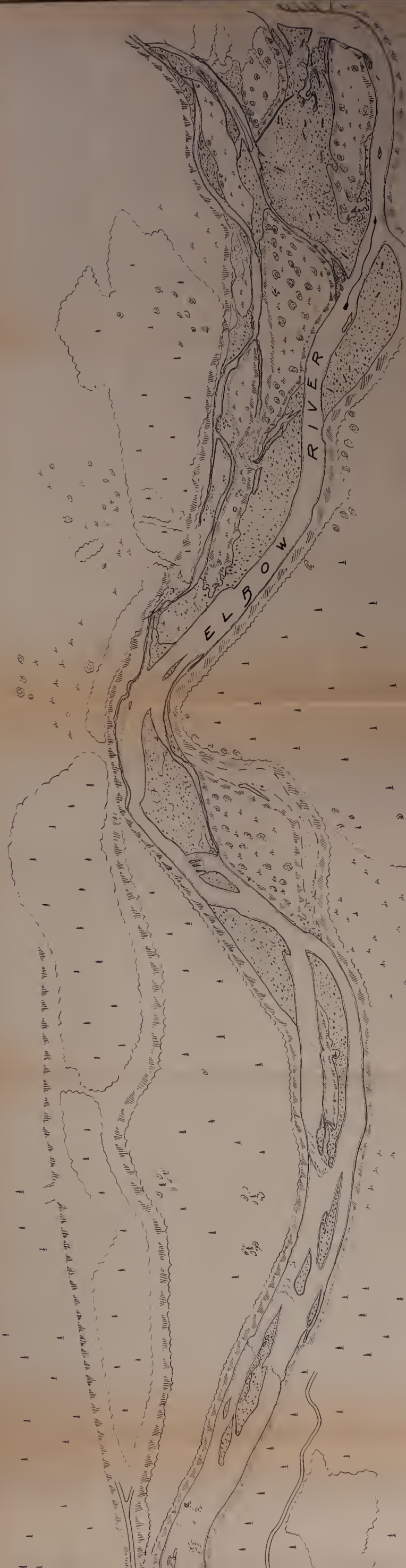
ELBOW RIVER AT BRAGG CREEK  
SCALE 1 INCH = 200 FEET  
DATE - MAY 26, 1967  
DISCHARGE - 800 C.F.S.



FIG. 4—9  
ELBOW RIVER AT BRAGG CREEK  
SCALE 1 INCH = 200 FT.  
DATE - JUNE 26, 1967  
DISCHARGE - 4500 C.F.S.



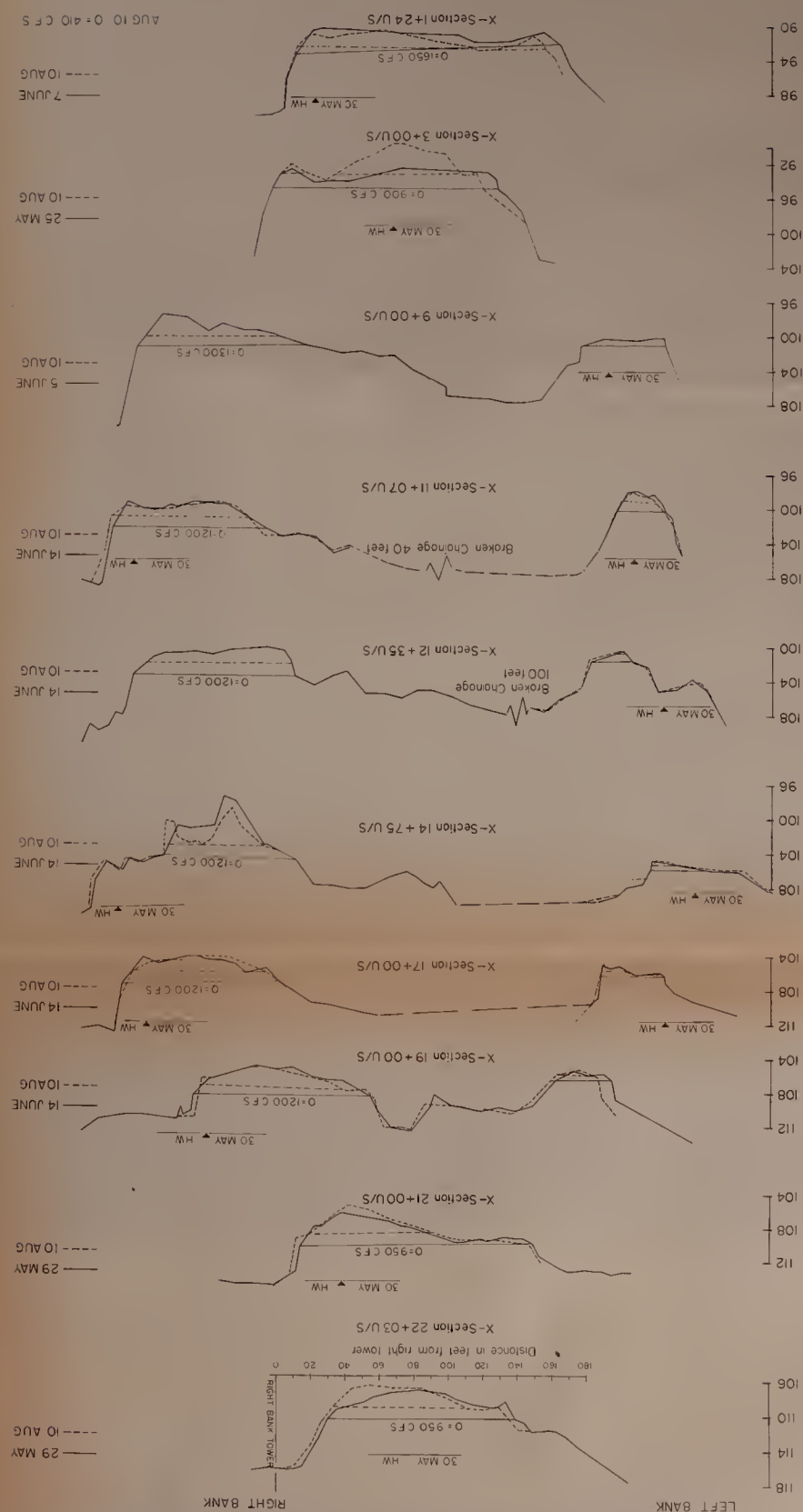
FIG. 4-9







Elevation in feet



ELBOW RIVER @ BRAGG CREEK  
CROSS SECTIONS, UPSTREAM FROM BRIDGE



### Cross Sections Downstream from Bridge

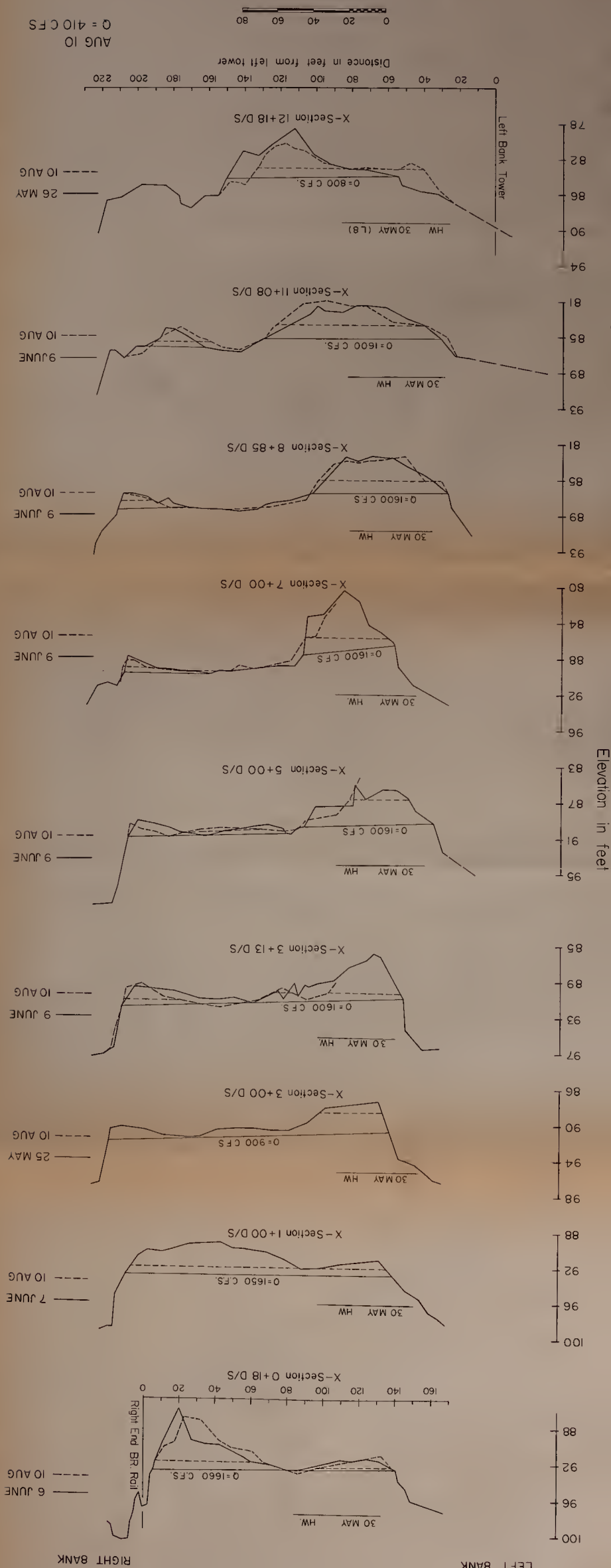


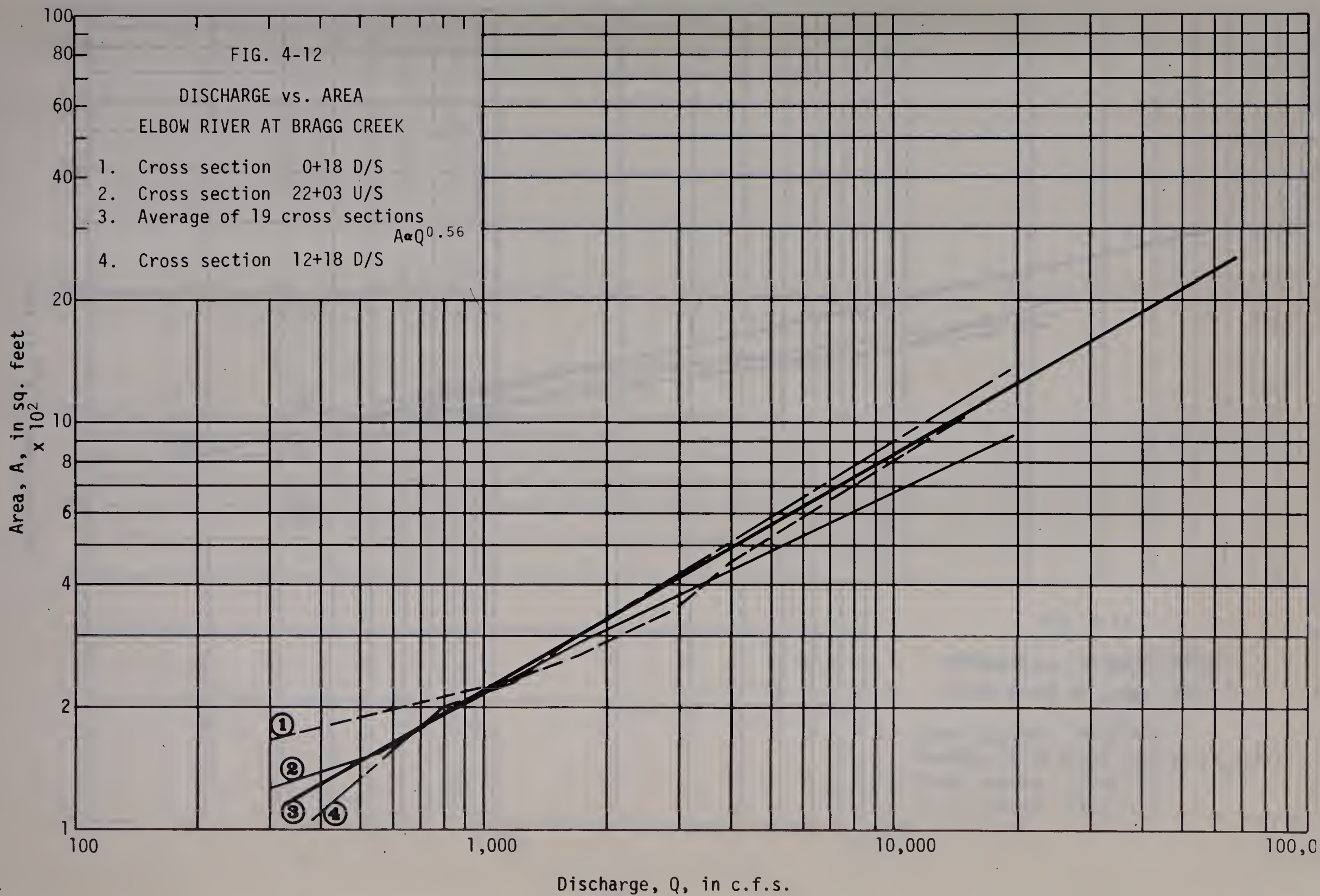


FIG. 4-12

DISCHARGE vs. AREA  
ELBOW RIVER AT BRAGG CREEK

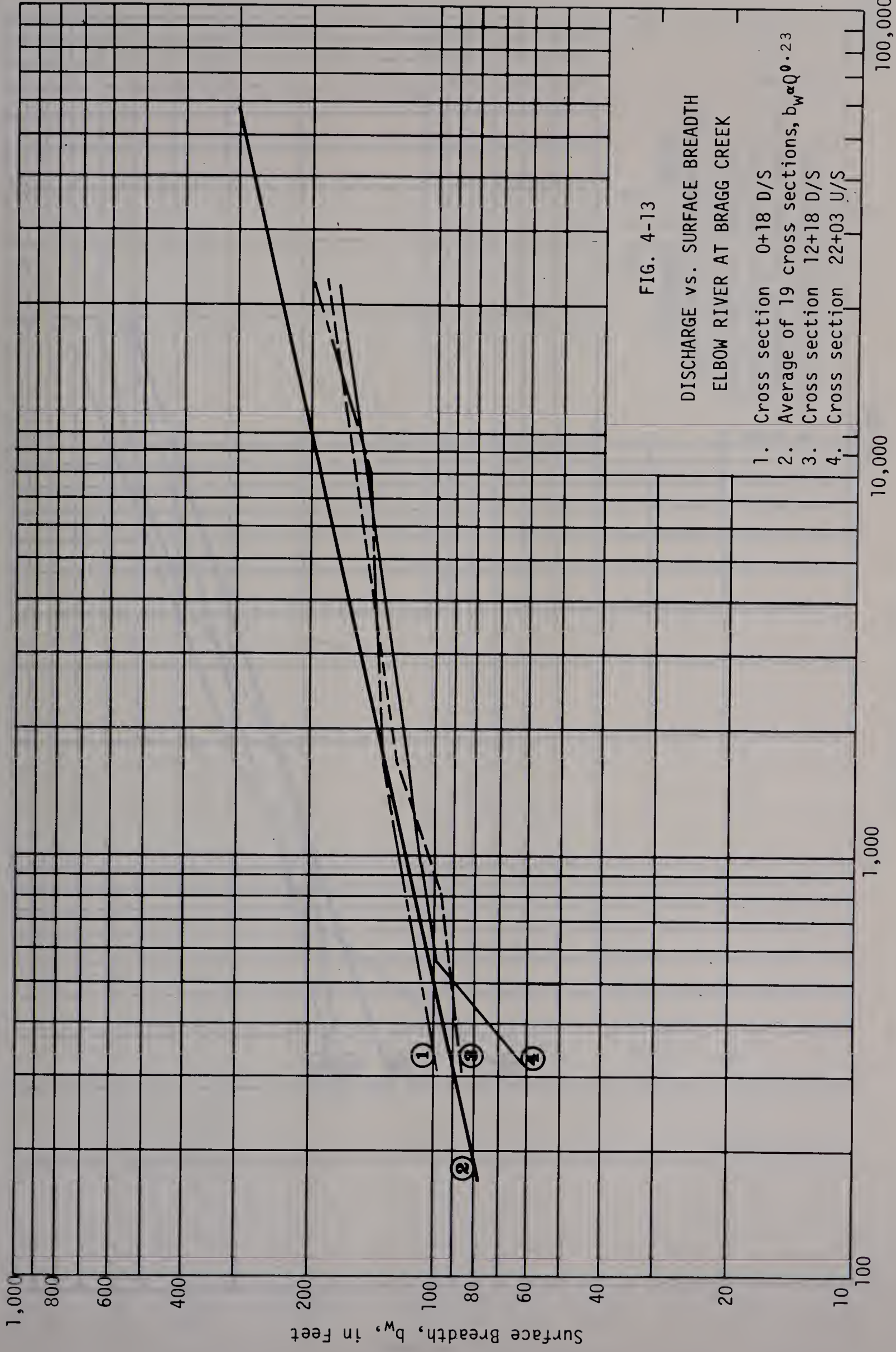
1. Cross section 0+18 D/S
2. Cross section 22+03 U/S
3. Average of 19 cross sections
4. Cross section 12+18 D/S

$$A \propto Q^{0.56}$$





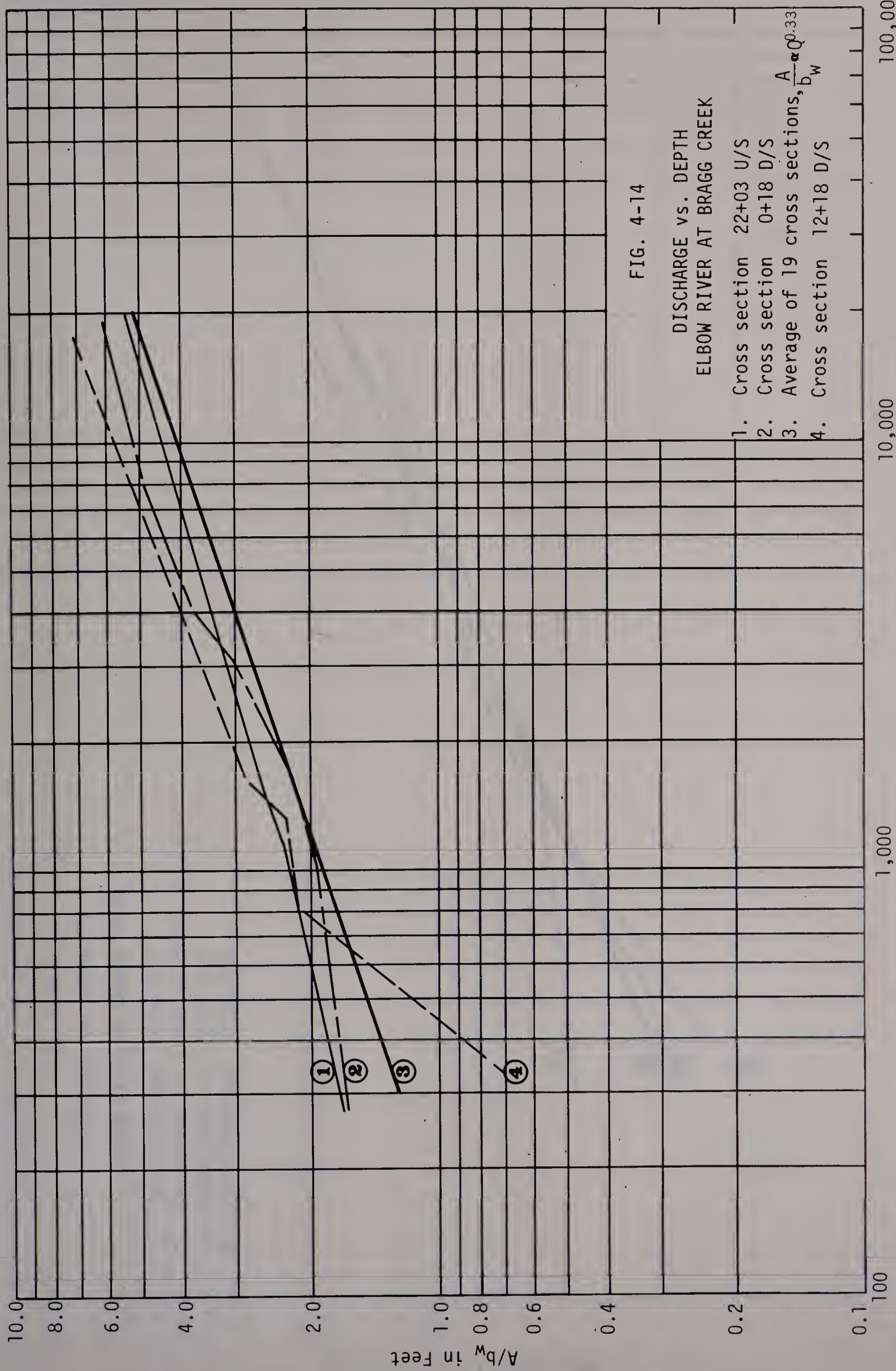




Discharge,  $Q$ , in c.f.s.

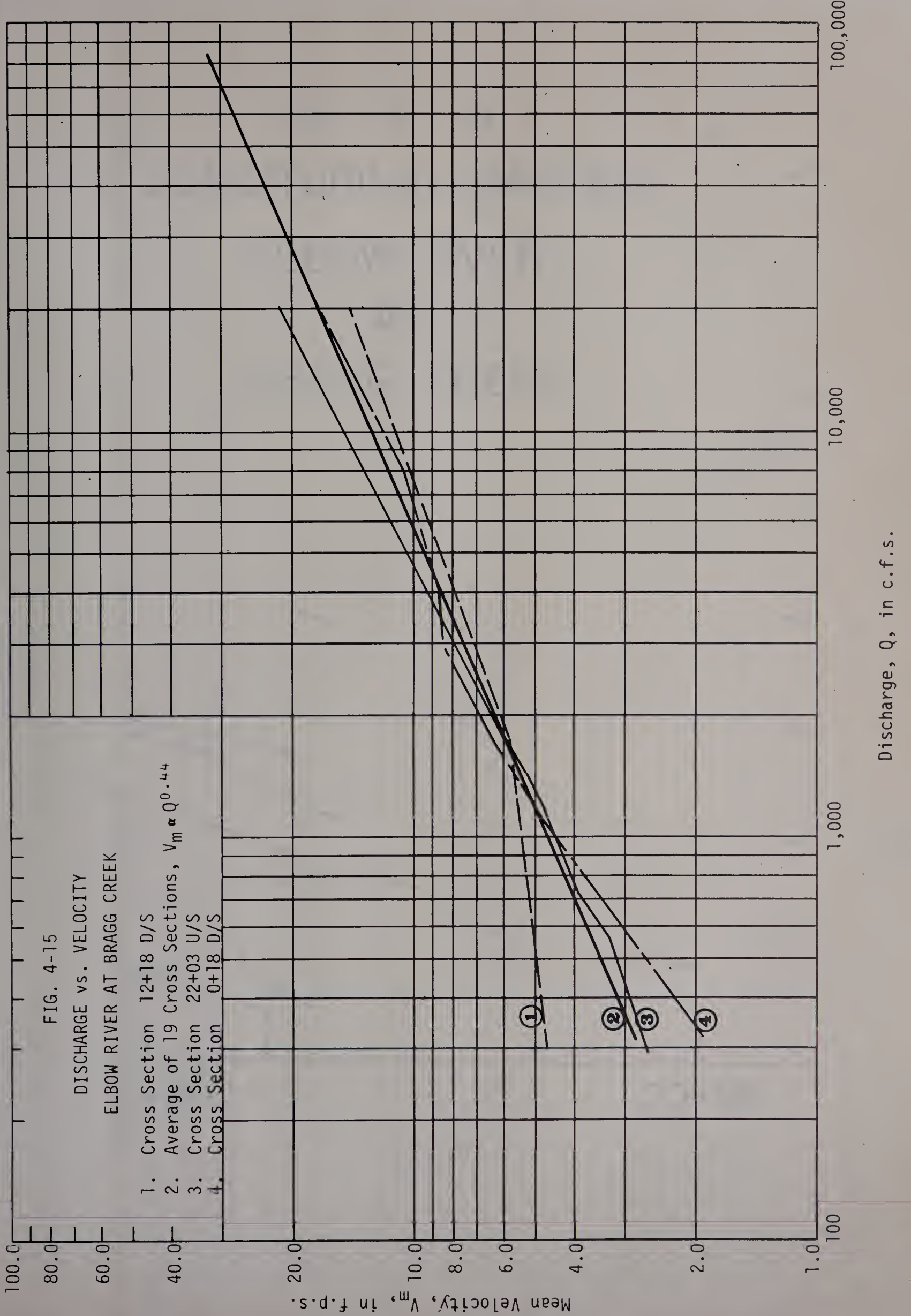






Discharge, Q, in c.f.s.



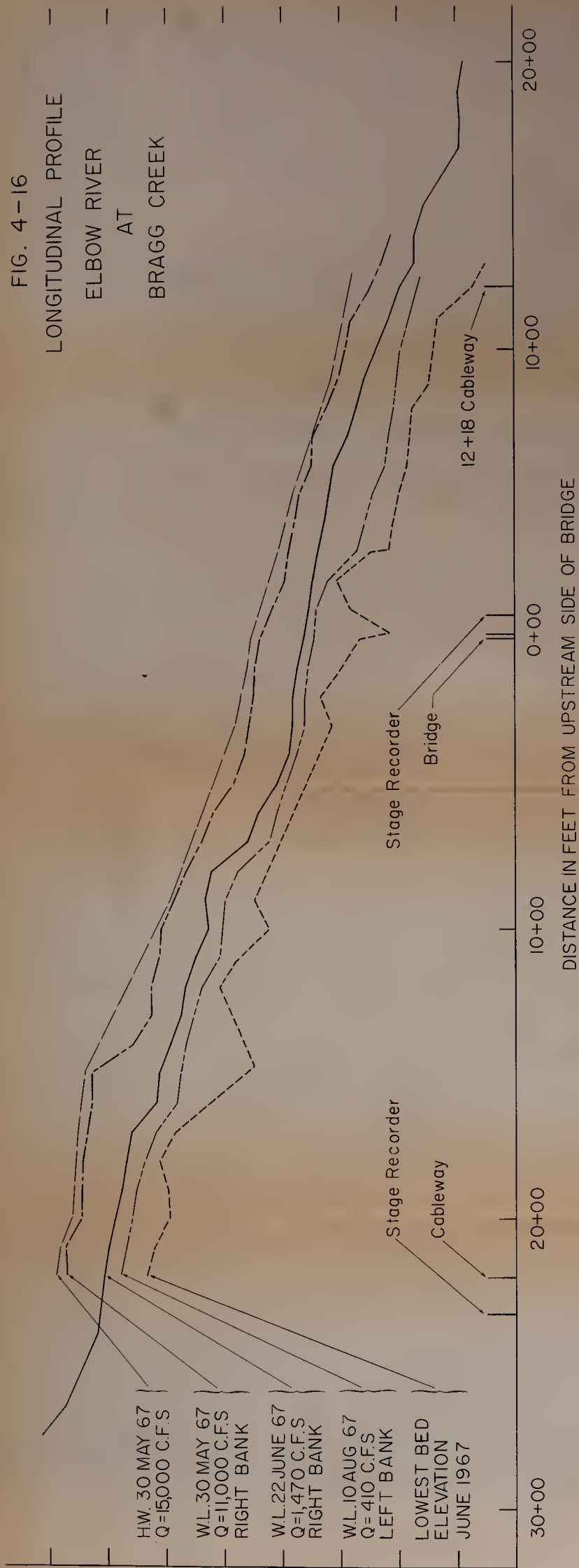








ELEVATION IN FEET, Assumed Datum 100.00 at Bridge B.M.





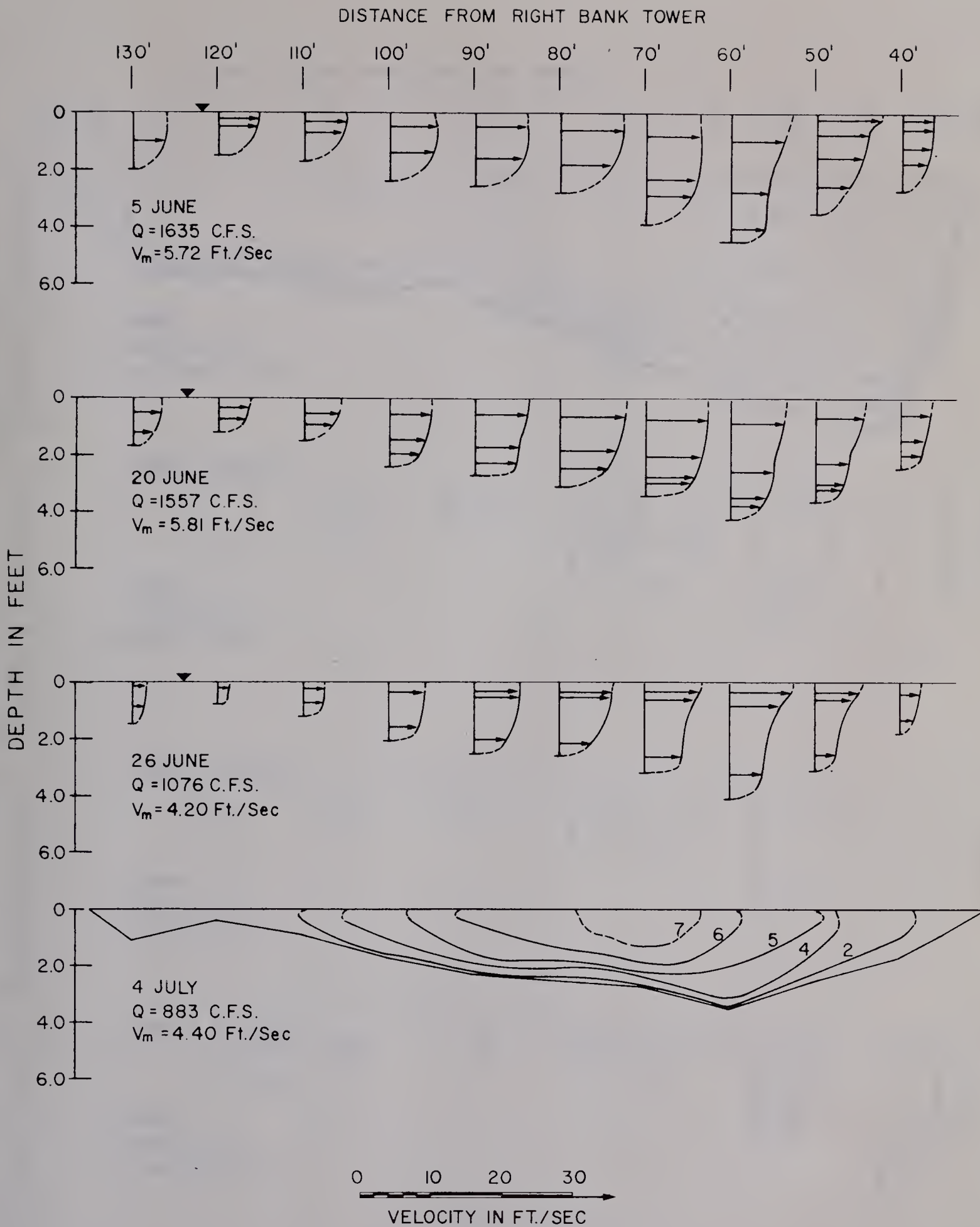
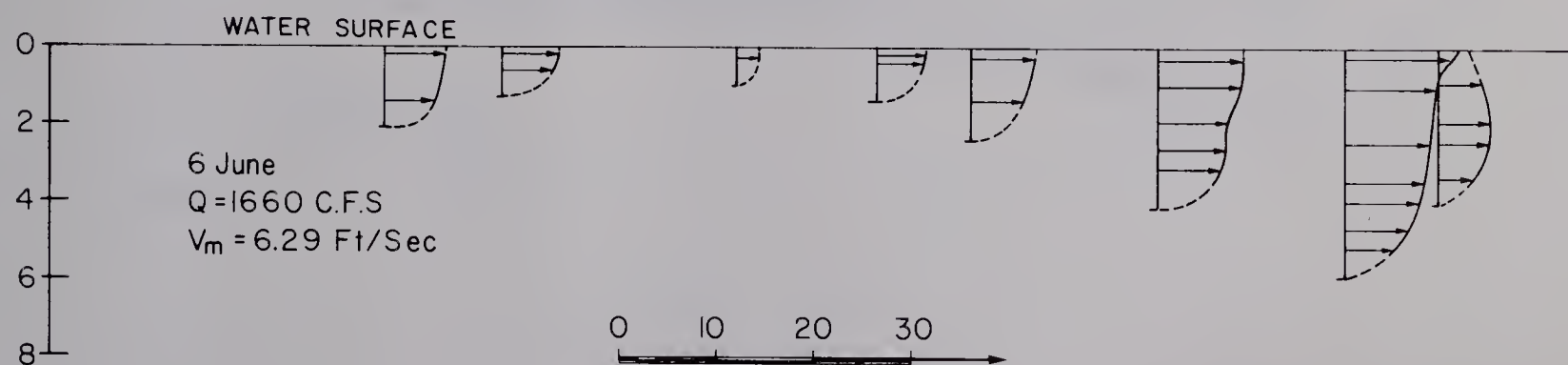
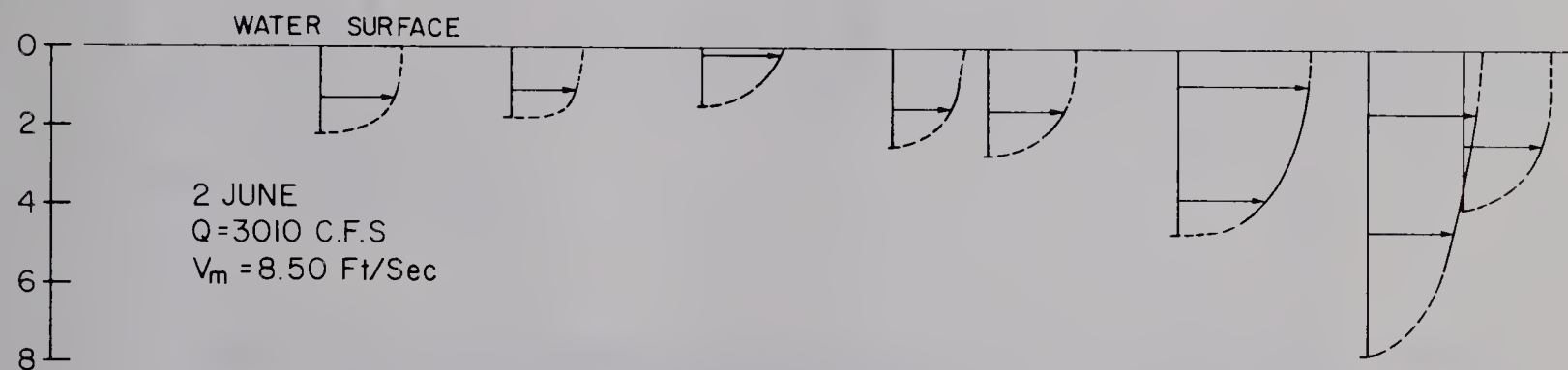
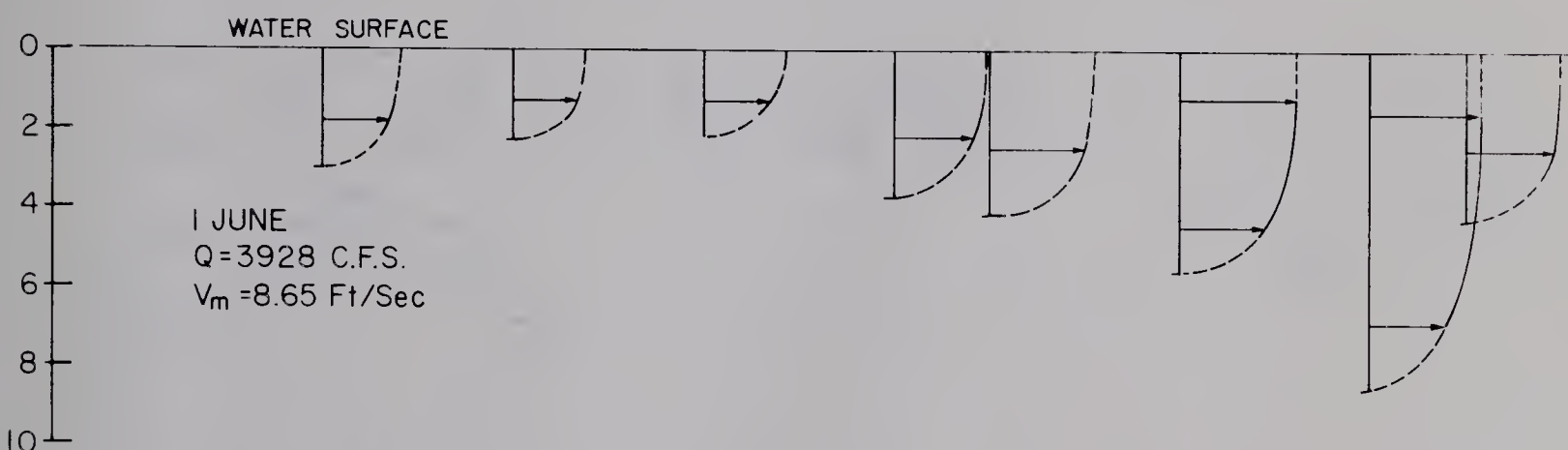
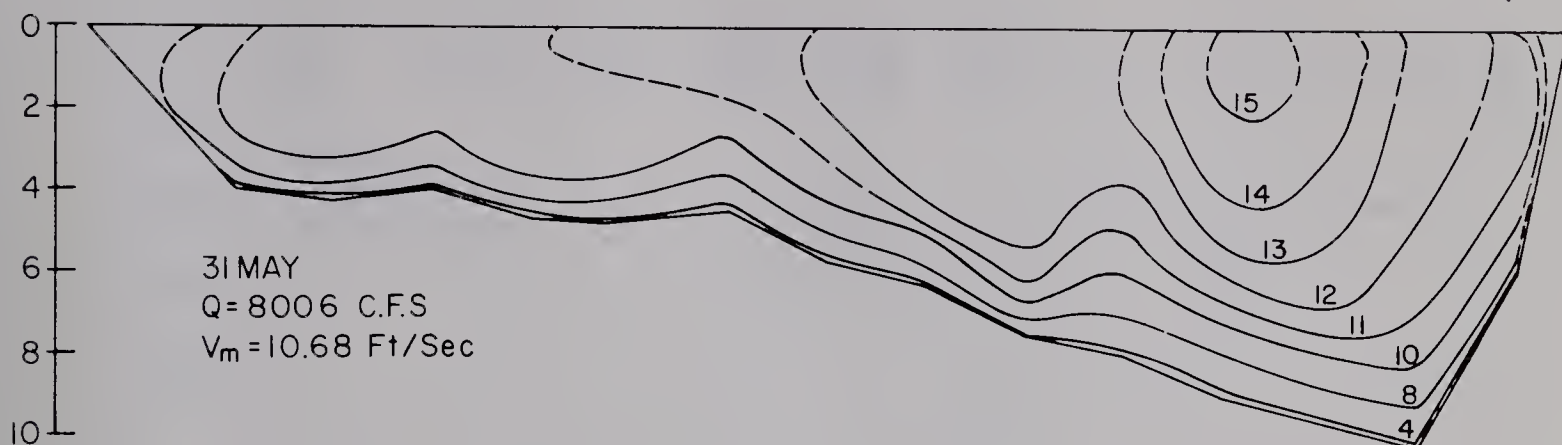


FIG. 4-17  
X-SECTION 22+03 U/S.  
VELOCITY DISTRIBUTION.



DISTANCE FROM RIGHT END OF BRIDGE.

136' 130' 120' 110' 100' 90' 80' 70' 60' 50' 40' 30' 20' 16'



0 10 20 30

VELOCITY IN FEET/SEC

FIG. 4-18 X-SECTION 0+18 D/S  
VELOCITY DISTRIBUTION





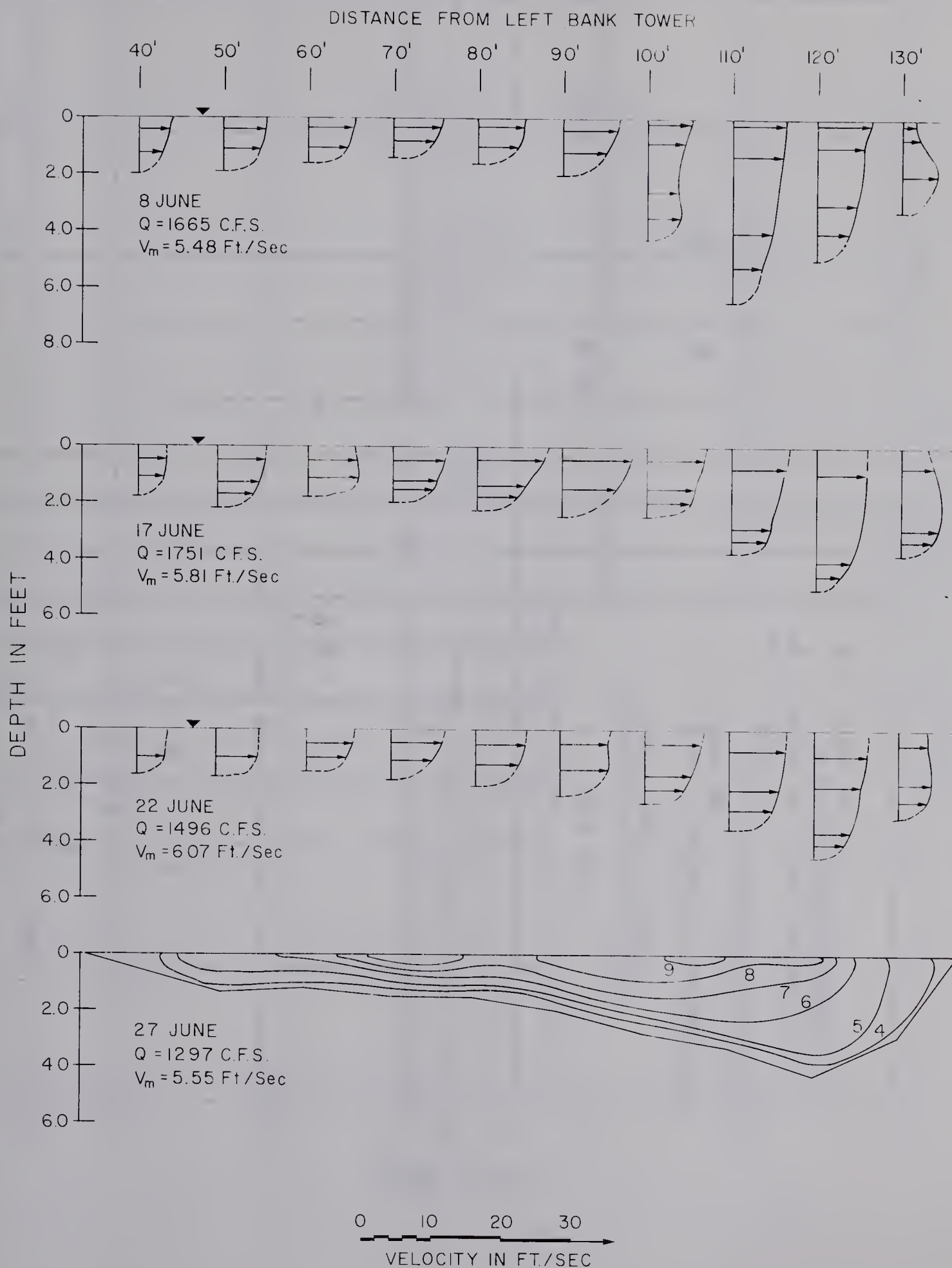
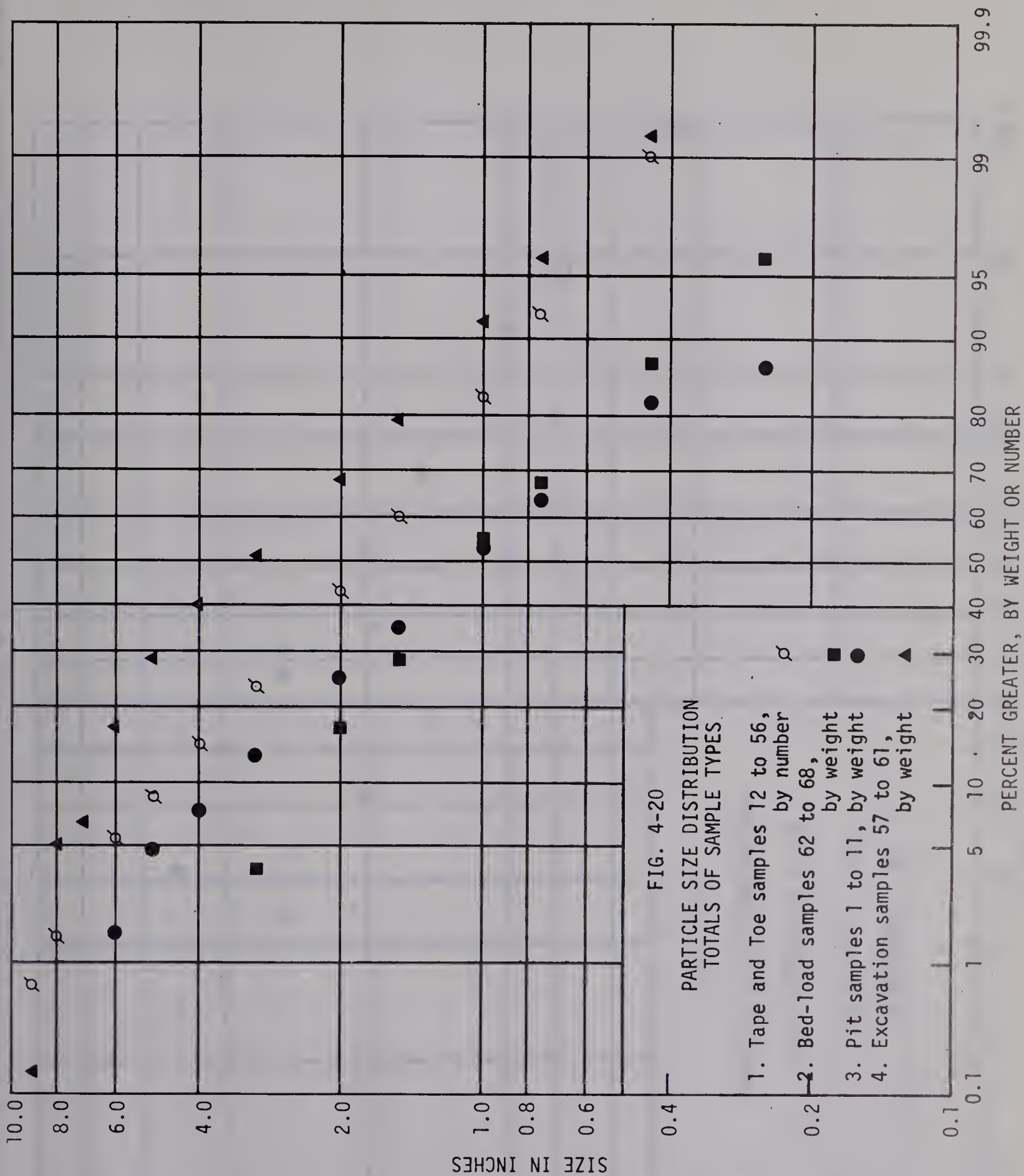
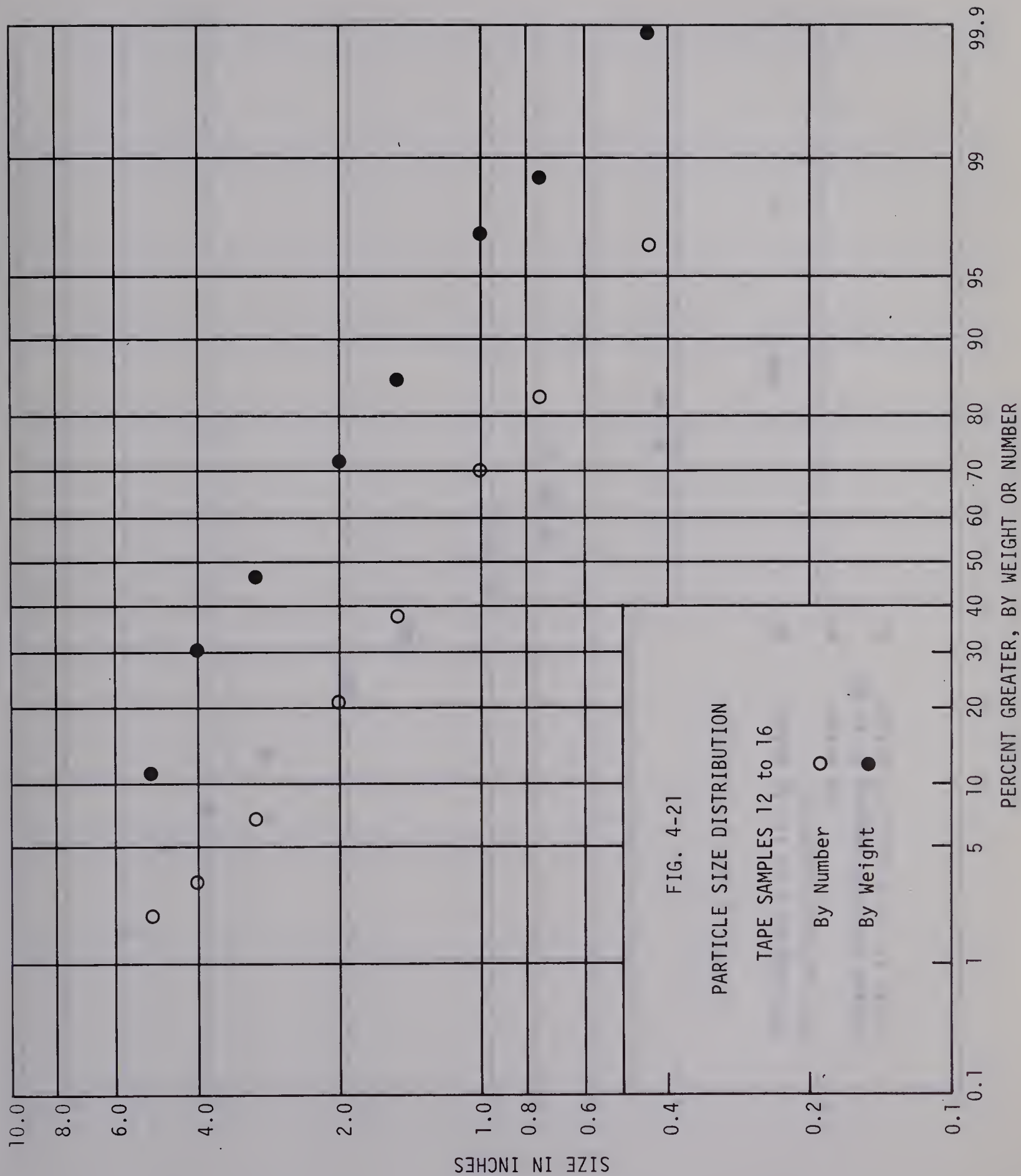


FIG.4-19  
X-SECTION 12+18 D/S  
VELOCITY DISTRIBUTION



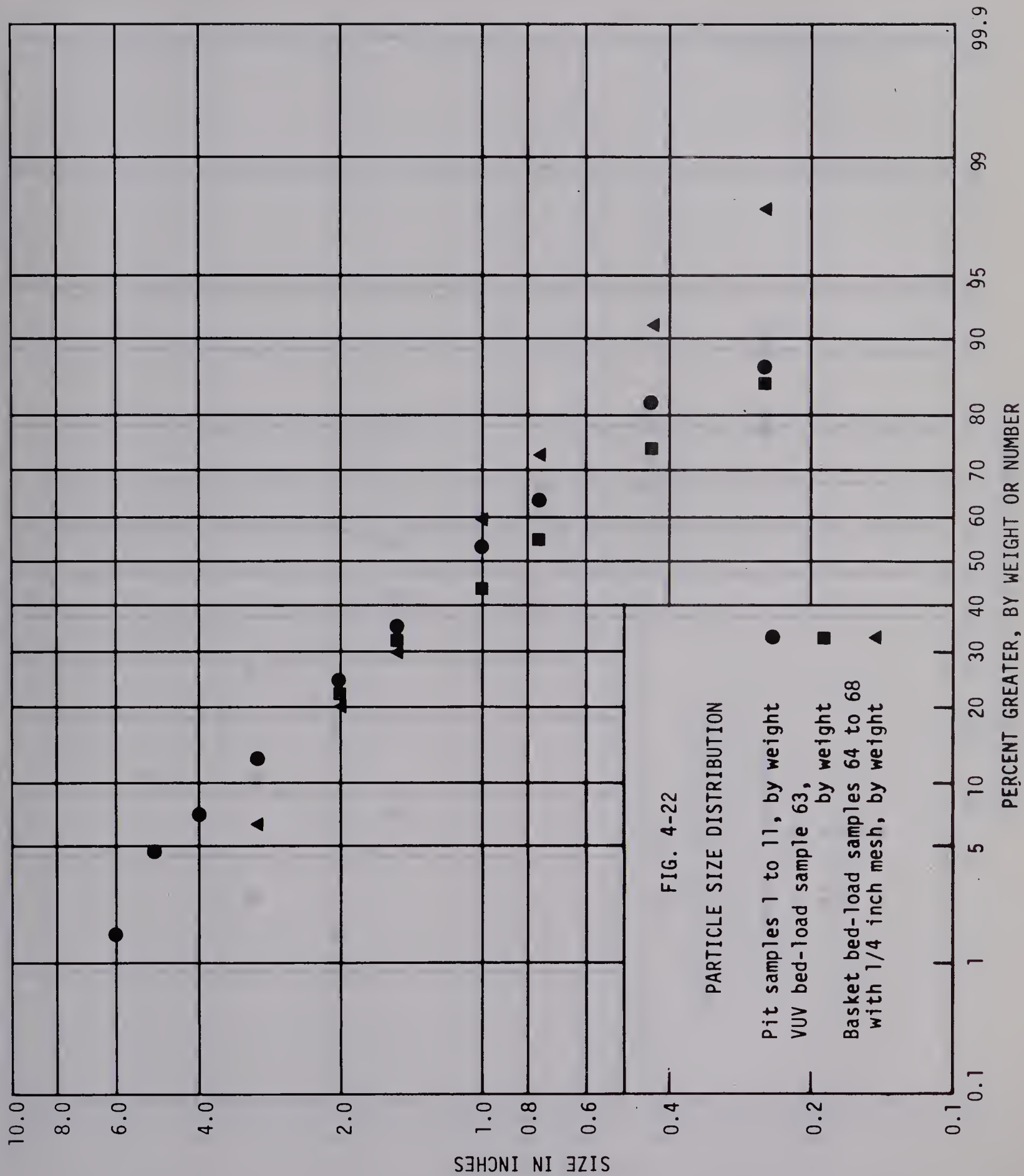




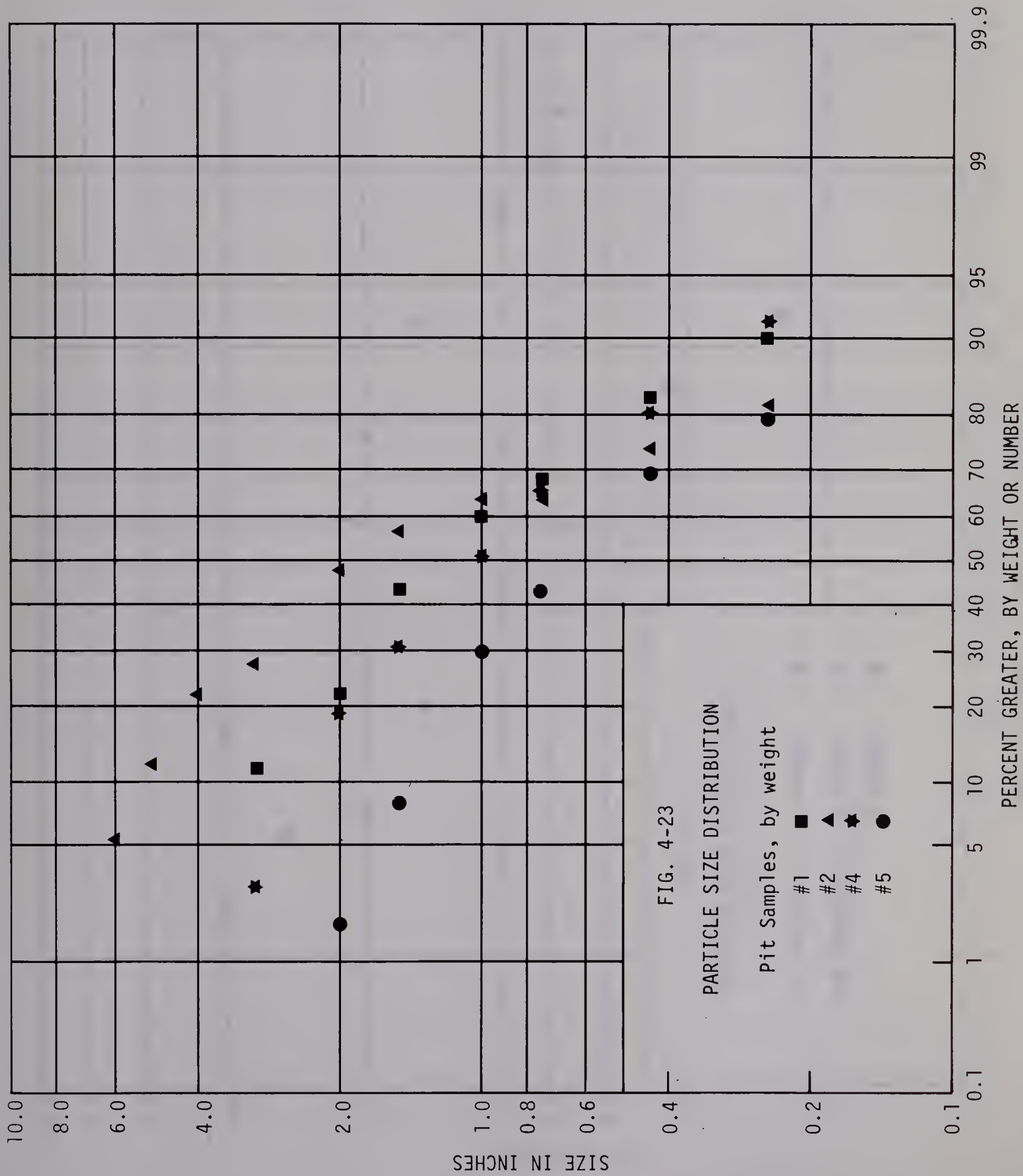






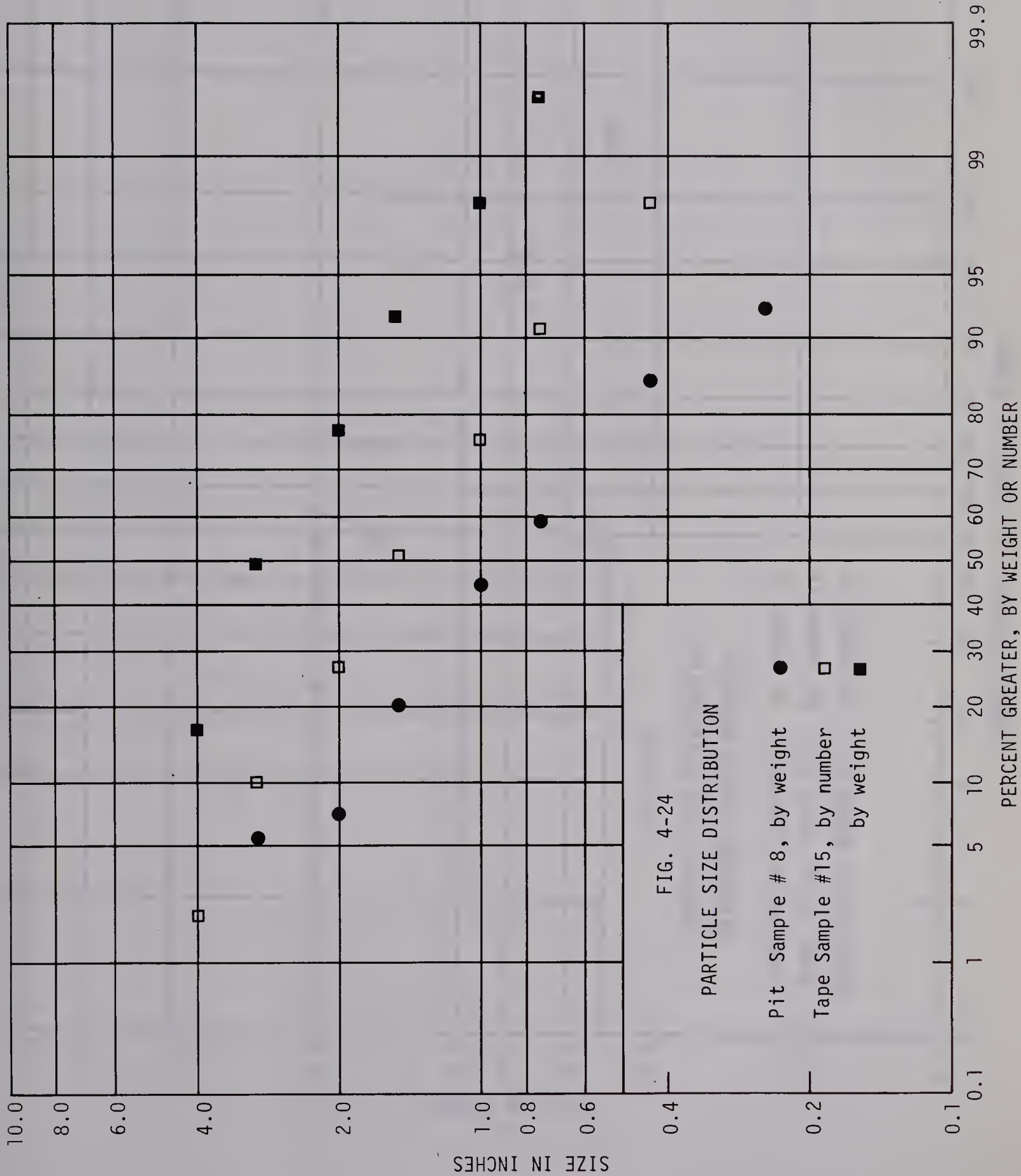




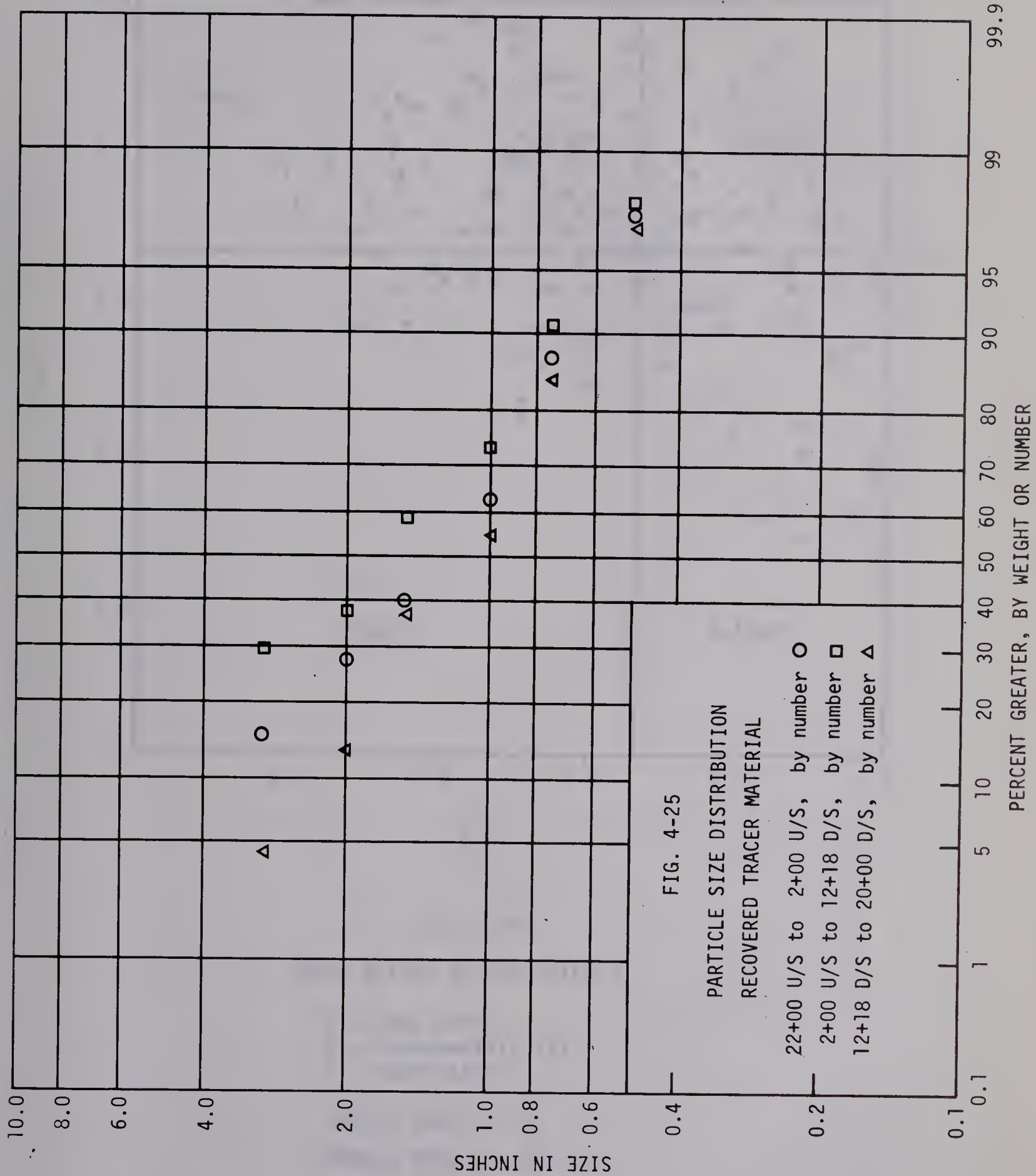














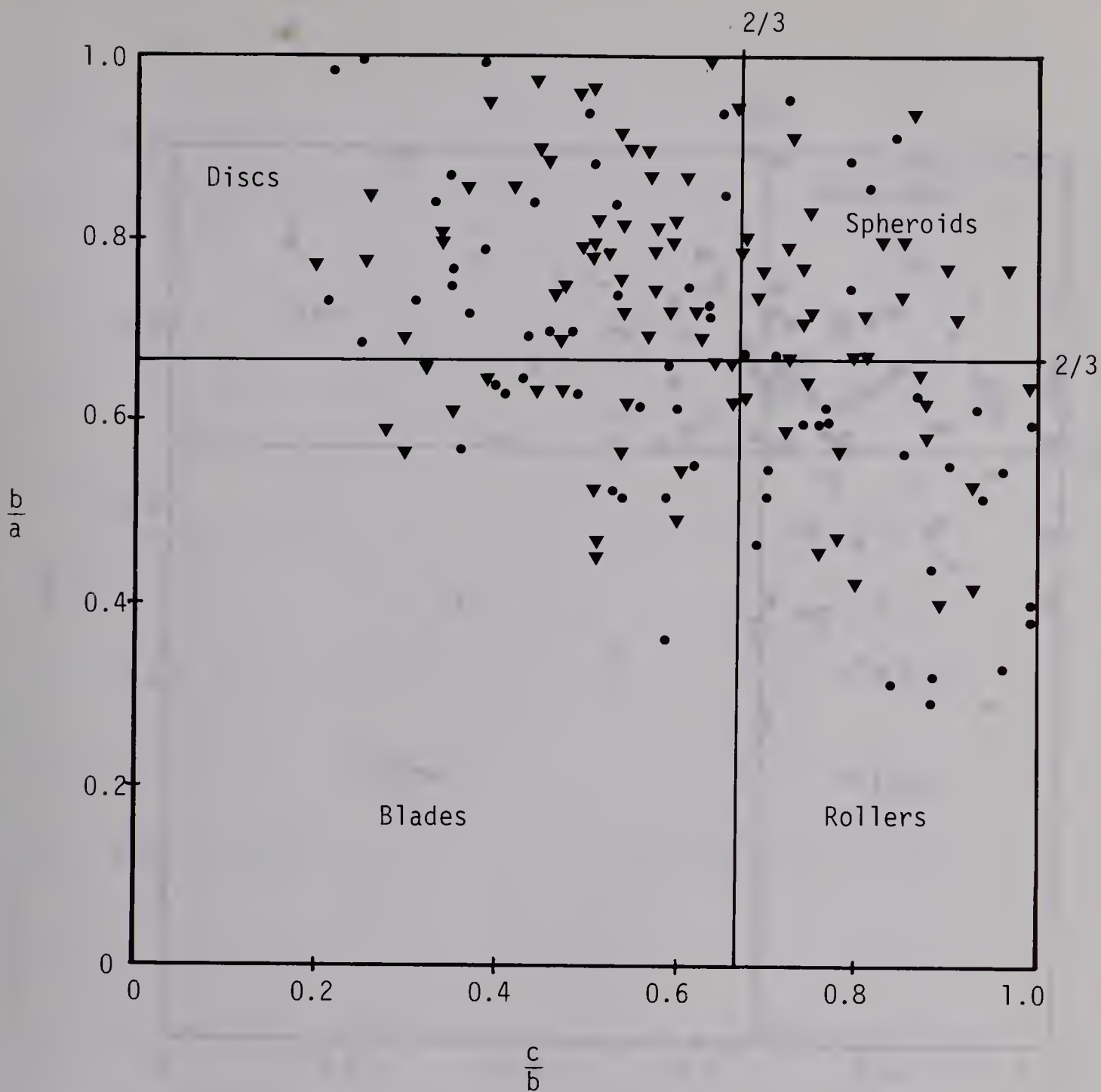


FIG. 4-26

#### SHAPE RATIOS OF BED MATERIAL

a - long axis  
b - intermediate axis  
c - short axis

Sample #36,  $b > 3"$  •

Sample #58,  $b > 3"$  ▼





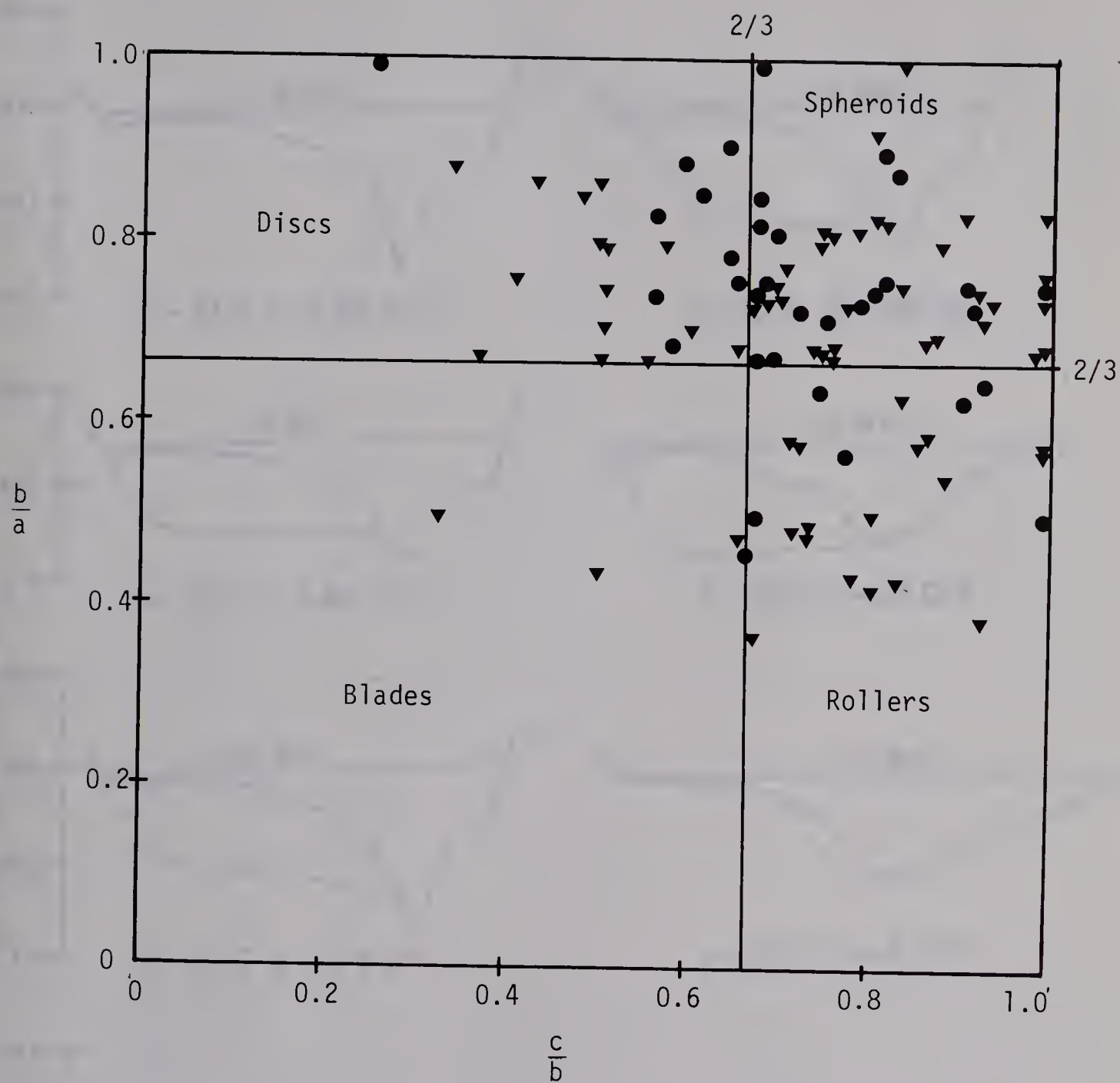


FIG. 4-27

# SHAPE RATIOS OF BED-LOAD MATERIAL

- a - long axis
- b - intermediate axis
- c - short axis

Sampled bed-load material ▼

Sampled bed-load tracer material ●



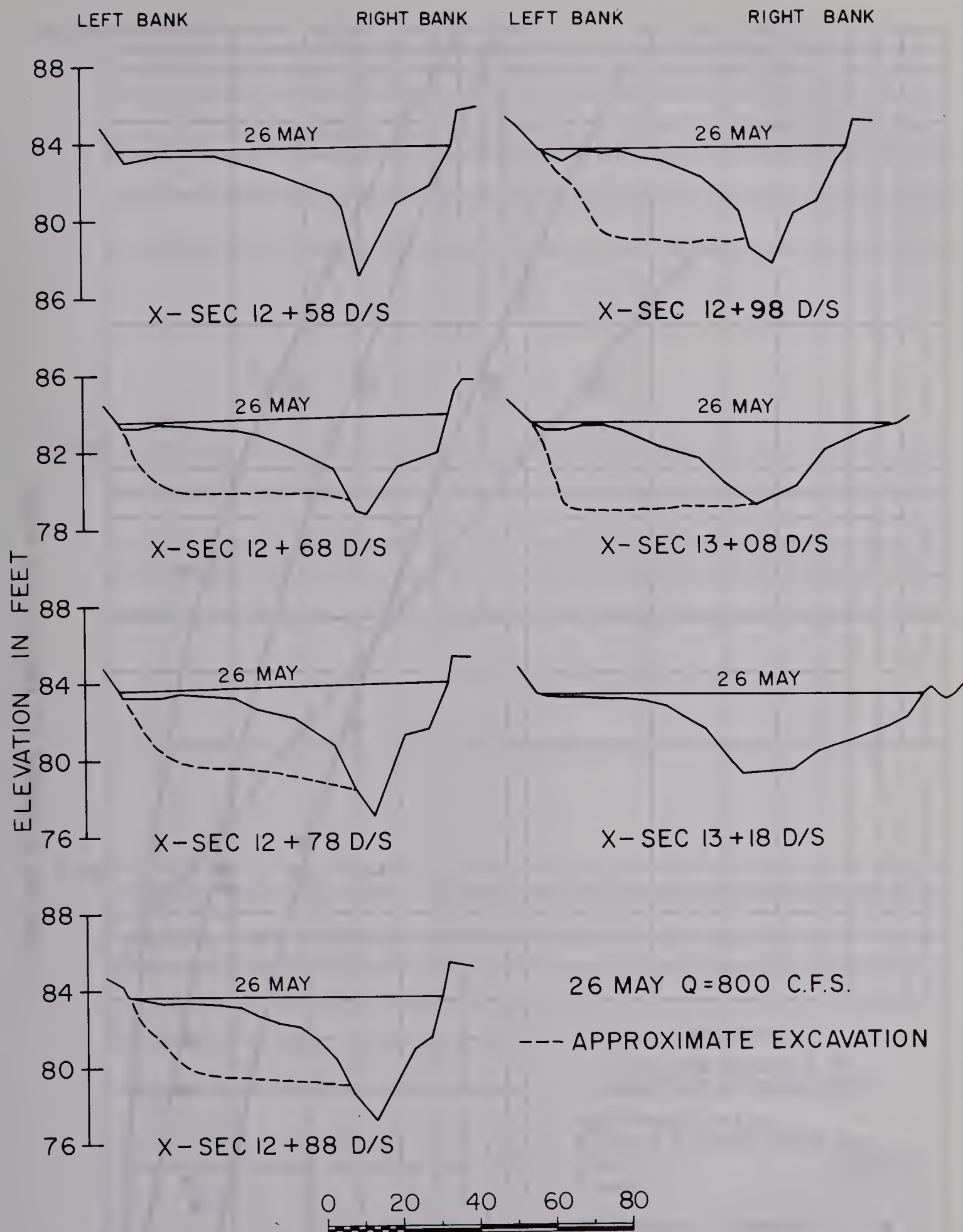
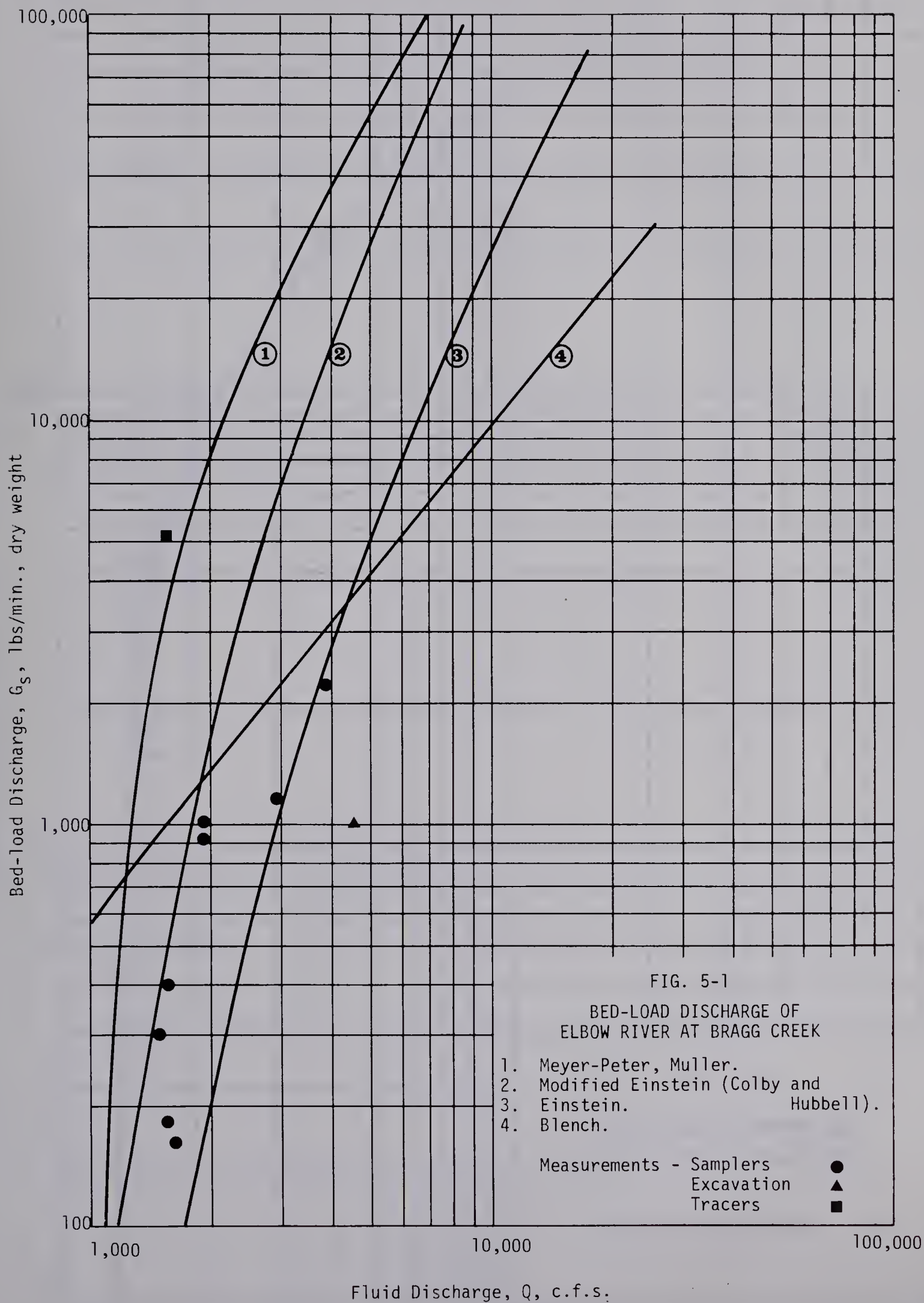


FIG. 4-28 X-SECTIONS AT EXCAVATION









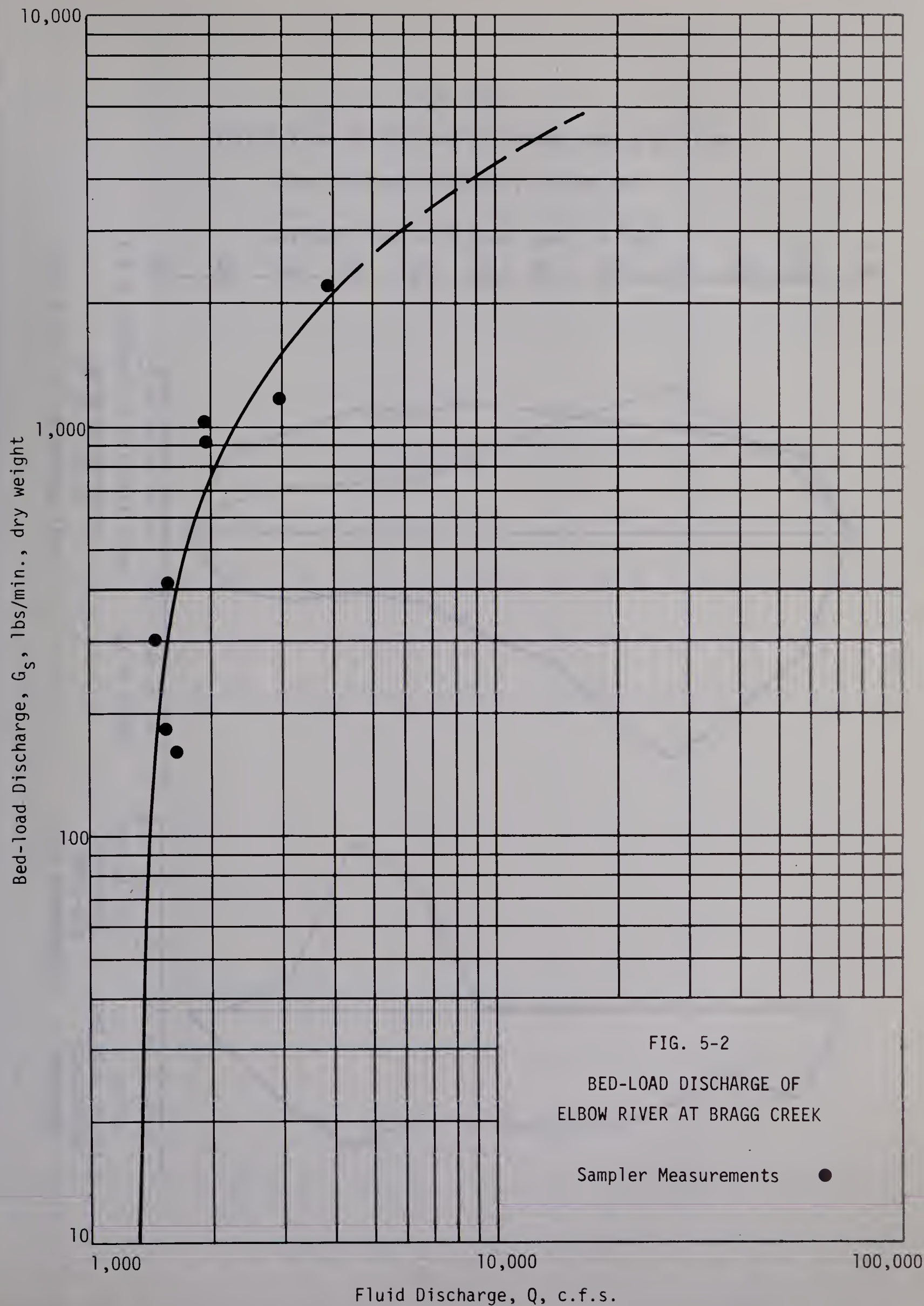


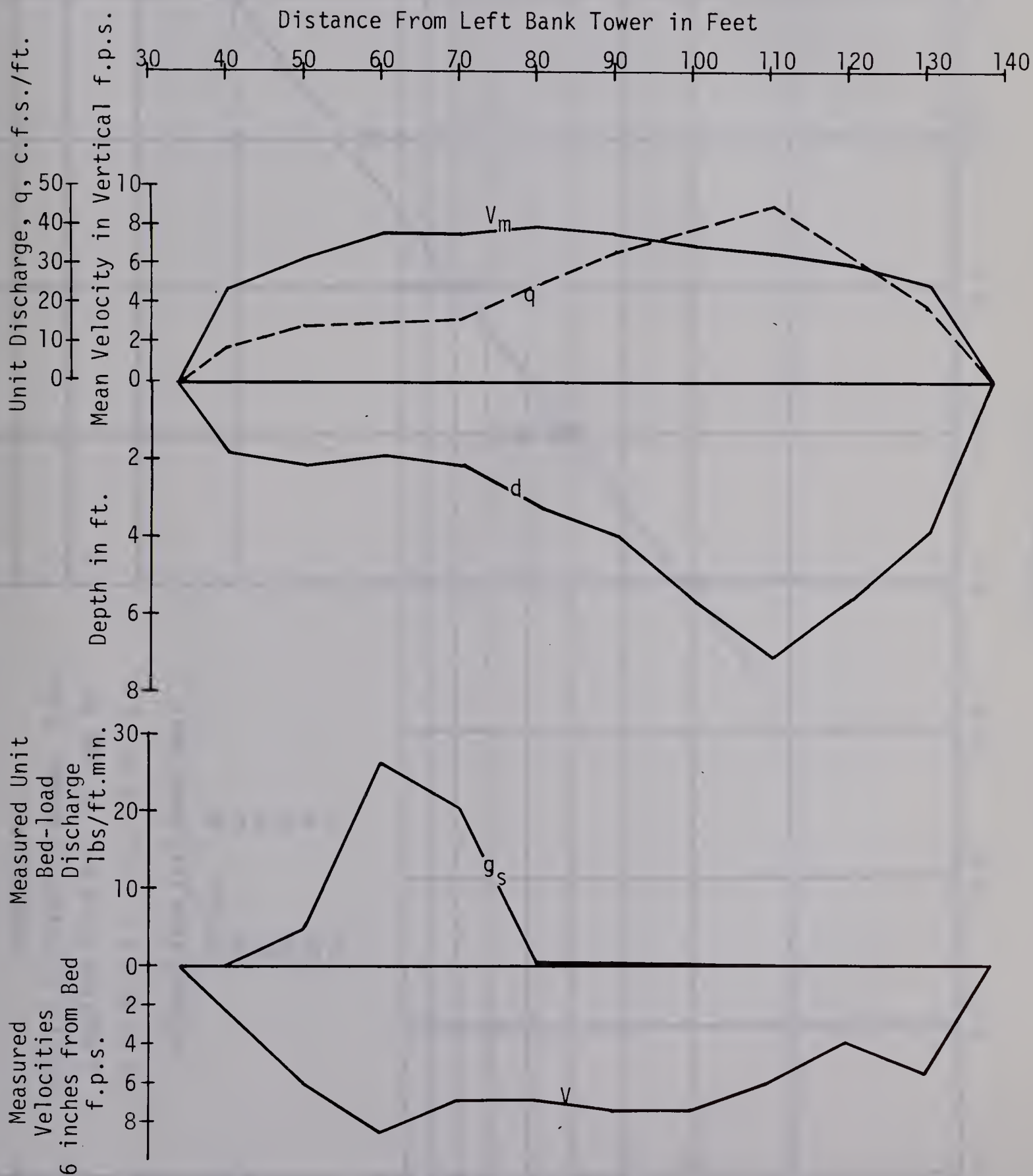




FIG. 5-3

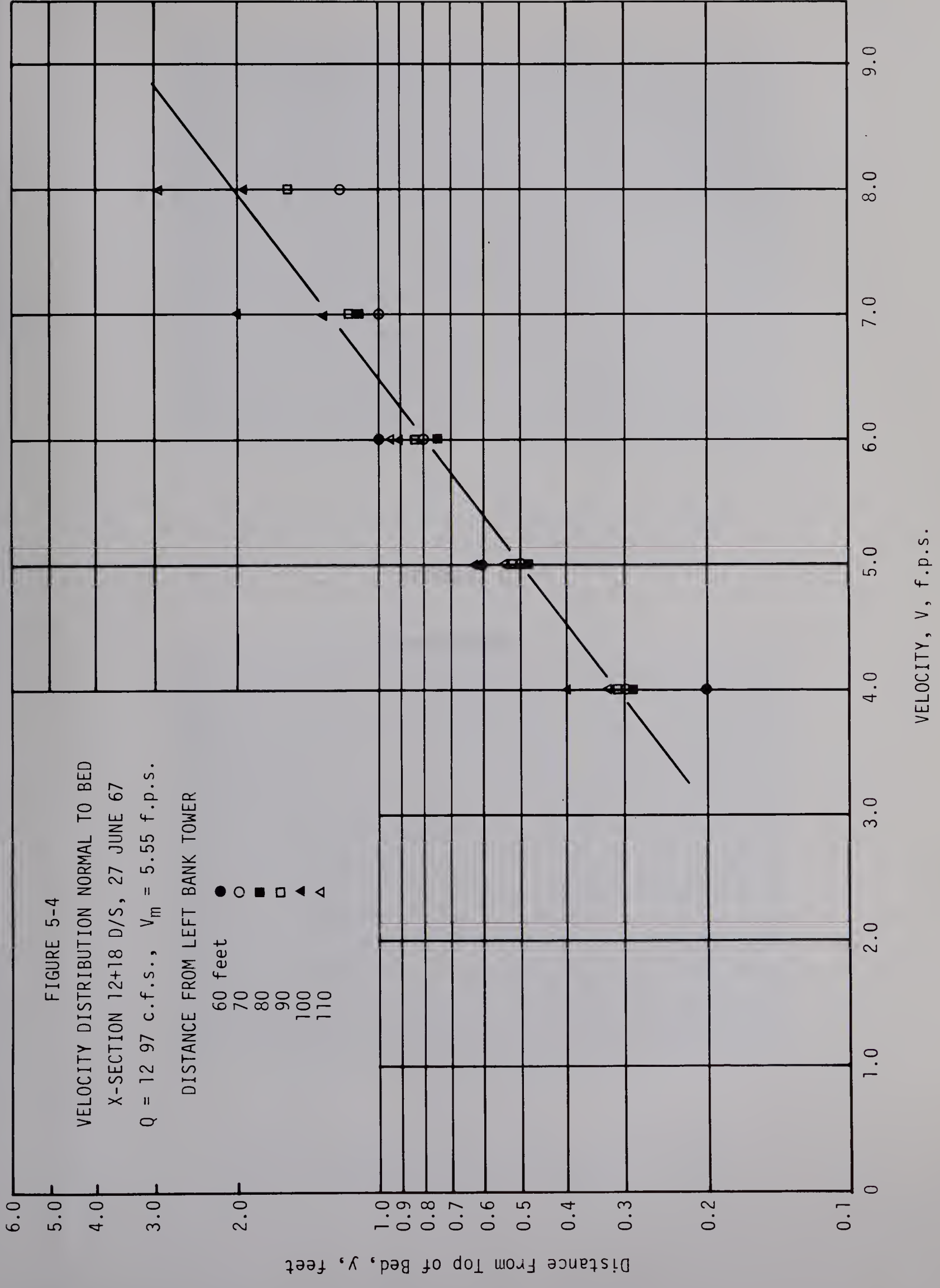
DISTRIBUTION OF BED-LOAD DISCHARGE ACROSS SECTION

Cross Section 12+18 D/S, 2 June 1967











## APPENDIX C

### PHOTOGRAPHS





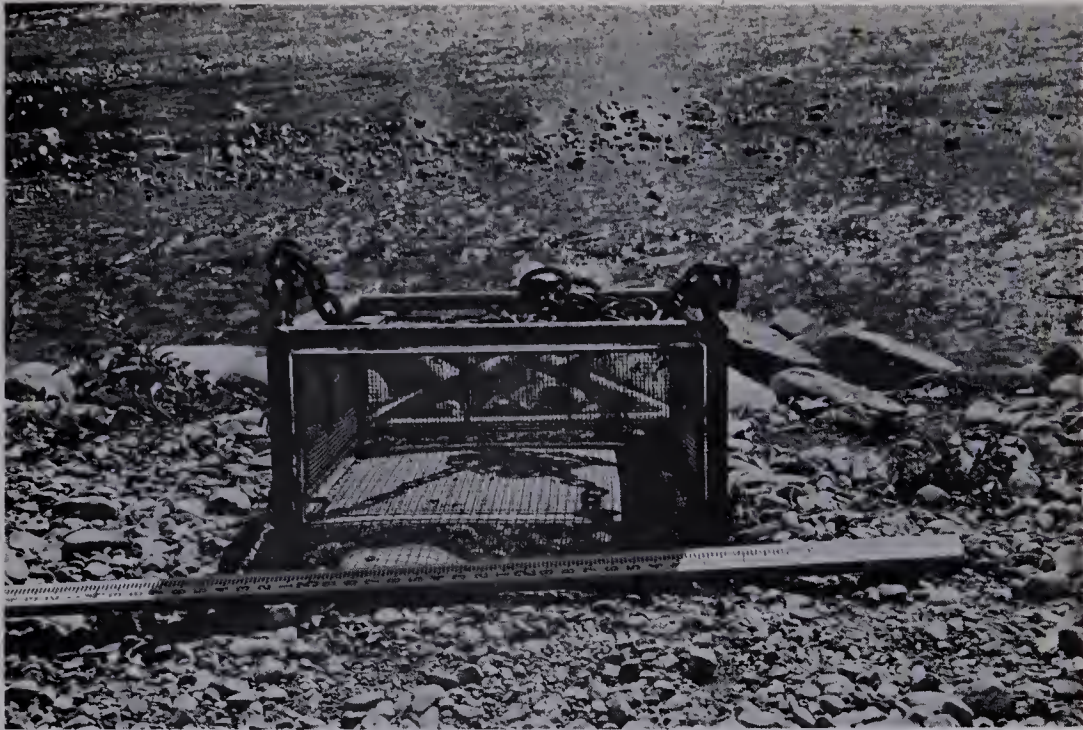


PLATE 3-1

Front View of Large Basket Sampler (24-10-30)  
With 1/4 Inch Mesh Basket



PLATE 3-2

Side View of Large Basket Sampler (24-10-30)  
With 1/4 Inch Mesh Basket





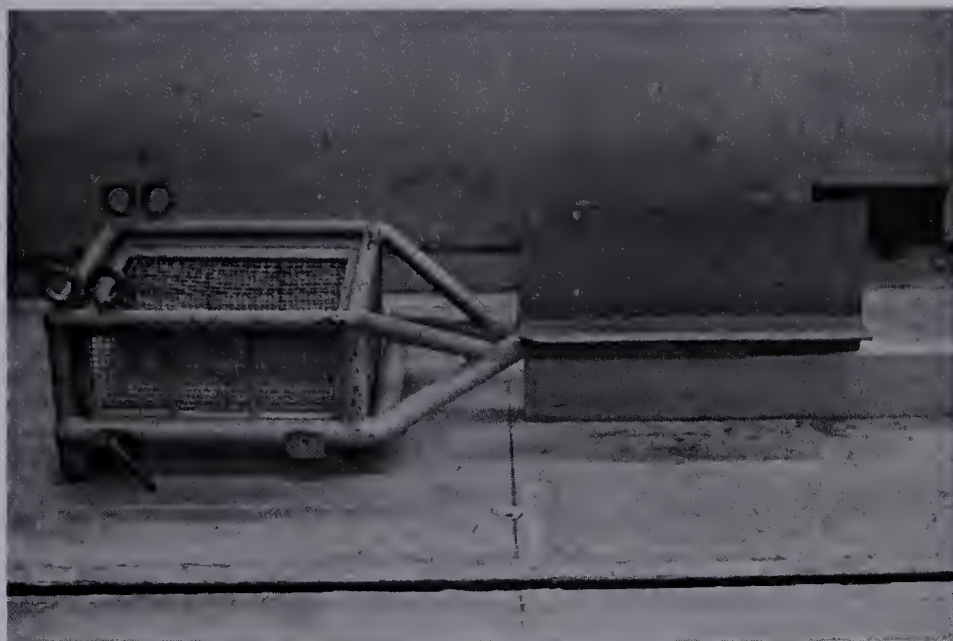


PLATE 3-3

Side View of Small Basket Sampler (12-6-15)  
With 1/4 Inch Mesh Basket



PLATE 3-4

Top-front View of Small Basket Sampler (12-6-15)  
With 1/4 Inch Mesh Basket





PLATE 3-5

Full Size VUV Sampler, Showing Mouth Opening

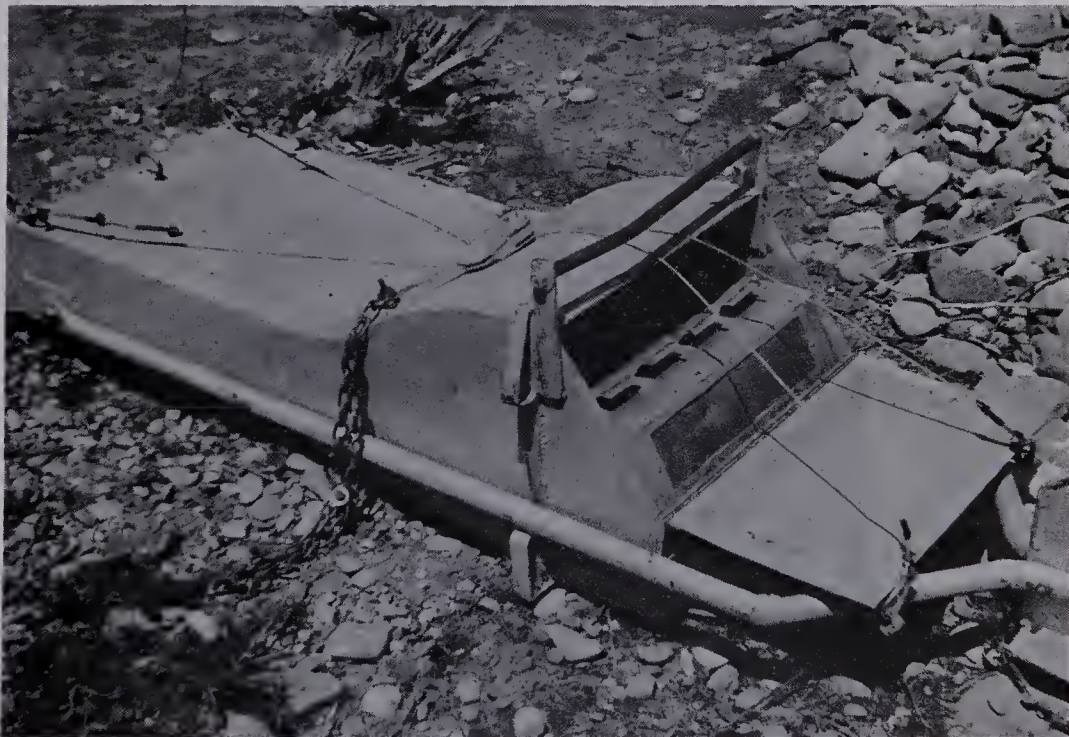


PLATE 3-6

Full Size VUV Sampler, Showing Rear Gate Open





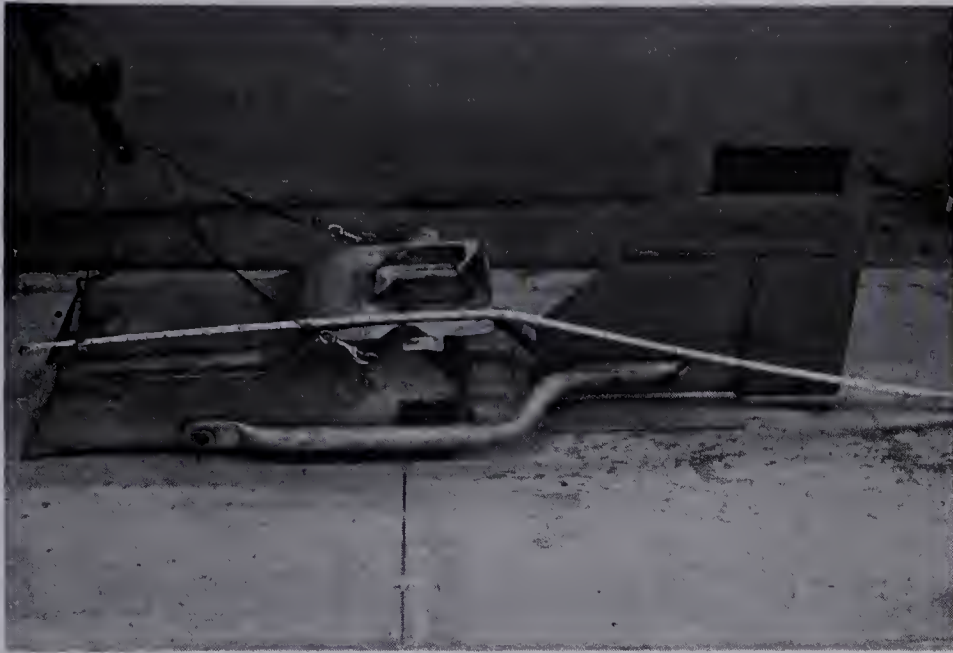


PLATE 3-7

Half Size VUV Sampler, Side View

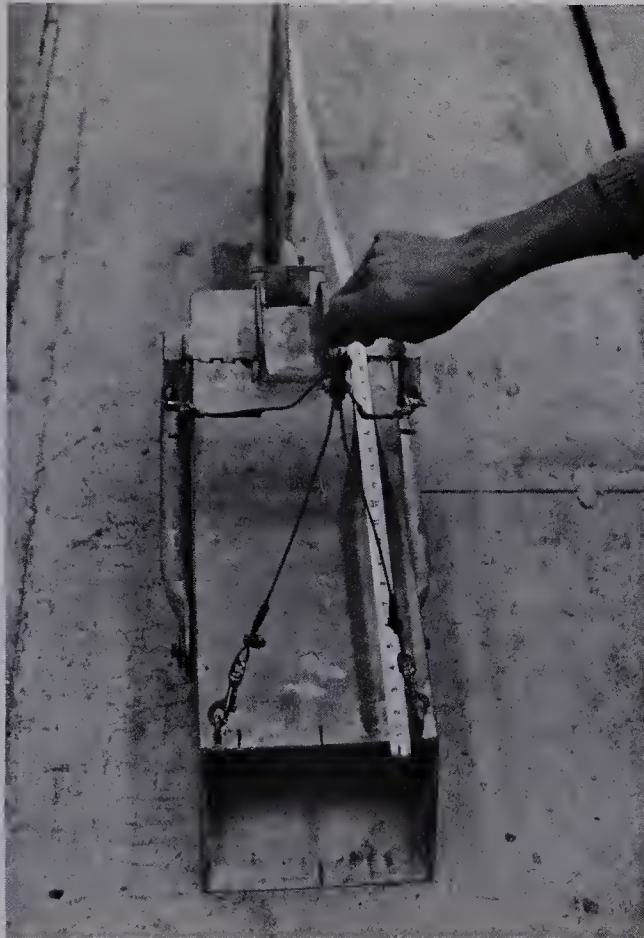


PLATE 3-8

Half Size VUV Sampler, Top-front View





PLATE 3-9

Lowering Large Basket Sampler at Station 110 Feet,  
12+18 D/S June 21, 1967. Photograph from Left Bank.



PLATE 3-10

Recovering Sampler to Left Bank. Large Basket Sampler  
With 1/4 Inch Mesh Basket. Photograph Looking Downstream.







PLATE 3-11

Hydrophone Assembly. From Right to Left; Weight (microphone), Cable, Amplifier, Headphones.



PLATE 3-12

Bottom View of Hydrophone Weight Showing Position of Enclosed Microphone.





PLATE 3-13

Dragline Equipment @ 12+18 D/S  
Working from Left Bank.









PLATE 4-1

ELBOW RIVER AT BRAGG CREEK

SCALE 1 INCH = 200 FEET

DATE - MAY 26, 1967

DISCHARGE - 800 C.F.S.








PLATE 4-2  
ELBOW RIVER AT BRAGG CREEK  
SCALE 1 INCH = 200 FEET  
DATE - JUNE 22, 1967  
DISCHARGE - 1500' C.F.S.

N



PLATE 4-2









PLATE 4-3

Upstream Stage Recorder from Right Bank at  
23+35 U/S.  $Q = 7,000$  c.f.s. May 31, 1967.



PLATE 4-4

Surface Wave, from Stage Recorder at 23+35 U/S  
on Left Bank.  $Q = 7,000$  c.f.s. May 31, 1967.





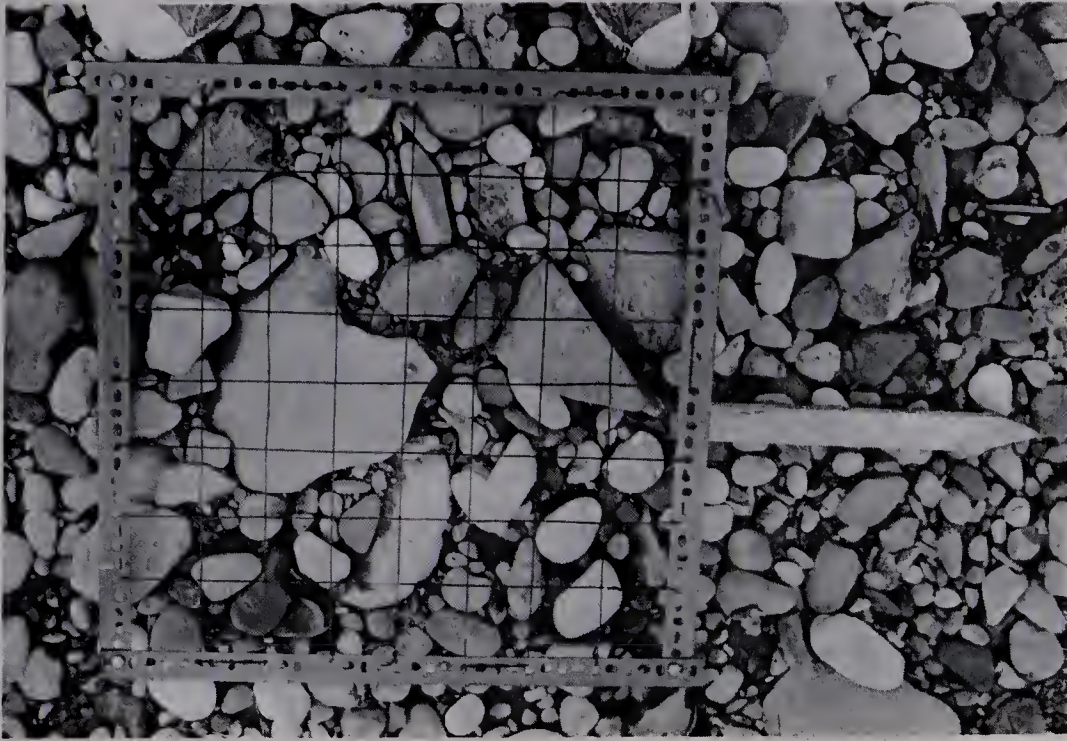


PLATE 4-5

Photograph of Grid on Bed Material. Grid 3 inches Square.  
Location - 21+00 U/S, Two Feet Left of Pit Sample No. 1.

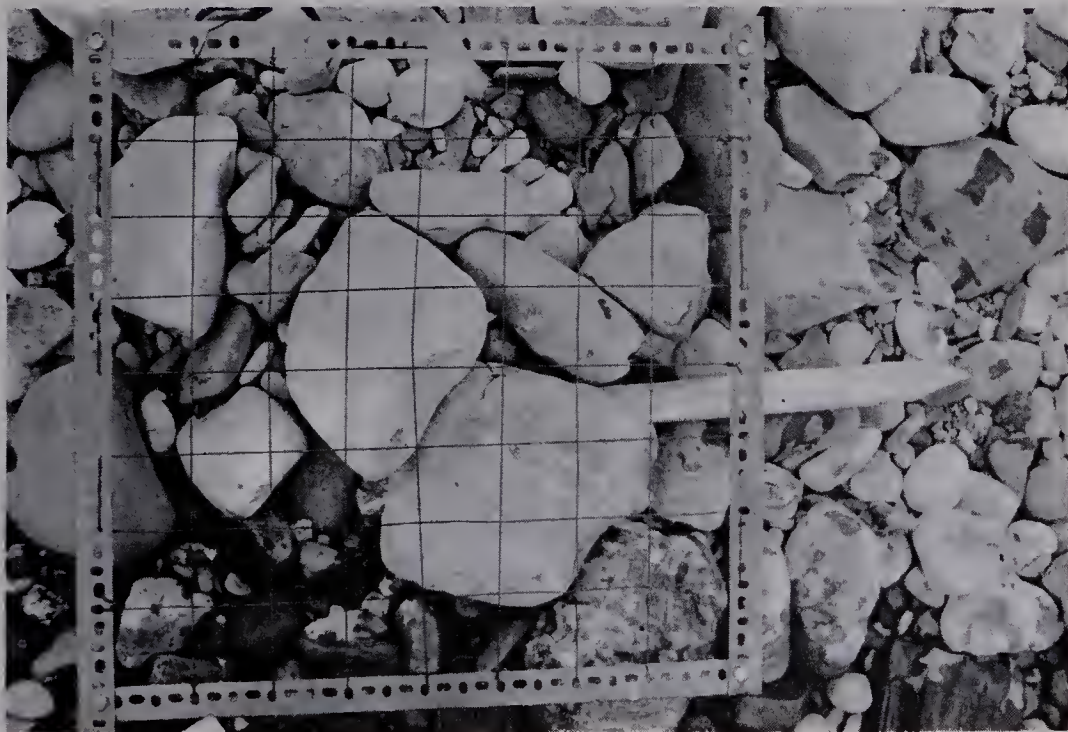


PLATE 4-6

Photograph of Grid on Bed Material.  
Location - 12+35 U/S, 10 feet U/S  
of Pit Sample No. 2.





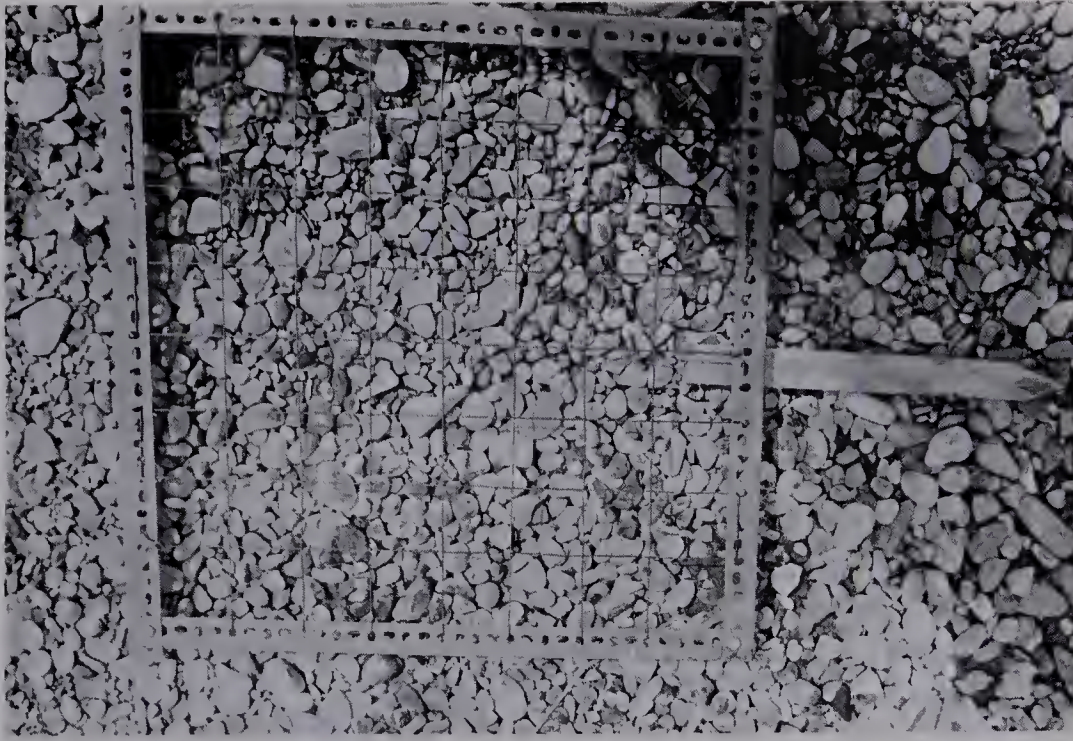


PLATE 4-7

Photograph of Grid on Bed Material. Location - 0+35 U/S,  
Top of Bar, 10 Feet Left of Pit Sample No. 4.

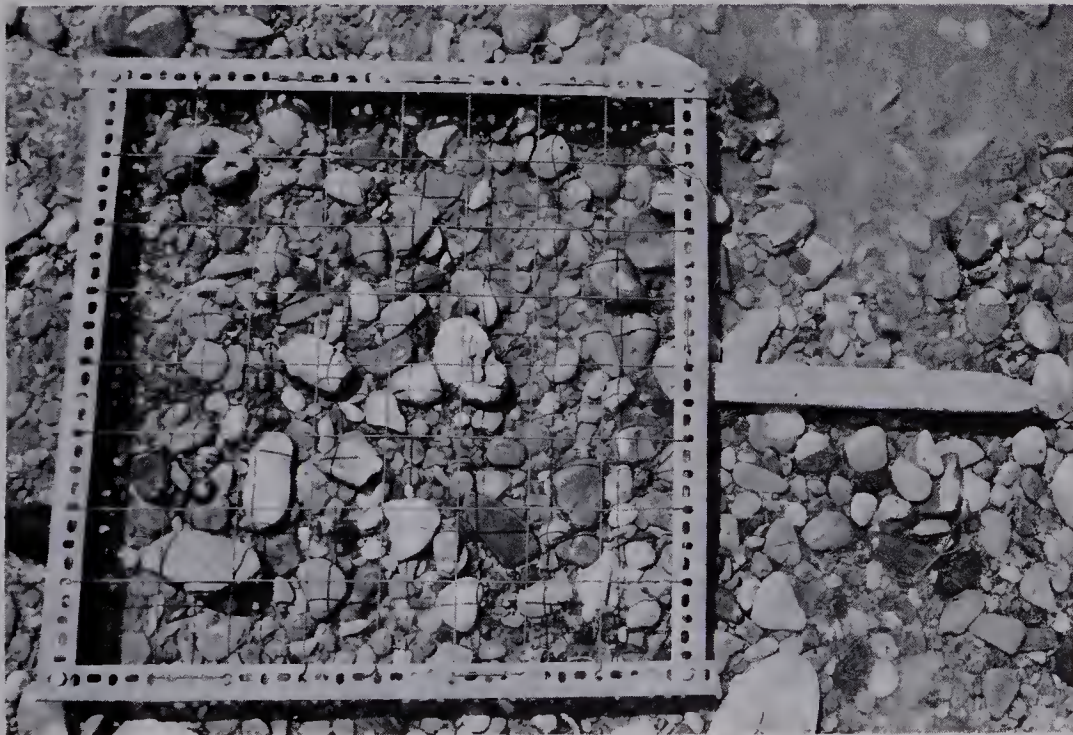


PLATE 4-8

Photograph of Grid on Bed Material. Location - 1+45 D/S,  
Top of Bar, 10 Feet Left of Pit Sample No. 5.







PLATE 4-9

Location of Tape Sample No. 15,  
Location 8+50 to 9+50 D/S, Looking Upstream.

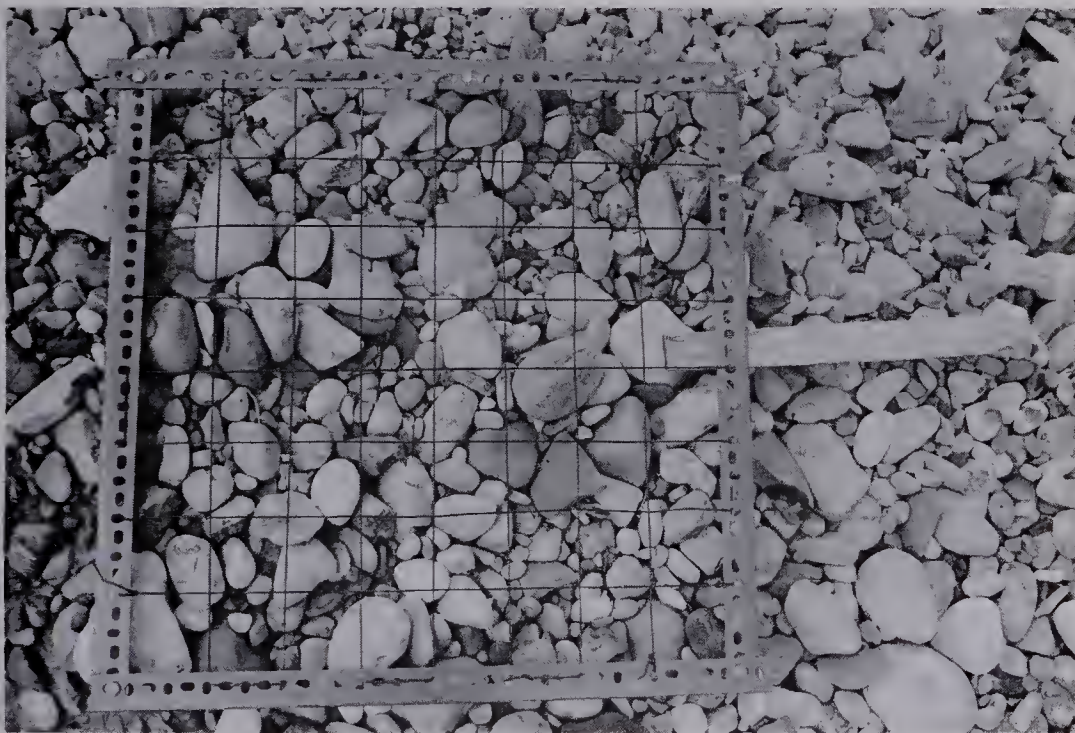


PLATE 4-10

Photograph of Grid on Bed Material.  
Location 9+00 D/S, 15 Feet D/S of Pit Sample No. 8.







PLATE 4-11

Location of Bed Excavation from Left Bank at  
12+38 D/S.  $Q = 7,000$  c.f.s. May 31, 1967.



PLATE 4-12

View from Right Bank at 12+00 D/S. Flow Over Bedrock  
in Foreground.  $Q = 7,000$  c.f.s. May 31, 1967.







PLATE 4-13

View from Left Bank at 12+18 D/S.  
 $Q = 400$  c.f.s. Aug. 17, 1967.  
 Bedrock on Right Bank.



PLATE 4-14  
 Bank Material Eroded  
 at High Flows.



















**B29882**